DEVELOPMENT AND VALIDATION OF NOVEL METHODS TO TRACK THREE-DIMENSIONAL SPINE KINEMATICS DURING DYNAMIC TRUNK MOVEMENTS USING A TIME-OF-FLIGHT RGB-D CAMERA

by

Wantuir Carlos Ramos Junior

A thesis submitted in partial fulfillment of the requirements for the
Master's degree in Human Kinetics

School of Human Kinetics
Faculty of Health Sciences
University of Ottawa

ABSTRACT

Low back pain (LBP) is a common and costly musculoskeletal disorder. Clinicians and researchers frequently assess dysfunction in LBP by observing patient's movement quality during pre-determined tasks using technically challenging and expensive motion capture devices. However, the cost and expertise needed to use these devices are direct barriers to their widespread adoption in clinical settings where direct benefits could be realized by LBP patients. RGB-D cameras are a potential inexpensive and less time-intensive motion capture alternative, which have been validated for analyses of gait, postural control, ergonomics, and human anatomy. However, as manufactured, RGB-D cameras are not ready for specific kinematic analyses, such as lumbar spine motion, as the native artificial intelligence (AI) models do not adequately detect the number and location of trunk joints to accurately track three-dimensional kinematics. In this thesis a proof of concept framework to adapt RGB-D cameras to accurately measure lumbar spine kinematics is presented, which is separated into two research studies: 1) validation of an RGB-D depth-based algorithm against an optoelectronic motion capture system of reference for measuring spine motion, and 2) the development of a markerless method of measuring lumbar spine kinematics.

In study one, 12 healthy young adults (6M, 6F) performed 35 cycles of repetitive flexion-extension with infrared reflective marker clusters placed over their T_{10}-T_{12} spinous processes and sacrum, while motion capture data were recorded simultaneously by one RGB-D camera and a 10-camera optoelectronic motion capture system. Lumbar spine joint angle range of motion (ROM) were extracted and compared between systems. Root mean squared error (RMSE) values were very low across all movement axes *($RMSE \leq 2.05° \pm 0.97°$)*, and intraclass correlations (ICCs) were considered excellent across all axes *($ICC_{2,1} \geq 0.849$)*, while Bland-Altman plots revealed that, on average, the RGB-D camera slightly

underestimated flexion-extension angles (≈ -1.88º) and slightly overestimated lateral bending and axial twisting angles (≈ 0.58º).

In study two, a single RGB-D camera was used to capture infrared, depth, and colour image data of 15 participants performing two batteries of 10 cycles of repetitive trunk flexion-extension under two conditions: marked (i.e. hand drawn markers on key anatomical locations on the back) and unmarked. The collected data were used to create a custom four module convolutional neural network (CNN; SpineNet) to segment the human back into upper back, lower back, and spine regions and to subsequently extract lumbar spine kinematics. SpineNet was trained and tested on ten marked participants in a train:test ratio of 80:20. Images of five additional participants without markers were used to evaluate SpineNet's generalizability. Quantitative image segmentation analysis on marked data had good similarity and accuracy between their prediction and ground truth across all individual modules *($mPA_{FG} \geq 0.8855$; $mJ_{BKG} \geq 0.8391$; $mJ_{FG} \geq 0.7884$; $fwJ_{BKG} \geq 0.9672$; $fwJ_{FG} \geq 0.8087$)* when the background class was ignored. Qualitative image segmentation analysis on unmarked data showed that Colourized and Surface Normal modules presented a more uniform and robust class morphology throughout frames than infrared (IR) and Fusion modules. All modules extracted kinematics similarly and were compared with their ground truth labels, showing low error levels across all movement axes (RMSE ≤ 3.66º), and good agreement on the flexion-extension and axial twist axes *($ICC_{2,1} > 0.907$; CI 95% [0.640, 0.990])*; however kinematic extraction in the lateral bend axis was poor *($-0.212 < ICC_{2,1} < 0.630$; CI 95% [-6,990, 0.910])*. Kinematic analysis on unmarked participants, done by inspecting average ensemble curves, showed that flexion-extension angles exhibited movement profiles (i.e. shape, timing, and peaks) that are comparable with previous research where similar data were collected.

In conclusion, this thesis provides a foundational proof of concept framework for using a single RGB-D camera for collecting and analyzing lumbar spine kinematics with or without

markers. The raw depth data were considered adequate for extracting lumbar spine kinematics from markers when compared to an optical motion capture system, and the application of an image segmentation AI model followed by the proposed method of kinematic extraction achieved adequate results for measuring lumbar spine kinematics on unmarked participants.

CO-AUTHORSHIP

This thesis contains materials from two manuscripts. The authorship is as follows:

Chapter 4: Ramos, W. C., Jr., Beange, K. H. E., & Graham, R. B. (2020). Concurrent validity of a custom computer vision algorithm for measuring lumbar spine motion from RGB-D depth data. *Under Review at Medical Engineering & Physics*.

Chapter 5: Ramos, W. C., Jr., Mavor, M. P., Boyle, A., & Graham, R. B. (2020). Development and testing of a custom markerless deep learning algorithm for spine segmentation and motion assessment using RGB-D images. *To be submitted to Computer Methods in Biomechanics and Biomedical Engineering.*

For each manuscript W. C. Ramos Jr. was responsible for: study conceptualization and design; acquiring, analysing and interpreting data; manuscript writing and review.

DEDICATION

I dedicate this work to my lovely wife Mariely Zago, whose support, affection, love, and endless dedication were essential so that I could continue walking and overcome this challenge. Thank you for staying with me throughout the journey, and let this be just the beginning of many more. The future is marvelous. I love you.

ACKNOWLEDGEMENTS

First, I would like to thank my supervisor Dr. Ryan Graham for accepting me as his student and for supporting me on this project for all these years. Thank you for always keeping the doors open and listening to me when I needed to, and thank you for creating this free research environment and for allowing me to take care of such a large and challenging research project.

Second, I would like to thank the invaluable inputs given by my colleagues Matthew Mavor, Kristen Beange and Alistair Boyle, your words and thoughts have deeply contributed to this project, thank you.

Third, I would like to thank all my lab mates for companionship and friendship, the advice and presence of all of you was fundamental and helped to make the journey much lighter.

Forth, I would like to give a special thanks to Danilo Catelli who helped to reopen the doors of the academic world to me at a crucial moment in my career. You were the one who helped me to revive the spark of interest in research and I will be forever grateful.

I also would like to thank all the love and support given by my family. Mom, Dad, William and Wivian, despite the distance, keeping contact with you during this time was fundamental for my success, thank you for being such good listeners and giving me all the support. Also, thanks to Faisca and Mingau that even unconsciously brought me unconditional love and care during all this time. I love you all.

Finally, Mariely, I really do not believe that any of this would be possible without you. Thank you for giving me all the support to make a dream come true, and thank you for letting me be part of yours. I love you!

“Last year I died, but this year I won’t”

Emicida & Belchior (AmarElo)

TABLE OF CONTENTS

LIST OF FIGURES

LIST OF TABLES

LIST OF EQUATIONS

NOMENCLATURE

2D, 3D	Two-dimensional, Three-dimensional
AI	Artificial Intelligence
AP	Anterior-Posterior
AT	Axial Twisting
BMI	Body Mass Index
CaRFs	Cascaded Ensembles of Randomized Decision Trees
CNN	Convolutional Neural Network
CoM	Centre of Mass
CRP	Continuous Relative Phase
FE	Flexion-Extension
FN	False Negatives
FP	False Positives
FPI	Foot Posture Index
fwJ	Frequency Weighted Jaccard Index
ICC	Intraclass Correlation Coefficients
IMU	Inertial Measurement Units
IR	Infrared
Kinect v1, v2	Kinect version 1, version 2
LB	Lateral Bending
LBP	Low Back Pain
LCS	Local Coordinate System
LoA	Limits of Agreement
MDRT	Multidirectional Reach Test
mJ	Mean Jaccard Index
ML	Medial-Lateral
mPA	Mean Pixel Accuracy
MSD	Musculoskeletal Disorder
PA	Pixel Accuracy
PD	Parkinson Disease
RGB	Red, green, blue
RGB-D	Red, green, blue, depth
RMSE	Root Mean Square Error
RNN	Recurrent Neural Network
ROI	Region of Interest
ROM	Range of Motion
SD	Standard Deviation
SN	Surface Normal
SVM	Support Vector Machine
TP	True Positives
TUG	Timed-Up-And-Go
V	Vertical
WSIB	Workplace Safety and Insurance Board

CHAPTER 1 GENERAL INTRODUCTION

Low back pain (LBP) is one of the most common musculoskeletal disorders worldwide, affecting approximately 80% of the population at some point during their lives (Schneider & Irastorza, 2010). The majority of LBP episodes resolve within a 4 week period; however, recurrence is common (Croft et al, 1998). In fact, 85% of people with LBP will suffer a recurrent case during their lifetime, and 20-44% will have a new acute episode within one year (Andersson, 1999). LBP also poses a large economic burden, with estimated medical expenditures ranging between $6-$12 billion annually in Canada alone, not including additional indirect costs occurred due to lost work time and productivity (Bone and Joint Canada, 2017). In Ontario, approximately 57,000 lost time claims were approved by the Workplace Safety and Insurance Board in 2016, of which roughly 10,000 were due to LBP (Workplace Safety and Insurance Board of Ontario, 2016).

In order to investigate causes of LBP and injury risk, researchers and clinicians frequently observe patients' movement quality during tasks that involve dynamic trunk motions. Usually, LBP patients have different kinematic movement profiles when compared to healthy controls; it is well-accepted that aberrant movement patterns are associated with low back dysfunction (Delitto et al., 1995). For instance, aberrant movement patterns during forward bending have consistently been observed in chronic LBP patients (e.g. Ashouri et al., 2017; Biely et al., 2014; Graham et al., 2014; Mokhtarinia et al., 2016). Alterations in kinematic patterns have also been observed in sit-to-stand tasks. For example, Shum and colleagues (2005) found limited mobility of the spine and hips in LBP subjects, as well as a significantly altered spine-hip joint coordination pattern relative to healthy control subjects. Additionally, Mazzone and colleagues (2016) found that participants with LBP have decreased lumbar extension range of motion (ROM) when compared to control participants during prone extension. Moreover, researchers have recently shown that they are able to

successfully classify LBP patient subgroups that differ based on the direction of painful movement (e.g., active extension pattern and flexion pattern groups; Hemming et al., 2018) using kinematic analyses.

Typically, researchers assess spine biomechanics and movement patterns using optoelectronic motion capture and other technically challenging and expensive devices in controlled laboratory environments (Bonnechère et al., 2016; Rosenberg et al., 2016). The high cost and complexity of these systems make the use of motion capture devices in clinical settings infeasible; thus, clinicians currently evaluate trunk motion using visual observations and interpretations of movements. Because these methods of visual assessment are subjective, interpretation and classification of movements may vary between clinicians, as well as between days. Introduction of objective assessments of movement quality can improve accuracy and reliability of measurements of movement quality in clinical settings. Recent work has reported a moderate agreement between clinicians' visual assessments relative to an electromagnetic motion tracking system, suggesting that data-driven analysis using motion capture systems may be useful for clinical assessments of movement quality, and, more specifically, identification of aberrant movements (Wattananon et al., 2017). It is likely that clinicians do not have the time or expertise required to operate such technically challenging devices (Papi et al., 2016); therefore, development of a portable, inexpensive, and easy-to-use motion capture tool would be beneficial to aid in the diagnosis and assessment of LBP disorders.

Researchers are currently investigating new methods to implement inexpensive, portable sensors and equipment to measure human movement in industrial and clinical settings. For example, Beange and colleagues (2019) investigated the performance of inertial measurement units (IMUs) for orientation estimation and motion tracking of the spine during trunk flexion-extension (FE) movements in comparison to optoelectronic motion capture. In their study, local dynamic spine stability, lumbopelvic coordination, and intersegmental motor

variability were measured on 10 participants during a repetitive trunk FE task; they found good to excellent agreement and reliability between systems across all variables. Similarly, Bauer and colleagues (2015) evaluated the validity and reliability of IMUs to measure lumbar spine ROM against a gold standard optical motion capture system during a series of movement dysfunction tests, and found that the IMUs provided valid estimates of spine ROM in the primary direction of movement. While IMU performance is regarded as clinically acceptable for motion tracking, the spatial resolution of anatomical landmarks in global space is difficult to obtain; this means that an IMU is only able to track orientation relative to itself (e.g., a starting position), or another IMU. Though many researchers attempt to track IMU motion in global space (e.g., Ricci et al., 2016; Zimmermann et al., 2018), these procedures are computationally expensive and advanced, and are dependent on careful IMU-to-segment placement and calibration techniques. As an alternative, researchers are exploring the use of red-green-blue-depth (RGB-D) cameras for tracking people's movement, as these sensors are able to provide positional data (i.e., position in global space) on top of orientation data (i.e., rotations).

The use of RGB-D cameras as motion capture devices started to became popular in 2010, when Microsoft released the Microsoft Kinect™ (Kinect; Microsoft Corporation, WA, USA), which allowed players to interact with their console by using gestures and spoken commands. Each Kinect is an RGB-D camera, as it is composed of a colour camera and a depth sensor that captures the player's motions. Similar technology was made available by other companies such as Asus, Orbecc, Intel and other companies have also released their own RGB-D cameras, still being developed and available today (e.g. Microsoft Azure, Asus Xtion, Orbecc Astra and Intel RealSense). Considering their cost (~$200 USD), portability, and simplicity of use, this new device has potential to be used as an alternative to gold-standard motion capture devices and other alternative motion capture devices (i.e., IMUs), allowing

researchers and clinicians to accurately measure spine kinematics during dynamic movements in more diverse settings (e.g., clinics, hospitals, patients' home, and research centres). RGB-D cameras have been tested for their validity as motion capture tools for research and use in clinical settings. More specifically, in the field of biomechanics, RGB-D cameras have been used to assess a number of kinematic measures during various tasks, such as: 1) postural control during forward reach, lateral reach and standing balance tasks (Clark et al., 2012); 2) spatiotemporal gait parameters during treadmill gait at normal and fast walking speeds (Auvinet et al., 2017; Eltoukhy et al., 2017); 3) clinical measurements of motor function during challenging gait tasks, balance tasks, and adaptive postural control tasks (Otte et al., 2016); and 4) in ergonomics to rapidly carry out workplace postural assessments and risk evaluations (e.g., RULA score evaluation; Plantard, et al., 2017). However, there has been very limited research completed using RGB-D cameras to carry out biomechanical assessments of the spine. Within the existing literature, researchers have been primarily focused on investigating accuracy, reliability, and reproducibility of RGB-D cameras as quantifying tools for spine posture and curvature assessments during standing static poses (Castro et al., 2017; Quek, et al., 2017; Hannink, et al., 2020), while very few aimed at assessing RGB-D cameras' accuracy and reliability to track dynamic spine movements. Moreover, while RGB-D cameras utilize a native skeletal model that locates and tracks joint centres to assess kinematics, this model is restricted to the predefined joint centres in the skeletal model algorithm, limiting the feasibility for traditional lumbar spine assessments.

Thus, the purpose of this thesis work was to develop and validate novel methods to assess 3D lumbar spine kinematics during dynamic movement tasks using data from an RGB-D camera. To achieve this, this thesis contains two parts: 1) assessment of the accuracy and reliability of a custom-developed motion tracking algorithm used to track infrared (IR) reflective markers placed over the lumbar spine from the RGB-D depth data, relative to

gold-standard optoelectronic motion capture equipment; and 2) further development of a deep learning algorithm to segment anatomical landmarks from the RGB-D images in order to extract 3D lumbar spine motion data without the use of IR reflective markers.

CHAPTER 2 LITERATURE REVIEW

2.1 Low back Pain

Low back pain (LBP) is a very prevalent musculoskeletal disorder, affecting approximately 80% of the world's adults at least once in their lifetime (Schneider, et al., 2010). Single acute cases usually resolve within 4 weeks, although recurrence is very common (Croft, et al., 1998; Kjaer et al., 2018), and a small number of cases (10-40%) turn into chronic LBP representing a major economic burden for society (Croft et al., 1998; Dillingham, 1995; O'Sullivan, 2005). In Canada alone, medical expenditures range from 6-12 billion dollars annually and these costs do not include losses in productivity and working hours. Furthermore, diagnosing LBP is challenging; a very small number of cases are linked to specific causes such as compression fracture, spondylolisthesis and ankylosing spondylitis, leaving about 90% of the cases classified as nonspecific, since their origin is unknown. Van Tulder and colleagues (1997) found evidence that nonspecific LBP is not strongly associated with image abnormalities. In fact, 40% to 50% of radiological images that presented degenerative changes and spondylosis were found in people without LBP (Roland & Van Tulder, 1998); therefore, medical imaging diagnostics might not be a useful tool for classifying LBP populations.

To better understand the underlying mechanisms and how best to treat LBP, clinicians typically analyse a patient's spine movement quality, and since it is well accepted that aberrant movements patterns are associated with low back dysfunction (Ashouri et al., 2017; Delitto, et al., 1995; Mokhtarinia, et al., 2016), their goal is to classify the movement as normal or aberrant (i.e., dysfunctional or harmful; Biely, et al., 2014; Silfies, et al., 2009). To evaluate a patient's movement, clinicians frequently use self reported questionnaires and clinical tests due to their simplicity (Lebel, et al., 2015; Smeets, et al., 2011); however, assessing lumbar spine motion with these methods comes with a high level of subjectivity (Carlsson & Rasmussen-Barr, 2013; Papi et al., 2018). In fact, several researchers investigated

the reliability of clinical assessments and found moderate to good interrater reliability and a high risk of bias (Alvarez, 2017; Biely et al., 2014; Carlsson & Rasmussen-Barr, 2013; Denteneer, et al., 2017; Fritz, et al., 2007; Hicks, et al., 2003; Rabin, et al., 2013). Introducing (or adding) objective measurements of movement (i.e., kinematic evaluation) is encouraged since it may help to improve reliability and accuracy in clinical assessments (Sánchez-Zuriaga, et al., 2011; Smeets et al., 2011) and, in many cases, it is possible to distinguish LBP patients from healthy controls through kinematic patterns (Sánchez-Zuriaga et al., 2011). However, these kinematic evaluations are mostly limited to research centres, as the traditional instrumentation that are capable of providing such evaluations (e.g. optoelectronic motion capture), are expensive, not portable, and requires a high level of training and expertise to use (Galna et al., 2014; Zhou & Hu, 2008). Thus, a method (or device) that that could enable objective kinematic assessments at a low cost, is highly portable, easy to use, has a high level of accuracy, and is reliable would greatly expand our clinical capabilities for conducting kinematic assessments and improve our clinical understanding of LBP.

2.2 RGB-D camera as an alternative motion capture device

RGB-D cameras are promising motion capture tools that are inexpensive and easy to use and can potentially be applied to movement assessments. RGB-D cameras are composed of a colour camera (RGB) and a depth sensor (D) that generates images where each pixel corresponds to the distance between the camera lens and any target on the camera's field of view, allowing motion tracking. One RGB-D camera in particular that contributed to the popularization of the technology is the Microsoft Kinect™ (Kinect). In 2010, Microsoft released the first version of the Kinect, a new motion capture gaming controller for the Xbox 360™ (Xbox 360; Microsoft Corporation, WA, USA) that allowed players to move the in-game avatars using their body's motion. On its first release, Microsoft's RGB-D camera used

a “structured light” matching method to sense depth; an infrared (IR) speckle light pattern (i.e., IR light clustered dots arranged in a known pattern) is projected over surfaces in front of the RGB-D camera , and then based on the distortion of the IR light pattern (i.e., size and IR clusters’ new pattern) it is possible to use trigonometry to estimate the distance between a surface and the sensor, generating a 3D depth image of what is inside the RGB-D camera’s field of view. Then, to automatically track body motion, the RGB-D camera applies a machine learning algorithm called “random forests” on its depth data output to identify anatomical landmarks, extracting predefined joint centres and fitting them onto a native “skeletal model”. In 2014, Microsoft released the second version of the RGB-D camera (Kinect version 2; Kinect v2) for its new console Xbox One™ (Xbox One; Microsoft Corporation, WA, USA). The updated features of the second version were: 1) the depth sensing technology was updated to a method called “time-of-flight”, which estimates distance based on how long an emitted IR light beam takes to travel from the camera, hit the target’s surface and bounce back; and 2) its native skeletal model received more joints on the hands and neck. While the updated depth sensing method truly enhanced the Kinect’s ability to track human motion, it also introduced slight disadvantages in comparison to the first version of the Kinect: accuracy of the new depth sensing method is more influenced by the colour of the target’s surface (squared error < 4 mm) and the device’s temperature (root mean squared error < 5.3 mm) as reported by Sarbolandi et al. (2015) and Wasenmüller & Stricker (2016). In contrast, the Kinect version one (Kinect v1) presents an offset error on depth sense that grows exponentially with object distance (i.e., offset below 10 mm for 0.5 m increasing to 40 mm for 1.8 m), while on Kinect v2 the depth sensing offset slightly varies with distance, remaining 18 mm on average (Sarbolandi, et al., 2015; Wasenmüller & Stricker, 2016). Thus, these characteristics should be considered when choosing the Kinect’s setup so that these errors can be easily mitigated with relatively simple measures, such as pre-warming Kinect for 25 minutes as recommended by Wasenmüller and

Stricker (2016). Although, given the advantages and disadvantages between Kinect versions, there is still no consensus on which version is better (Clark, et al., 2019) as one might be better suited for certain applications than the other (Sarbolandi, et al., 2015; Wasenmüller & Stricker, 2016), therefore findings using Kinect v1 and other RGB-D cameras that use "structured light" depth sensing technology are still relevant.

Since the release of the first RGB-D cameras, scientists have been researching their validity as an alternative motion capture device in research and clinical settings due to its portability, low cost, and easiness to use when compared to traditional motion capture systems (Galna et al., 2014; Zhou & Hu, 2008). The RGB-D cameras' validity has been researched in many biomechanical settings such as: gait analysis (Geerse, et al., 2015), postural control and balance (Clark et al., 2015), functional tasks (Moreno, et al., 2017), clinical assessment of motor function (Otte et al., 2016), postural assessment and risk evaluation in workplaces (Plantard, et al., 2017), static posture evaluation (Castro et al., 2017), and spine curvature assessment (Quek, et al., 2017). Overall, results have been positive regarding RGB-D cameras' validity, agreement, and reliability. RGB-D camera validation studies during gait assessments, balance tests, functional assessments, posture and anatomical assessments are discussed in detail below. These papers were chosen due to their relationships with this thesis in terms of: a) their final goals – i.e., to validate the RGB-D camera(s) to measure human movement in clinical and research settings and b) their methods, which includes using RGB-D camera(s) depth data and sometimes IR to track anatomical landmarks, and, therefore, presented results are more pertinent to our work.

2.3 Gait analysis

Gait assessments are frequently performed by clinicians aiming to evaluate gait abnormalities caused by diseases (e.g. Parkinson's and Stroke) and track patients' progress during rehabilitation (Benson, et al., 2018; Dugan & Bhat, 2005; Saleh & Murdoch, 1985;

Simon, 2004; Whittle, 1996). In an effort to make gait assessments more widely accessible, researchers have validated methods to use RGB-D cameras as objective quantifying tools for gait analysis through kinematic and spatiotemporal variables. In the literature, it is well accepted that some spatiotemporal variables extracted from the RGB-D cameras' native skeletal data are valid and reliable such as gait speed, step length, step time and stride length (Clark et al., 2019; Geerse et al., 2015; Müller, et al., 2017; Springer & Seligmann, 2016). However, there is some conflicting evidence regarding other variables such as foot swing velocity, step width and stride time (Clark, et al., 2013; Dolatabadi, et al., 2016; Eltoukhy, et al., 2017; Mentiplay et al., 2015; Xu, et al., 2015). Despite the discordant evidence, Müller and colleagues (2017) demonstrated that it is possible to improve the accuracy of spatiotemporal variables (i.e., walking speed, step length, stride length, step width and step time) by positioning multiple RGB-D cameras with different viewpoints. By averaging the RGB-D camera's native skeletal data measured from both left and right sides of the participant's body rather than measuring the native skeletal data from a single side, Müller et al. (2017) had a reduced occlusion rate, which resulted in an improved level of agreement across all outcome variables when compared to an optoelectronic motion capture system $(0.434 \leq ICC_{2,1\ Single\ side} \leq 0.991;\ 0.505 \leq ICC_{2,1\ Both\ sides} \leq 0.999)$. Although there is conflicting evidence of the accuracy of some spatiotemporal variables, Müller et al. (2017) showed that using multiple viewpoints does improve the accuracy of the skeletal data; therefore, studies intending on investigating spatiotemporal gait variables should use multiple RGB-D cameras with overlapping views to ensure a complete view of their participants.

RGB-D camera validation studies that investigated kinematic variables also show conflicting evidence when using skeletal data. Xu and colleagues (2015) validated an RGB-D camera against an optoelectronic system to measure gait parameters of the hip and knee joints during treadmill walking. Xu et al. (2015) found poor angular displacement registration using

the RGB-D camera's native skeletal data. Xu et al. (2015) also reported high root mean square error *(RMSE)* indices for the knee and hip range of motion (ROM) in the flexion and extension movement axis *(RMSE > 11.8° ± 8.6°)*; hip joint ROM angles were underestimated during flexion and overestimated during extension, and the RGB-D camera calculated unrealistic negative angles for the knee joint. However, despite the errors found in magnitude of the knee and hip joint angles, ensemble averages of angular displacement across all gait cycles calculated by the RGB-D camera followed the optoelectronic reference system movement profile's trend (knee: r = 0.81; hip r = 0.91). Therefore, the RGB-D camera's native skeletal model is calculating similar movement patterns albeit with a substantial difference in magnitude. Differently from Xu and colleagues (2015), Geerse and colleagues (2015) investigated the linear displacement of all 19 joints of the RGB-D camera's native skeletal model over a 10 metre over ground walking task. Geerse and colleagues (2015) found good to excellent agreement in the anterior-posterior (AP) movement plane for all joints except for the hip, moderate to excellent agreement for medial-lateral (ML) movement plane and moderate to good for trunk, head and upper limbs in the vertical (V) axis *(0.736 < $ICC_{AP\ All\ joints\ except\ hip}$ < 0.973; 0.587 < ICC_{ML} < 0.903; 0.567 < $ICC_{V\ trunk,\ head\ and\ upper\ limbs}$ < 0.900)*. However, overall agreement indices for the hip and lower limb joints were poor on AP and V movement planes *(0.386 < $ICC_{AP\ hip}$ < 0.479; 0.163 < $ICC_{V\ hip\ and\ lower\ limbs}$ < 0.616)*. Despite outcome variables and metrics being different, it appears that Geerse and colleagues (2015) and Xu and colleagues (2015) reported similar findings: the hip and knee joints produce high error indices. Conversely, Eltoukhy and colleagues (2017) reported excellent agreement for linear displacements of the hip in the ML and vertical axes *(0.68 < ICC < 0.80)*, and excellent agreement for angular displacement of the hip and knee during treadmill walking *(0.84 < ICC < 0.91)*. However, these variables were presented with very large confidence

intervals *(-0.45 < CI < 0.96)*, which corroborates with the evidence of high error in the hip and knee joint positions of the RGB-D camera's native skeletal model. Thus, the aforementioned studies provide evidence for the usability of the RGB-D camera's native skeletal model for gait assessment using spatiotemporal and kinematic variables of the trunk and upper limb joints; however, hip and lower limb joints are not as reliable, which can be detrimental for clinical gait evaluations.

While research endeavours using the RGB-D camera's native skeletal model produce mixed results, studies that calculate kinematic variables using the RGB-D camera's depth data directly to track participants with and without IR reflective markers have achieved adequate validity against gold standard motion capture systems. As an example, Auvinet and colleagues (2017) investigated the validity of the RGB-D camera's native skeletal model and depth data (i.e., markerless method) compared to an optoelectronic system (i.e., marker-based method) by calculating continuous relative phase (CRP) of the shank and thigh for assessing the longitudinal asymmetry index of participants. It was found that the RGB-D camera's native skeletal data was not adequate to measure the longitudinal asymmetry index. The correlation between the longitudinal asymmetry index assessed with the RGB-D camera's native skeletal data and the optoelectronic system had a low positive correlation coefficient *(r < 0.45)*, while the assessment made using depth data had a very high positive correlation with the reference system *(r = 0.92)*. The authors associated the low correlation coefficient of the RGB-D camera's native skeletal data on measuring the longitudinal asymmetry index to its lack of precision on automatically identifying the lower limb joints, while comparing body segments directly from the depth data was more robust for assessing the longitudinal asymmetry index (Auvinet et al., 2017). Thus, this study shows that the RGB-D camera's native skeletal data is unreliable for assessing longitudinal asymmetry, and using the RGB-D camera's depth data can provide more reliable results.

Studies where the RGB-D camera is used to track markers also corroborate with the argument that working directly from depth data, by selecting joints or anatomical landmarks of interest and ignoring skeletal data, yield better results. As an example, Chakraborty and colleagues (2020) validated a marker based method that uses augmented reality markers (small cards similar to QR codes) to track and select data points directly from depth data against an optoelectronic motion capture reference system during treadmill walking. Chakraborty and colleagues (2020) also tested how errors in angular displacement change with two different camera positions: directly behind the participant or placed laterally (right side). They found that errors in angular displacements of the knee and hip joints were approximately 4° *(RMSE ≈ 4°)* when the RGB-D camera was positioned behind the patient and approximately 10° *(RMSE ≈ 10°)* when the RGB-D camera was positioned on the side, which represents an improvement in comparison with the study done by Xu and colleagues (2015) that used RGB-D camera's native skeletal data and obtained an error of approximately 12° *(RMSE ≈ 12°).*

Thus, when appraising available literature that validate RGB-D cameras for gait assessment, these devices are partially capable of evaluating spatiotemporal and kinematic variables using skeletal data (Clark, et al., 2013; Xu et al., 2015). By incorporating several RGB-D cameras with different viewpoints into a study design, skeletal data can be improved, making spatiotemporal and kinematic variables more reliable (Müller et al., 2017); however, the skeletal model has poor reliability when tracking the lower limbs (Geerse et al., 2015). When using the depth data directly researchers have shown improvements in data acquisition making kinematic variables more reliable than the skeletal model when compared to an optoelectronic motion capture system (Auvinet et al., 2017; Chakraborty et al., 2020).

2.4 Postural control and functional assessments

Researchers and clinicians commonly do postural control tests to investigate a wide number of disorders, as performance on these tests are linked to fall risk, ligament injury, chronic ankle sprains, and neurological disorders. Typically, these tests have only one outcome measure and are made visually by clinicians, which adds subjectivity and evaluates only one aspect of the patient's physical function (Vernon et al., 2015; Yang et al., 2014). While these assessments are useful for clinicians, they are prone to ceiling effects and are not capable of quantifying different movement strategies (Clark et al., 2012; Visser et al., 2008). Thus, using instrumented motion capture tools can help clinicians to objectively analyse a patient's movement better by assessing their movement strategy, and potentially helping discriminate between different populations (Clark et al., 2012; Jaspers et al., 2011).

In postural control research, RGB-D cameras have been used for various tasks to assess physical function and have been shown to have good validity, reliability and agreement against a reference motion capture system (Clark et al., 2012, 2015; Eltoukhy et al., 2018; Galna et al., 2014; Moreno et al., 2017; Yang et al., 2014). RGB-D cameras' native skeletal data had excellent concurrent validity for linear displacements of the joints of the hand, sternum, pelvis, knee, and ankle, and angular displacements of the trunk when validated against an optoelectronic system for three balance tasks: single leg balance, forward reach, and lateral reach (Clark et al., 2012). Yang and colleagues (2014) also found positive results when they validated the RGB-D camera's native skeletal data against an optoelectronic motion capture system of reference during another three standing tasks: single limb stance and double limb stance with feet together and feet apart. Yang et al. (2014) measured linear displacement and velocity of the participant's centre of mass (CoM), finding excellent reliability *($ICC_{2,1} > 0.88$)* between systems across all tasks. However, problems were reported for tasks with a smaller motion amplitude; the RGB-D camera's native skeletal data recorded lower velocities and the

CoM path trajectories were smoother than the reference system, thus indicating a lack of precision for tasks involving finer movements.

Postural control research investigating RGB-D camera validity on a young healthy population and an elderly clinical population found a positive outcome when collecting RGB-D camera native skeletal data for balance assessment (Eltoukhy et al., 2018). In Eltoukhy and colleagues' (2018) experiment, CoM excursion was measured on both populations during a single leg balance task and an ankle sway task with eyes open and closed. Eltoukhy et al. (2018) found excellent consistency, agreement and concordance on both groups (i.e., young and elderly) and across all explored variables: average sway length, CoM excursion and velocity along AP and ML movement planes; the only exception was average sway length for the elderly group, which obtained good consistency, moderate agreement and poor concordance *($ICC_{2,k} = 0.735$; $ICC_{3,k} = 0.568$; $r_c = 0.372$)*. In addition, Galna and colleagues (2014) investigated the RGB-D camera's temporal accuracy (e.g. cycle-to-cycle duration of hand clasping) and spatial accuracy (linear and angular displacements) during a series of functional tasks in people with Parkinson's disease (PD) and healthy controls in comparison to an optoelectronic system of reference. For both populations, temporal accuracy measurements had limits of agreement (LoA) less than 19.6%, excellent intraclass correlation *($ICC_{2,1} > 0.919$)* and excellent Person's correlation coefficients *($r > 0.950$)*, indicating excellent agreement and accuracy between systems. However, agreement and accuracy were overall considered poor for spatial accuracy. On healthy controls, LoA during standing trunk flexion and hand clasping tasks exceeded 134%, agreement between systems and accuracy levels were also low *($LoA > 134\%$; $r < 0.302$; $ICC_{2,1} < 0.301$)*, and similar trend was found on PD population *($LoA > 61\%$; $r < 0.487$; $ICC_{2,1} < 0.166$)*. Also, poor accuracy levels were reported across populations for angular displacements during standing trunk flexion, lateral trunk flexion, elbow flexion, shoulder flexion and abduction *($0.301 < ICC_{2,1} < 0.724$)*, and for linear

displacements during hand clasping and pronation supination tasks *(0.012 < $ICC_{2,1}$ < 0.699)*. Thus, these results show that the RGB-D camera's native skeletal data is valid to measure duration of tasks but not the joint angles and their linear displacements during the execution of finer movements, as for example, hand clasping.

Galna et al. (2014) findings are in agreement with a study done later on by Clark and colleagues (2015) using an RGB-D camera, where smaller amplitude movements were not correctly registered during double limb standing tasks, which might be due to the built-in RGB-D camera data filtering that smooths small oscillations (Clark et al., 2015, 2019). Clark and colleagues (2015) validated an RGB-D camera for a series of seven standing balance trials, finding good to excellent overall validity between the RGB-D camera and an optoelectronic motion capture system of reference, although, as the amplitude of the tasks got smaller, the RGB-D camera's validity decreased. Thus, the results ranged from good to excellent validity both for linear and angular displacements across all larger amplitude tasks: limits of stability, forward reach, lateral reach, single leg standing balance with eyes closed *(0.74 ≤ r ≤ 0.98)*. However, for finer movement tasks, linear displacements in the ML axis for single leg standing balance with eyes open, double leg standing balance with eyes open and with eyes closed were poor *(-0.18 ≤ r ≤ 0.62)*. Thus, these findings show that the RGB-D camera's native skeletal data is unsuitable for measuring small amplitude movements. Furthermore, the poor results on finer movements were attributed to the RGB-D camera's built-in algorithms that could filter out small oscillations (less than 2 mm) on skeletal data, creating a system less sensitive to small movements (Clark et al., 2015, 2019). Therefore, the unsatisfactory performance found are caused by the intrinsic characteristics of the RGB-D camera and the its native skeletal model (i.e., built-in filters), in addition, errors found in this study were also associated with the camera's position and poor detection of the anatomical landmarks and joint centres. For some of the performed tasks, such as standing trunk flexion, the RGB-D camera might have a better

performance if it were positioned at 45° laterally to the participant to avoid occlusions (Galna et al., 2014). While for other tasks, where the RGB-D camera's position was optimal, the RGB-D camera may achieve a better spatial accuracy results by implementing movement tracking methods that use RGB-D camera's depth data instead of its native skeletal data (Galna et al., 2014; Hotrabhavananda, et al., 2016; Schwarz, et al., 2012; Xiao, et al., 2012).

Moreno and colleagues (2017) compared kinematic variables of the trunk derived from skeletal data from an RGB-D camera against an inertial motion unit sensor (IMU) during two functional assessments: multidirectional reach test (MDRT) and timed-up-and-go test (TUG). This RGB-D camera used "Structured Light" to measure depth and produces skeletal data, similarly to the Kinect version one (Kinect v1). For the MDRT test, skeletal data and IMU data were strongly positively correlated, however, correlation was poor for TUG test during the walking phase *($r_{displacement} > -0.327$; $r_{velocity} > -0.083$)*. The authors attribute the poor performance on the TUG test during the walking phase to the camera's position, where participants moved too far away and too close to the camera's field of view limits, which is detrimental to the data collection accuracy (Moreno et al., 2017). Other possible problems that may have occurred, and have already been reported in the literature, are the RGB-D camera's native skeletal model's inability to detect turning (Ono & Takahashi, 2019) and the accuracy loss in the skeletal data when a person is moving from sitting to standing to walking, since the joints can be confused with the chair (Galna et al., 2014), or there could still be problems with the skeletal data between standing up from the chair, walking towards the turning point and returning towards the chair, since the RGB-D camera cannot detect turning (Hotrabhavananda et al., 2016; Ono & Takahashi, 2019). Thus, since the issues found are related with the skeletal data's inaccuracy, a logical step would be improving the automatic anatomical landmark detection algorithms, or using depth data directly to evaluate the desired movement tasks (Hotrabhavananda et al., 2016; Schwarz et al., 2012; Xiao et al., 2012).

In summary, skeletal data provided by RGB-D camera depth sensors, including Kinect's, built-in machine learning algorithm are valid for assessing balance and functional assessment of a number of tasks that have a large movement amplitude (e.g. single leg balance and single limb stance). For these tasks, the RGB-D camera's native skeletal data achieves good to excellent rates of agreement, validity, and correlation with gold standard motion capture systems for kinematic variables such as linear displacement and velocity of CoM, and body joints linear and angular displacements. In contrast, the RGB-D camera's native skeletal data was considered inadequate for measuring movements during tasks of smaller amplitudes, such as double limb stand balance test with eyes open, and in more complex functional assessments, such as TUG, which involves patients turning in front of the camera and standing up from a chair. Furthermore, the poor results obtained may be due to failures in the RGB-D camera's algorithm for detecting anatomical landmarks and body joints, since it was reported that the RGB-D camera cannot properly identify turning and can also mislabel people's limbs while sitting on a chair (Clark et al., 2015; Galna et al., 2014; Moreno et al., 2017; Ono & Takahashi, 2019). Therefore, improving the skeletal model, or finding alternative methods to identify and track anatomical landmarks using the RGB-D depth data is essential for improving the RGB-D camera's validity, specially during more complex tasks and the ones with small movement amplitude (Galna et al., 2014; Schwarz et al., 2012; Stone & Skubic, 2011; Xiao et al., 2012).

2.5 Anatomical evaluation

In general, performing anatomical evaluations are static in nature. In these evaluations, shape, volume, position and relationships between the anatomical parts assessed are important, for example, assessing acromial 3D spatial positions is important as they are used to calculate shoulder angles during spinal posture evaluation (Castro et al., 2017). Normally, this type of evaluation uses the RGB-D camera's depth data instead of its skeletal data, since researchers

are usually not interested in whole-body motion and joint locations, but are interested in the surface of the analyzed anatomical region.

A good example of anatomical evaluation is foot posture assessment, which is a potentially useful screening test for assessing injury risk and can also be used as a predictor of foot dynamics during gait (Mentiplay et al., 2013; Paterson, et al., 2015). Mentiplay and colleagues (2013) have validated an RGB-D camera for measuring foot posture against visual assessments and an optoelectronic motion capture system of reference. They used the RGB-D camera's depth sensor to evaluate five items of the foot posture index (FPI), which consists of checking anatomical characteristics of six different parts of the foot's anatomy; 1) if the talar head is medially or laterally positioned; 2) if the infra curvature shape of the malleoli are more concave or convex in comparison with supra curvature; 3) if the calcaneal plane is inverted or everted; 4) if the talo-navicular joint region is concave or the joint is bulging; 5) if the medial longitudinal arch is acutely angled or flat; and 6) if the forefoot is adducted or abducted in relation of rearfoot (Mentiplay et al., 2013). Mentiplay and colleagues (2013) could not use the RGB-D camera to assess the talar head, since there is no detectable difference on the anatomical surface of the foot for that item, and thus the talar head must be palpated. The RGB-D camera's validity and intra-rater reliability against the optoelectronic system and visual assessment were evaluated through Spearman's rho (ρ), finding moderate to good validity to identify four out of five anatomical landmarks of the foot $(0.51 \leq \rho \leq 0.85)$. Moreover, the RGB-D camera had a better intra-rater reliability in comparison to visual assessment $(0.62 \leq \rho_{\text{camera}} \leq 0.68;\ 0.17 \leq \rho_{\text{visual assessment}} \leq 0.63)$. Thus, despite the mixed results, the RGB-D camera has shown potential for assessing foot posture.

Another example of an anatomical evaluation done using an RGB-D camera, is a study done by Castro and colleagues (2017), where the RGB-D camera's depth data was used to acquire anatomical surface information to assess people's tendency of having scoliosis. The

authors performed a preliminary case study using the RGB-D camera to measure shoulder angulation during habitual standing posture and Adam's forward bending test in 98 participants with or without any clinically determined history of back injury (i.e., diagnostics and/or prescribed treatment), sports activity, and exposure to heavy loads. Participants' back, spine, scapular region, and the superior part of the sacrum iliac region were scanned and reconstructed as a 3D surface, then anatomical landmarks of interest (i.e., C7 and acromia) were manually selected for calculating the shoulder angle. Despite the study not validating the RGB-D camera against any device or visual assessment, the authors were successful in measuring patients' shoulder angles by applying their method and relating shoulder angles that are bigger than 1° with their patients' antecedents of back injury (injuries, treatments, sports activity and exposure to heavy loads). Thus, showing evidence of feasibility for a possible application of the RGB-D camera as an initial screening tool in clinics using only its depth data.

Another possible application for RGB-D cameras on spine biomechanics is to directly measure patients' thoracic kyphosis as in Quek and colleagues (2017). The researchers validated an RGB-D camera's depth data against a flexible ruler that molds to the shape of the participants spine (Flexicurve) to evaluate thoracic kyphosis during standing and sitting. The researchers found an excellent concurrent validity between methods *(ICC = 0.76–0.82)* with LoA below 10% during standing and sitting positions across all variables: thoracic kyphosis indices and angles (Quek et al., 2017), once again showing evidence of the usefulness of the RGB-D cameras for anatomical evaluation.

2.6 Summary

RGB-D cameras have been used in and validated for a variety of gait assessment tasks, postural control tasks, and anatomical assessments, with mixed results. Considering gait analysis, using skeletal data for assessing spatiotemporal variables seems adequate (Geerse et al., 2015), although tracking can be further improved by adding more RGB-D

cameras to the system (Müller et al., 2017). However, skeletal data cannot appropriately evaluate kinematic variables of gait (Xu et al., 2015), while studies that use markers to track movement for gait analysis are more successful (Chakraborty et al., 2020). In postural control tasks, it appears that the built-in skeletal model is adequate for collecting gross movement patterns (Clark et al., 2015), although during certain postural control tasks where fine movement patterns are of interest, the RGB-D camera performs poorly compared to optoelectronic motion capture systems (Clark et al., 2015). It also appears that using the depth data from the RGB-D camera rather than the skeletal model improves reliability (Clark et al., 2019). On anatomical assessments, RGB-D cameras have achieved high level of accuracy in comparison with visual assessments and optoelectronic motion capture systems (Mentiplay et al., 2013b), including spine curvature assessment (Quek et al., 2017).

CHAPTER 3 PURPOSE AND HYPOTHESIS

3.1 Purpose

The main motivation of this thesis project was to develop an inexpensive and portable tool capable of quantifying lumbar spine motion in the field using an RGB-D camera.

More specifically, the purpose was to create a novel framework that takes raw red-green-blue-depth (RGB-D) data and manipulates them to measure dynamic lumbar spine movement. This project is divided into two independent research studies: 1) the development and assessment of a method to track infrared (IR) reflective markers from raw depth data relative to gold-standard optoelectronic motion capture equipment for tracking lumbar spine motion (**Study 1**); and 2) further development of this algorithm by implementing deep-learning to segment regions of the back from the RBG-D camera data streams in order to segment and measure spine kinematics without the use of IR reflective markers (**Study 2**).

3.2 Hypothesis

Study 1: *Concurrent validity of a custom computer vision algorithm for measuring lumbar spine motion from RGB-D depth data* .

It was hypothesized that the RGB-D camera's depth sensor data would be valid for quantifying lumbar spine motion and would have an excellent level of agreement and reliability in comparison with the optoelectronic motion capture system.

Study 2: *Development and testing of a custom markerless deep learning algorithm for spine segmentation and motion assessment using RGB-D images.*

It was hypothesized that our artificial intelligence (AI) model would correctly segment and classify regions of the back and spine from RGB-D camera images in comparison with manually labelled ground truth images to allow for adequate quantification of lumbar spine kinematics without the use of IR reflective markers.

CHAPTER 4 CONCURRENT VALIDITY OF CUSTOM COMPUTER VISION ALGORITHM FOR MEASURING LUMBAR SPINE MOTION FROM RGB-D CAMERA DEPTH DATA

4.1 Abstract

Using RGB-D cameras as an alternative motion capture device can be advantageous for biomechanical spine motion assessments of movement quality and dysfunction due to their lower cost and complexity. In this study, we evaluated an RGB-D camera performance relative to gold-standard optoelectronic motion capture equipment; 12 healthy young adults (6M, 6F) were recruited to perform repetitive spine flexion-extension, while wearing infrared reflective marker clusters placed over their T_{10}-T_{12} spinous processes and sacrum, and motion capture data were recorded simultaneously by both systems. Custom computer vision algorithms were developed to extract spine angles from depth data. Root mean square error *(RMSE)* was calculated for continuous Euler angles, and intraclass correlation coefficients *($ICC_{2,1}$)* were calculated between minimum, maximum, and average range of motion angles in all movement planes. *RMSE* was low *($RMSE \leq 2.05°$)*, and reliability was excellent *($ICC_{2,1} \geq 0.889$)* across all movement planes. In conclusion, the proposed algorithm for tracking 3D lumbar spine motion during a sagittal movement task from one RGB-D camera is reliable in comparison to gold-standard motion tracking equipment. Future research will investigate accuracy and validity in a wider variety of movements, and will also investigate the development of novel methods to measure spine motion without using infrared reflective markers.

4.2 Introduction

Low back pain (LBP) is one of the most prevalent and costly musculoskeletal disorders in the world, affecting up to 80% of people at some point in their lifetime. While a small number of cases have a definitive diagnosis and associated treatment, the vast majority of cases are classified as non-specific, meaning there is no known pathoanatomical cause (Dillingham, 1995). For this group of patients, researchers and clinicians typically assess spine

movement quality during a set of movement dysfunction tests with the goal of classifying normal and abnormal (i.e., dysfunctional or harmful) movements (Silfies, et al., 2009; Biely, et al., 2014a). Clinical assessments often involve subjective visual appraisal of movement quality performed by a trained clinician; however, there is poor inter- and intra-rater reliability (Biely, et al., 2014; Fritz, et al., 2007; Hicks, et al., 2003; Stanton et al., 2011). Conversely, researchers in laboratory settings typically utilize optoelectronic motion capture to obtain objective measurements of spine movement quality; however, these systems are costly and technologically challenging, which limits their feasibility for use in clinics.

To overcome these challenges and improve clinical spine movement assessment, researchers have investigated the feasibility of alternative devices to objectively measure spine motion in clinics. For example, wearable inertial measurement units (IMUs) have been validated for tracking trunk motion and assessing spine neuromuscular control during repetitive trunk flexion-extension (FE) tasks (Beange et al., 2019), as well as for assessments of common clinical movement dysfunction tests (Bauer et al., 2015). It was established in these studies that spine range of motion (ROM) measurements were within or slightly above the clinical benchmark for accuracy of human movement tracking (i.e., < 2° error, or between 2° and 5° with additional subjective interpretation; McGinley et al., 2009), and that they were reliable for measuring typical movement dysfunction parameters (Bauer et al., 2015; Beange et al., 2019). While IMU performance is regarded as clinically acceptable for motion tracking, the sensors are subject to gravitational drift, and sensor location is also difficult to obtain (i.e., an IMU is only able to track *orientation* relative to itself, or another IMU). Many researchers attempt to track IMU location in global space (e.g., Ricci et al., 2016; Zimmermann et al., 2018); however, these procedures are computationally expensive and advanced, and are dependent on careful IMU-to-segment placement and calibration techniques. Some commercially available devices are capable of providing estimates of lumbar spine range of motion (ROM) and movement

quality in clinical settings (e.g., DorsaVi Professional Suite; DorsaVi, Victoria, AUS); however, these systems come with proprietary motion-tracking algorithms, which are prohibitive for conducting custom assessments of spine movement quality and dysfunction. As an alternative, researchers are exploring the use of depth sensors for tracking people's movement, as these sensors are able to provide position and orientation data, and it is possible to customize methods of movement assessment from raw depth data.

RGB-D cameras are gaining popularity as an alternative method for motion tracking in clinical and research settings. These cameras use their depth data stream and native machine learning algorithms to locate pre-defined joint centres for tracking full-body motion (aka the built-in "skeletal model"). RGB-D cameras are less expensive and require less time than traditional optoelectronic motion capture equipment for tracking human motion, and they can be easily installed within clinical settings. The performance and implementation of these cameras have been studied for the assessment of various experimental and clinical outcome measures relative to gold-standard motion tracking equipment, such as: 1) clinical measurements of motor function and postural control (Auvinet et al., 2017; Clark et al., 2012; Otte et al., 2016); 2) spatiotemporal gait parameters during ground and treadmill walking (Auvinet et al., 2017; Dolatabadi et al., 2016); and 3) spatial accuracy (i.e., location and orientation) of landmarks during various movement tasks (Cippitelli et al., 2015; Macpherson et al., 2016; Otte et al., 2016).

The majority of studies that utilize RGB-D camera systems for tracking human motion achieve adequate results using the integrated skeletal model (Clark et al., 2013; Dolatabadi, et al., 2016; Otte et al., 2016). Specifically, Otte et al. (2016) found excellent reliability while evaluating the spatial accuracy of RGB-D cameras for clinical assessments of whole body motion, obtaining nearly perfect correlation ($r > 0.99$) with optoelectronic motion capture when tracking "spine base" (approximately L_5/S_1), "spine mid" (approximately T_{12}/L_1),

and "spine shoulder" (approximately T_4) landmark locations (as defined by the native skeletal model) in the sagittal plane, strong correlation in the frontal plane *($r \geq 0.85$)*, and moderate correlation in the transverse plane *($0.46 \leq r \leq 0.70$)*. Clark et al. (2012) compared measurements of spinal posture between the skeletal data relative to optoelectronic motion capture equipment; pairwise comparison of *ICCs* showed no significant differences between devices during single leg balance and both lateral and forward reach, and correlation between systems was very strong across all movement axes *($0.93 < r < 0.99$)*. Lastly, Dolatabadi and colleagues (2016) evaluated the performance of the native skeletal model in estimating spatiotemporal gait parameters (e.g., stance time, step time, step length, and velocity) relative to optoelectronic motion capture, and achieved good to excellent reliability between systems ($0.73 \leq ICC_{2,1} \leq 0.98$). Researchers in these studies recorded data using a frontal view of the participants; however, for evaluating lumbar spine movement tasks, the camera must be positioned in a posterior-anterior view (i.e., behind the participant) to capture the anatomical landmarks of interest, which restricts the ability to use the built-in skeletal model. Thus, development of custom motion tracking algorithms from raw depth data are necessary for clinical assessment of lumbar spine motion. Prior to clinical integration, these algorithms must be validated relative to gold-standard motion tracking equipment to meet the clinical benchmark for human motion tracking.

In a meta-analysis conducted by Cuesta-Vargas and colleagues (2010) concerning the use of IMUs as an alternative for human motion tracking, it was concluded that IMUs should be considered only as a tool, and that their validity for tracking human movement is task- and site-specific, and also heavily dependent on the specific pre-/post-processing algorithms used to assess motion from raw sensor data (Cuesta-Vargas et al., 2010). Applying the same premise to RGB-D cameras, they are tools for tracking motion, and, therefore, it is necessary to evaluate their performance according to the same standard.

Some researchers have developed custom methods of tracking human motion from raw RGB-D camera depth data and achieved adequate results. Macpherson and colleagues (2016) positioned the RGB-D camera behind participants and recorded depth data in order to measure pelvis and trunk kinematics during treadmill locomotion, finding moderate to very strong correlations *(0.3 < r < 0.9)* during walking and running. Similarly, Cippitelli and colleagues (2015) developed a method using the RGB-D camera's depth sensor to measure changes in full-body positioning using sagittal plane views, and achieved superior performance of their method over the built-in skeletal model when compared to gold-standard optoelectronic motion capture (Cippitelli, et al. 2015). Lastly, Auvinet et al (2017) developed a custom framework to extract lower extremity kinematics from the RGB-D camera's depth data (using both frontal and posterior view points) to measure intersegmental coordination and gait asymmetry during treadmill walking. Results for this study showed excellent correlation between the RGB-D camera's depth data and gold-standard optoelectronic motion capture equipment when measuring gait asymmetry from both view points; however, intersegmental coordination computed with the RGB-D camera's skeletal data was not reliable (Auvinet et al., 2017).

Of the aforementioned studies, two looked at trunk kinematics using the built-in skeletal model (i.e., Clark et al., 2012; Otte, et al., 2016), and one looked at lower back kinematics using custom motion tracking algorithms (i.e., Macpherson et al., 2016). To the best of authors' knowledge, there are no studies validating RGB-D camera depth data against an optoelectronic motion capture system when comparing lumbar spine motion during a dynamic trunk FE task; therefore, the goal of this study was to develop and validate a computer vision method to track lumbar spine motion from an RGB-D camera's depth data using infrared (IR) reflective markers during a repetitive FE task relative to gold standard optoelectronic motion capture equipment. Based on results from previous studies, as well as previous work that evaluated the performance of wearable IMUs for spine motion tracking using similar methods, it was

expected that the RGB-D camera would achieve a similar level of performance (i.e., low root mean square error (*RMSE*) for continuous angles and excellent reliability when measuring minimum (min), maximum (max), and ROM angles).

4.3 Methodology

4.3.1 Participants

Twelve healthy adults (6M/6F) were recruited from the general university population via poster-advertising and word of mouth. Participant demographics are reported in Table 4.1. Participants who were unable to complete the trunk movement tasks without experiencing pain or fatigue, and participants who had suffered from a low back injury within six months prior to data collection were excluded from this study.

Table 4.1 *Mean (SD) Participants Demographics.*

	Height (cm)	Weight (kg)	Age (years)	BMI (kg/m2)
Male	176.2 (5.2)	77.4 (2.6)	26.7 (6.0)	25.0 (1.6)
Female	163.4 (6.1)	55.4 (11)	21.3 (2.5)	20.6 (2.9)
All	169.8 (8.6)	66.4 (14)	24.0 (5.2)	22.8 (3.2)

All participants were recruited from the general university population. All participants met the inclusion criteria outlined on participant information letter (Appendix A). SD = standard deviation; BMI = body mass index.

4.3.1.1 Consent

Participants received a copy of the research consent form prior to their involvement in the study. Researchers also provided a verbal explanation of the study at the time of participation. Any questions or concerns were addressed prior to obtaining informed consent. Participants were informed that they were able to withdraw at any point in the study.

4.3.1.2 Participant Preparation

Prior to data collection, participants were asked to change into custom-made motion capture spandex clothing. Once the participant had changed, demographic information (i.e., age and sex) were recorded, and anthropometric (i.e., height and weight) data were collected using a physician scale (Detecto 339, Detecto, USA). Passive IR reflective marker

clusters (12.7 mm, B & L Engineering, USA) were placed superficial to the T_{10}-T_{12} vertebrae (i.e., “trunk”) and the sacrum (i.e., “pelvis”; Figure 4.1).

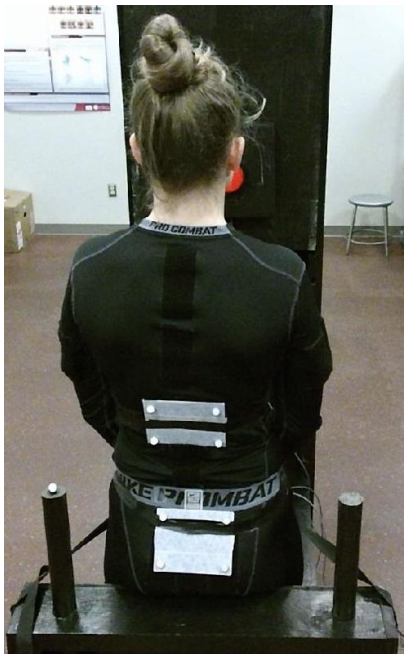

Figure 4.1 *Marker placement and experimental setup.*

4.3.2 Equipment and Experimental Setup

During the data collection session, kinematic data were collected simultaneously from one RGB-D camera (Kinect v2, Microsoft Corporation, Redmond, WA, USA) at 30 Hz and a 10-camera motion capture system (Vantage V5, Vicon, UK) at 120 Hz. The RGB-D camera was positioned 1.0 m behind the participant at a height of 1.70 m, with the camera pointing 30º downward from the horizontal towards the participant’s back (Figure 4.2). This camera position allowed adequate visualization of the participant’s back during execution of the movement task, avoiding camera occlusions and ensuring the detection of their full range of motion. The RGB-D camera’s depth data were captured using the “Kinect Image Acquisition Toolbox” from MATLAB (R2018b, The MathWorks Inc., USA). To synchronize both the RGB-D camera and the optoelectronic motion capture systems, a common temporal event was created by moving a passive IR reflective marker placed behind the participant to signal start time.

4.3.3 Task Protocol

Participants performed 35 cycles of trunk FE at a rate of 30 beats/minute controlled by a metronome (i.e., 15 cycles/minute) while constrained at the hip, thus ensuring the measured ROM represents trunk movement FE exclusively, instead of a combination of the lower limbs, pelvis, and trunk movement. To control for ROM, participants touched targets placed at specific locations with arms outstretched in front of them; one target was located 50 cm anteriorly at knee height, positioned parallel with the floor, and the other at shoulder height and at arm's length away, positioned perpendicular to the floor (Beange et al., 2019; Granata & England, 2006). One cycle was defined as the participant moving from standing position (touching shoulder height target), into forward flexion (touching knee height target), and back to standing (touching shoulder height target; Figure 4.2).

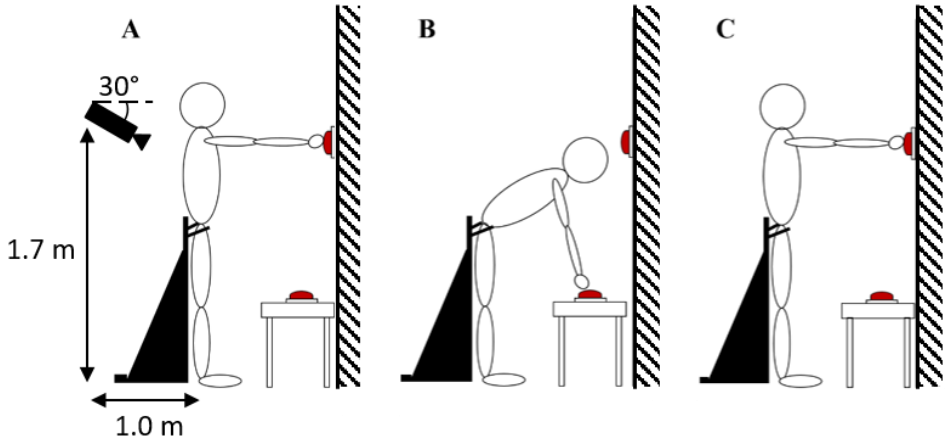

Figure 4.2 *Experimental setup and task protocol. (A) Participants begin in upright standing position with arms outstretched in front of them; then, (B) participants move into full flexion; and finally, (C) participants return to upright standing position for the completion of one full cycle.*

4.3.4 Data Analysis

To compare spine kinematics between systems, each system underwent identical post-processing for direct comparison. For the RGB-D camera's depth data, an additional step was required that involved a series of image processing algorithms to track the 3D location of IR reflective markers from depth data. Additionally, optoelectronic motion capture system data were downsampled to ensure the trials for each system were equal-length. Lastly, data from

both systems were filtered using an effective 4th order low-pass Butterworth filter, with a cut-off frequency of 2 Hz.

4.3.4.1 Depth Image Processing Algorithm

Several steps were involved in the custom-developed computer vision algorithm; these included: 1) manually selecting a region of interest from the depth images where IR reflective markers would be likely to appear throughout the video; 2) applying a logical operator on each image to find pixels that had value equal to zero (indicating reflection of IR reflective light and therefore the presence of markers); 3) filtering pixel regions based on their properties (i.e., major axis length and area), which must match IR reflective markers size and shape (i.e., 12.7 mm diameter sphere; this was done using the *"regionprops"* function in MATLAB); 4) calculating marker *(x,y)* global coordinates based on the centroid position of each pixel region *(i,j)* on the image plane; and finally 5) calculating marker *(z)* global coordinates based on the average of the pixel values in the vicinity of each pixel region. This process produced 3D global coordinates *(x,y,z)* for each IR reflective marker.

4.3.4.2 Kinematics

Both systems underwent identical calculation of lumbar spine kinematic variables for direct comparison. First, individual local coordinate systems were defined using trunk and pelvis marker clusters; individual markers were labelled: T_{Rupper}, T_{Rlower}, T_{Lupper}, T_{Llower}, P_{Rupper}, P_{Rlower}, P_{Lupper}, and P_{Llower} (Figure 4.3; where T and P refer to trunk and pelvis marker clusters, respectively, and subscripts R and L represent right and left markers, respectively, when facing the participants' back). The origin of the trunk cluster was defined at T_{Rlower}. To create the mediolateral x-component of the trunk, a unit vector $\hat{\imath}$ was defined using Equation 4.1. Next, an auxiliary vector $\hat{v}$ was created as a temporary y-component unit vector (i.e., superior direction; Equation 4.2). This vector was used to create the z-component unit vector $\hat{k}$ (i.e., posterior direction), which was defined as the cross product between $\hat{\imath}$ and

$\hat{v}$ (Equation 4.3). Finally, the y-component unit vector $\hat{j}$, was adjusted by taking the cross product between $\hat{k}$ and $\hat{\imath}$ (Equation 4.4).

$$\hat{\imath} = \frac{T_{Llower} - T_{Rlower}}{\|T_{Llower} - T_{Rlower}\|} \tag{4.1}$$

$$\hat{v} = \frac{T_{Rupper} - T_{Rlower}}{\|T_{Rupper} - T_{Rlower}\|} \tag{4.2}$$

$$\hat{k} = \hat{\imath} \times \hat{v} \tag{4.3}$$

$$\hat{j} = \hat{k} \times \hat{\imath} \tag{4.4}$$

The resulting right-handed rotation matrix (Equation 4.5) describes the orientation of the rigid body in 3D global space:

$$R_{Trunk} = \begin{bmatrix} \hat{\imath}_x & \hat{\imath}_y & \hat{\imath}_z \\ \hat{j}_x & \hat{j}_y & \hat{j}_z \\ \hat{k}_x & \hat{k}_y & \hat{k}_z \end{bmatrix} \tag{4.5}$$

This process was repeated for the pelvis cluster (i.e., the origin is defined as P_{Rlower} , and the rotation matrix R_{Pelvis} is obtained identically). A rotation matrix describing relative motion between trunk and pelvis marker clusters was calculated, and Euler angles were extracted using an X-Z-Y rotation sequence (corresponding to FE-lateral bend (LB)-axial twist (AT) axes).

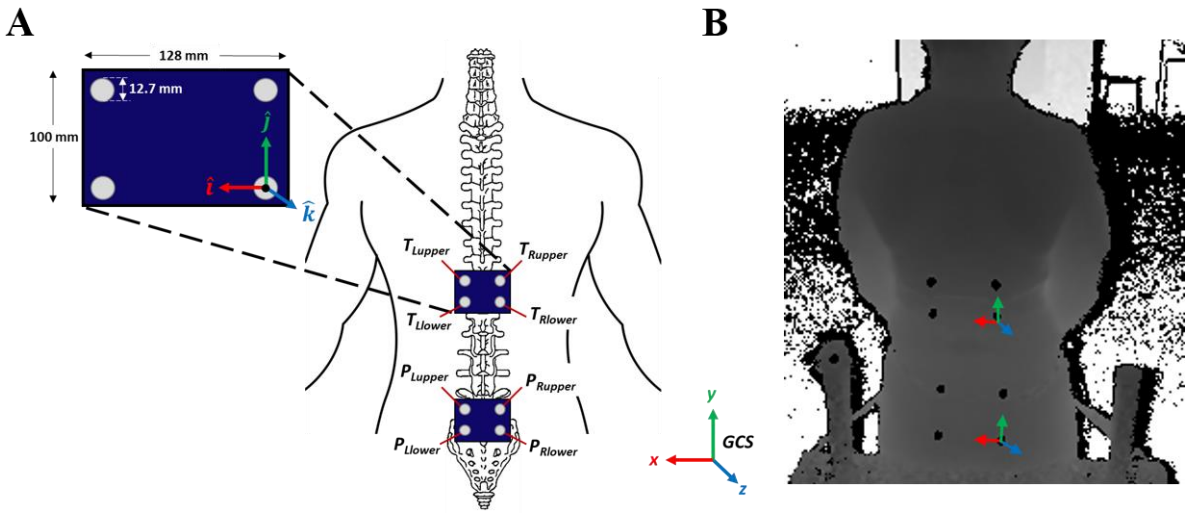

Figure 4.3 *Infrared reflective marker setup. (A) Trunk and pelvic marker clusters with individual marker labels. The trunk marker cluster with local coordinate system is shown in the zoomed in image. The global coordinate system is shown in the bottom right. (B) Depth image with local coordinate systems defined over each marker cluster.*

4.3.4.3 Range of Motion

To obtain lumbar spine ROM (i.e., trunk relative to pelvis), the following steps were taken: 1) the FE, LB, and AT time-series' were divided into individual movement cycles by identifying peak angles (which correspond to upright standing) in the FE plane; then, 2) each individual cycle was normalized to 101 data points (i.e., 0-100% of the cycle); next, 3) the mean ensemble curve (representing the average movement across all cycles) was obtained by calculating the mean angle across all cycles, at each percentage of the movement; and finally 4) FE, LB, and AT ROM were calculated according to Equations 4.6 - 4.8.

$$ROM_{FE} = \left|\theta_{max}^{FE} - \theta_{min}^{FE}\right| \quad (4.6)$$

$$ROM_{LB} = \left|\theta_{max}^{LB} - \theta_{min}^{LB}\right| \quad (4.7)$$

$$ROM_{AT} = \left|\theta_{max}^{AT} - \theta_{min}^{AT}\right| \quad (4.8)$$

4.3.5 Statistical Analysis

To quantify the magnitude of error of the RGB-D camera relative to optoelectronic motion capture system, *RMSE* was calculated across the entire trial; two-way random intraclass correlation coefficient's ($ICC_{2,1}$) were used to assess reliability between min, max, and ROM angles, and Bland-Altman plots were constructed to assess absolute agreement between ROM

measurements obtained by each system. All statistical analyses were performed using SPSS statistical software for windows (SPSS 23, IBM Corporation, USA).

4.4 Results

RGB-D camera and optoelectronic motion capture system relative lumbar spine angles were extracted and compared. *RMSE* of continuous planar angles, and $ICC_{2,1}$*'s* of min, max, and ROM angular measurements were used to quantify performance of the RGB-D camera depth data and proposed image processing algorithms relative to the optoelectronic motion capture system. Overall, our method of extracting angles from RGB-D camera's depth data produced very low *RMSE* in comparison with optoelectronic motion capture system *($RMSE_{FE}$ = 2.05° ± 0.97°; $RMSE_{LB}$ = 0.65° ± 0.37°; $RMSE_{AT}$ = 0.84° ± 0.38°)*. Mean ensemble curves (i.e., representing the average motion across all cycles and across all participants) and associated standard deviations *(SDs)* were plotted for visual appraisal (Figure 4.4).

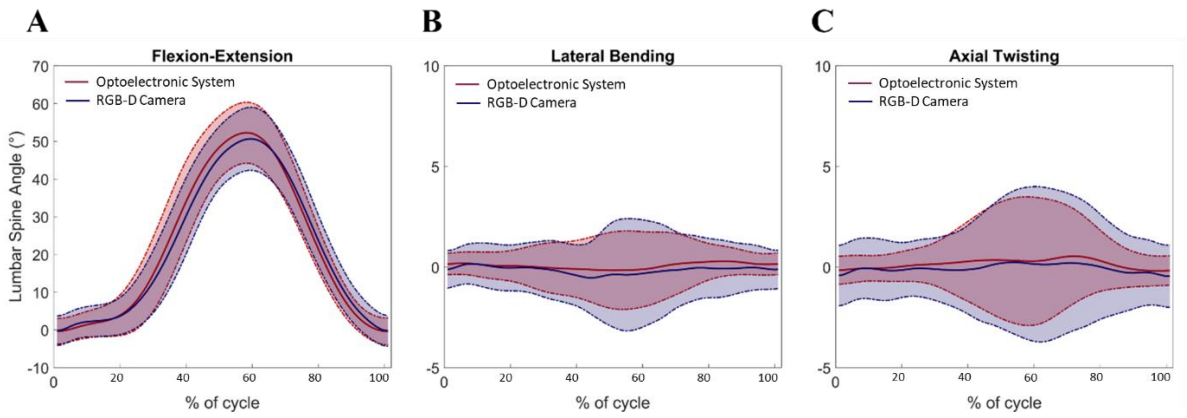

Figure 4.4 *RGB-D camera (blue) vs optoelectronic motion capture system (red) averages (solid) and standard deviations (dashed) of the lumbar spine joint angle of A) flexion-extension, B) lateral bending, and C) axial twisting movement axes. Y-axis range for B) and C) are different than A) for better visualization.*

Cycle-to-cycle min, max, and ROM angles and their respective SDs from both systems were calculated and directly compared; they are organized and presented in Table 4.2. For analysis of reliability between systems, $ICC_{2,1}$'s for relative min, max, ROM angles of cycle-to-cycle data were compared across FE, LB, and AT movement axes, and exhibited

excellent reliability *($ICC_{2,1} \geq 0.849$)* in comparison with gold standard motion capture equipment; specific results are listed in Table 4.3. Bland-Altman plots were also constructed to identify any instrument bias when measuring planar ROM (Figure 4.5); these plots show that the RGB-D camera systematically underestimated ROM in the FE plane, and overestimated ROM in the LB and AT planes.

Table 4.2 *Mean (SD) relative cycle-to-cycle range of motion, and minimum and maximum angles.*

	Flexion-Extension		**Lateral Bending**		**Axial Twisting**	
	Optoelectronic	**RGB-D**	**Optoelectronic**	**RGB-D**	**Optoelectronic**	**RGB-D**
ROM	53.4° (7.7°)	51.5° (7.6°)	1.9° (1.0°)	2.5° (1.4°)	2.7° (1.8°)	3.0° (1.4°)
max	52.9° (8.6°)	51.2° (8.5°)	0.9° (1.2°)	1.0° (2.0°)	1.5° (1.6°)	1.4° (2.4°)
min	-0.4° (3.5°)	-0.3° (4.1°)	-1.0° (1.1°)	-1.5° (1.6°)	-1.2° (2.3°)	-1.6° (2.7°)

ROM = range of motion; max = maximum; min = minimum; SD = standard deviation.

Table 4.3 *Reliability analysis ($ICC_{2,1}$; 95% CI lower-upper) between the optoelectronic motion capture system and the RGB-D camera lumbar spine angles.*

		Flexion-Extension	**Lateral Bending**	**Axial Twisting**
$ICC_{2,1}$	*ROM*	0.979 (0.453-0.996)	0.889 (0.290-0.973)	0.898 (0.654-0.970)
	max	0.973 (0.851-0.993)	0.914 (0.700-0.975)	0.849 (0.460-0.957)
	min	0.930 (0.754-0.980)	0.865 (0.521-0.961)	0.921 (0.736-0.977)

ROM = range of motion; max = maximum; min = minimum; $ICC_{2,1}$ = intraclass correlation coefficient; CI = confidence interval.

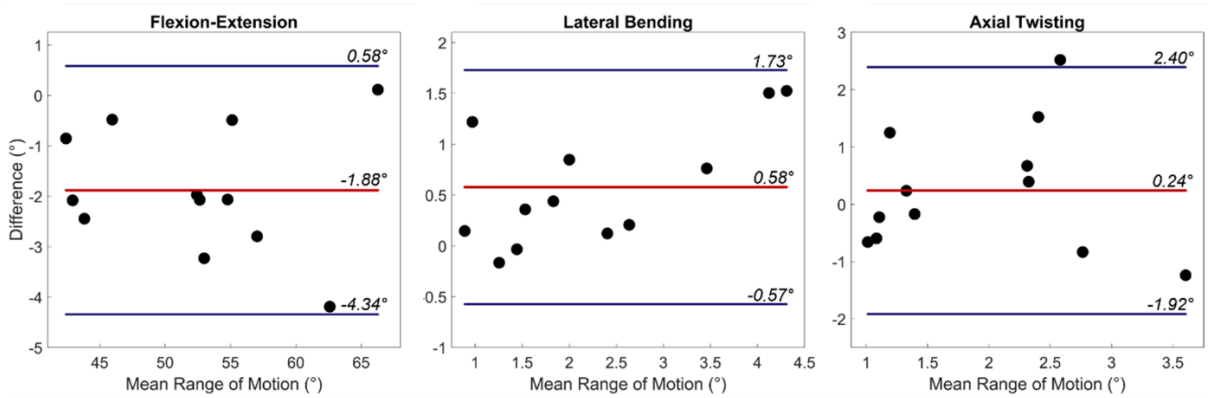

Figure 4.5 *Bland-Altman plots for lumbar spine range of motion measurements between the optoelectronic motion capture system and RGB-D camera. The red lines represent mean measurement difference between systems, and the blue lines represent mean ± 1.96SD (standard deviation).*

4.5 Discussion

In this study, we developed a custom image-processing method to track lumbar spine motion from one RGB-D camera depth data during repetitive spine FE, and we were able to show that our method performs well when compared to a gold-standard optoelectronic motion capture system. *RMSE* of continuous motion, and absolute agreement and reliability of lumbar spine angular measurements were assessed across all movement axes between systems. Overall, our method of tracking lumbar spine motion from RGB-D camera's depth data produced low *RMSE (RMSE* $\leq 2.05° \pm 0.97°$*)* with optoelectronic motion capture system data. Although *RMSE* was highest overall in the FE plane, the error as a percentage of total ROM was lowest (i.e., ~ 9.0%); percentage error in the LB and AT planes was relatively high (i.e., > 40%), but this is likely due to random measurement noise (Beange et al., 2019). $ICC_{2,1}$*'s* were also excellent between systematic measurements of min, max, and ROM angles; it was best in the FE plane (i.e., along the main axis of movement; $ICC_{2,1,FE} \geq 0.930$), and slightly worse (but still excellent) in LB and AT planes *(*$ICC_{2,1,LB} \geq 0.865$*;* $ICC_{2,1,AT} \geq 0.849$*).* Lastly, upon observation of the Bland-Altman plots, it is evident that overall measurement agreement between systems is excellent, but there is some systematic error when measuring ROM; nevertheless, this difference is within the acceptable limits for clinical motion tracking (i.e., less than 2°). These results combined show that using RGB-D cameras is a realistic and feasible option for clinical motion capture of the spine.

Similar to the current study, Macpherson and colleagues (2016) tracked an RGB-D camera's depth data with a custom developed algorithm that identified the centroid of individual IR reflective markers. They compared linear and angular displacements of the trunk and pelvis between the RGB-D camera and the optoelectronic motion capture system during walking and running on a treadmill. While correlations between linear displacements were very strong to nearly perfect, correlations of angular displacements ranged from moderate to strong.

It is likely that their methods to obtain angular displacement from linear marker trajectories lacked the sophistication needed to accurately obtain these angles in the presence of trigonometric noise. Macpherson and colleagues (2016) utilized only 4 IR reflective markers (placed over the right and left posterior superior iliac spines and bilaterally over the 10^{th} rib) to track motion of the trunk and pelvis, and for each marker, a 42-point rectangular cloud was superimposed onto the image surrounding the marker. The mean marker depth was used as the camera-marker distance (i.e., anterior-posterior direction), and the medial-lateral and superior-inferior locations of the marker were calculated using trigonometry and manufacturer information regarding the field of view. To calculate angular positions, vectors joining left-sided and right-sided markers were created (representing the FE plane axis), and the projected angles of these vectors on the LB and AT planes were recorded for the trunk and pelvis rotations. This process was vastly different than the method proposed in our study, with the main difference being that they utilized synthetic superimposed marker data to track angular positions. The use of synthetic data was necessary in their study as their marker setup involved only 2 markers per anatomical region (their marker tracking algorithm was unable to discern more closely positioned markers). We believe that the method used in the current study performed better as it did not involve the use of synthetic markers, and the process for obtaining rotations from rigid-body marker clusters placed over the trunk and pelvis has been used extensively in literature (Beange et al., 2019; Mavor & Graham, 2015; Ross, et al., 2015). Additionally, Macpherson and colleagues (2016) used a different RGB-D camera, the Kinect v1, which was a previous version of the system; our study used the Kinect v2 which has been proven to have better accuracy and precision when tracking motion (Samir et al., 2016; Wasenmüller, 2016). Lastly, Macpherson and colleagues' (2016) movement protocol for the involved fast-paced treadmill running, which can cause excess skin-motion artifact noise at heel contact, and can affect motion tracking; we believe that our

movement protocol is less strenuous and therefore likely to avoid excessive noise caused by skin-motion.

While the results from the current study are promising, there are some limitations to consider. First, the spatial resolution of the selected RGB-D camera decays with distance (Yang et al., 2015); as such, there may be increased error (and poorer agreement and reliability) as a direct result of the nature of the given task (i.e., as the participant moves farther away into a fully flexed position, spatial resolution decays). To address this in future studies, the utilization and synchronization of two or more RGB-D cameras that are capable of recording the full capture volume with high-quality spatial resolution may be a feasible option. This may also help to reliably capture more complex movements in future studies (e.g., repeated LB, multidirectional movements, etc.). Additionally, the pre-programmed capture frequency for the selected RGB-D camera is 30 Hz, which is much lower than the collection frequency used for the selected optoelectronic motion capture system in this study (i.e., 120 Hz). This has potential to result in discrepancies between systematic measurements of ROM, as operating at a lower frequency can result in missing data/missing phenomenon (e.g., peak angles may occur between frames). Unfortunately, the collection frequency is imbedded in the selected RGB-D camera and cannot be modified, so it is an inherent limitation that cannot be improved. Nevertheless, given that the frequency of the movement protocol in the current study is low, we believe that a capture frequency of 30 Hz is sufficient. Lastly, this study aimed to validate the use of RGB-D cameras as quantitative tools for measuring spine kinematics during a repetitive trunk FE task on healthy participants; in order to be considered feasible for clinical motion tracking of the spine in people with LBP, it must first be validated on LBP patients. Overall, this study generates evidence of low levels of error, and excellent agreement and reliability between systems, making it a feasible option for lumbar spine motion tracking in clinical settings.

4.6 Conclusion

In conclusion, the proposed method had excellent performance (i.e., low error and excellent agreement and reliability) for tracking lumbar spine motion using RGB-D camera's depth data in a standardized setting compared to optoelectronic motion capture equipment; thus, the proposed method can be considered as a valid method for quantifying lumbar spine movement using one RGB-D camera. Future studies should investigate the validity of using RGB-D cameras to track human movement in a wider variety of settings (i.e., other camera positions and angles), during additional movement tasks (e.g., repeated LB and AT, and activities of daily living), and on clinical populations. Furthermore, future studies should develop deep learning methods to segment and classify trunk/spine anatomical landmarks, allowing similar kinematic analysis to be done without the use of IR reflective markers.

CHAPTER 5 DEVELOPMENT AND TESTING OF A CUSTOM MARKERLESS DEEP LEARNING ALGORITHM FOR SPINE SEGMENTATION AND MOTION ASSESSMENT USING RGB-D IMAGES

5.1 Abstract

SpineNet, a four-module deep learning network that uses infrared and depth (i.e., colourized and surface normal) data from an RGB-D camera, was developed to segment a participant's back into spine, upper back and lower back classes and calculate lumbar spine kinematics during a repetitive trunk flexion-extension task. To train SpineNet, a dataset containing videos of 15 participants performing the task under two different labelled conditions (unmarked and marked) was created. An 80:20 training and testing ratio with marked participants was used; five unmarked participants assessed generalizability. Image segmentation achieved high levels of accuracy and similarity no matter what type of RGB-D camera data was used as input (i.e., infrared, colourized, surface normal or fused data). Lumbar spine kinematics (i.e., ROM) extracted from SpineNet were appropriate in the flexion-extension movement axis, but performed poorly in the lateral bend axis for marked participants. Average ensemble curves of lumbar spine kinematics of unmarked participants presented profiles (i.e. shape, timing, and peaks) that are comparable with previous research where similar data were collected.

5.2 Introduction

Clinicians assess dysfunction in low back pain (LBP) by quantifying a patient's movement quality (Silfies et al., 2009; Biely et al., 2014a), since aberrant movement patterns are associated with low back dysfunction (Delitto et al., 1995; Ashouri et al., 2017; Mokhtarinia et al., 2016). Movement quality evaluations are often undertaken by a trained clinician through visual assessments or are self-reported by the patient using questionnaires (Lebel et al., 2013), but these approaches are subjective and have low reliability (Hicks et al., 2003;

Stanton et al., 2011; Spinelli et al., 2015). In laboratory environments, objective optoelectronic motion capture systems have been used to classify LBP patients based on their movement patterns (Hemming et al, 2018). Although these devices would profoundly improve clinical assessment of LBP, their complexity, transportability, and costs prove to be significant barriers to clinicians (Zhou & Hu, 2008).

RGB-D cameras are gaining popularity as an alternative motion capture tool. These devices use their depth data stream and an artificial intelligence algorithm (i.e., "randomized decision forest") to identify anatomical landmarks of a human in images without using markers to locate joint centres, generating a native "skeletal model" for tracking whole-body motion. Previous research using the RGB-D camera's skeletal data has found it to be valid for gait analysis (Geerse et al., 2015), postural control assessments (Clark et al., 2012), evaluating motor control function (Otte et al., 2016) and ergonomics (Plantard et al., 2017). Although deemed valid, it is noted that the RGB-D camera's native skeletal model is not suitable for fine movement tasks such as those found in some postural control tasks (Clark et al., 2012). Using only the depth data, researchers have found increased reliability when calculating angular displacement of the thigh and shank during treadmill walking compared to the skeletal model when comparing both models to an optoelectronic motion capture system (Auvinet et al., 2017). Researchers have also validated the RGB-D camera's depth data for anatomical evaluations: Mentiplay et al. (2013b) validated foot posture evaluations against visual appraisal, and Quek et al. (2017) have successfully used it to detect scoliosis. In our previous work, we validated three-dimensional (3D) lumbar spine kinematics calculated using depth data collected from a single RGB-D camera against an optoelectronic motion capture system using infrared (IR) reflective markers (See Chapter 4). Using the RGB-D camera's depth data allows for a posterior-anterior camera view and avoids the skeletal model's limitations of only having three reference points for the entire spine: "spine base"

(approximately L_5/S_1), "spine mid" (approximately T_{12}/L_1), and "spine shoulder" (approximately T_4), which wouldn't allow for the calculations of 3D lumbar spine kinematics. Although, our previous research achieved low RMSE values *($RMSE \leq 2.05°$)* and high $ICC_{2,1}$ values *($ICC_{2,1} \geq 0.849$)* between motion capture devices, it would be more advantageous for clinicians and their patients if a markerless motion capture method were available.

Image semantic segmentation using Convolutional Neural Networks (CNN) is a Deep Learning technique that has the potential to automatically identify and track unmarked anatomical landmarks of the human back using images from RGB-D cameras. This is a very popular and promising method, which has been used in several applications, such as scene understanding in urban traffic images (Kim et al., 2020) and segmentation of anatomical structures in x-rays (Novikov et al., 2018). To do semantic segmentation using RGB-D cameras, some authors take advantage of these cameras multiple data streams (i.e., Colour and IR) and its depth sensor, encoding the depth data and fusing it with other data streams throughout the AI's architecture (Eitel et al., 2015a; Gupta et.al., 2014; Hazirbas et al., 2017; Rahman et al., 2017). Encoding depth data has been a successful approach to convert high-precision[1] grey-scale depth images to lower-precision[2] RGB colour images. For example, Gupta and colleagues (2014) improved object detection and segmentation on indoor scenes when they encoded surface normal information based on depth data and used it as input on a Depth CNN to extract the object's features, and Eitel and colleagues (2015) found a promising alternative depth encoding method when they mapped depth data into a jet colormap, obtaining

[1] Depth data from the selected RGB-D camera are 13-bit (0-8000) single channel images of 512 by 424 pixels. While its colour images are 8-bit, three channel RGB images of 1920 by 1080 pixels.

[2] "Colourized" depth data for this work were 8-bit (0-255) three channel (red, green, blue) images of the same image dimensions. Nominally this gives 24-bits of data per pixel and any fixed mapping of depth to colours should be sufficient to encode the depth data per pixel without loss.

high accuracy results that were comparable to surface normal depth encoding when used on their object classification CNN. Some CNN implementations adopt data fusion techniques that combine the RGB-D camera's multimodal data. Rahman and colleagues (2017) created a CNN that combined three RGB-D camera's data streams (i.e., RGB, and two modalities of encoded depth data; encoded jet colourmap and 3D surface normal), with a late Fusion module, which merges three RGB data stream feature maps to classify household objects. Rahman et al (2017) compared their AI architecture and data encoding techniques against a state-of-the-art Nonlinear Support Vector Machines (SVM) object recognition model that uses RGB-D data (Lai et al. 2011), Cascaded Ensembles of Randomized Decision Trees (CaRFs) (Asif et al., 2015), and a convolutional-recursive deep learning method (CNN-RNN), which is a combination of CNN and Recurrent Neural Network (RNN) implementation (Socher et al., 2012). Their results had an accuracy of 92.1 ± 1.3 %, which was superior to the compared methods that achieved accuracy levels between 83.9 ± 3.5 % and 91.3 ± 1.4 %. Another example of an architecture that applies data fusion was created by Hazirbas and colleagues (2017), which used semantic segmentation to classify indoor scenes using Colour images from RGB data stream and unencoded depth data. Their AI architecture used RGB and depth data as inputs and implemented a "slow fusion" method, where depth and RGB feature maps where merged all along its architecture, improving the AI model accuracy and similarity compared to using RGB data or depth data exclusively (Hazirbas et al., 2017).

To break down the barriers to adopting objective motion capture technology in clinical practices for the assessment of LBP, we propose an AI model (SpineNet) that automatically detects anatomical landmarks and calculates spine kinematics through a single RGB-D camera aimed at a posterior-anterior view of a participant completing a trunk flexion-extension task. In the current paper, we propose and evaluate a proof of concept experiment, where we outline the methods used to collect the appropriate RGB-D camera's data streams and the development

of a novel CNN that segments anatomical landmarks of the back by: 1) encoding depth data by colourization and converting to 3D surface normal; 2) using the U-Net architecture and layer types (i.e., convolution, transposed convolution, concatenation of feature maps); and 3) by fusing multimodal data by adopting late fusion to combine the different types of data.

In this this work, we also show preliminary data to display feasibility of calculating lumbar spine kinematics extracted by SpineNet on marked and unmarked people. Lumbar spine ROM extracted from image predictions of marked people was tested against its own ground truth labels to check agreement and error, while lumbar spine kinematics extracted from image predictions of unmarked people were assessed through average ensemble curves that were compared against studies that have explored similar trunk flexion tasks studies (Laird et al., 2019; McGill et al., 1999; Ng, et al., 2001).

5.3 Methodology

5.3.1 Data Acquisition

Data were acquired from fifteen healthy male adults who were recruited from the university population. Participants' mean height, weight, age and BMI were 177.0 cm *(standard deviation (SD) = 7.9)*, 77.5 kg *(SD = 10.1)*, 31.7 years *(SD = 6.8)*, and 24.7 kg/m^2 *(SD = 2.3)*, respectively. Participants who were unable to complete the trunk movement tasks without pain or experienced a low back injury within six months prior to data collection were excluded. The study was approved by the University of Ottawa ethics review board (H08-17-26).

During the data collection session, participants were instructed to perform two series of 10 continuous trunk flexion-extension cycles at a pace of 30 beats per minute (i.e., 15 cycles per minute) controlled by a metronome. Trunk kinematic data were collected by one RGB-D camera (Kinect v2; Microsoft Corporation, Redmond, WA) at 30 Hz positioned approximately one metre behind the participant at a height of 1.70 m, with the camera angled 30º down from

the horizontal (Figure 5.1). For each participant, the camera angle and position were adjusted slightly to ensure adequate coverage of the participant's movements. Kinect Studio 2.0 (Microsoft Corporation, Redmond, WA) was used to capture the RGB-D camera data.

Participants were asked to remove their shirt and wear spandex shorts to fully expose the back. The first series of 10 trunk flexion-extension cycles were performed without drawn markers. Next, point markers were drawn on the participant's back using a black dry-erase marker: from C_7 to S_1, a series of straight horizontal lines of seven point markers were drawn across the back on every second vertebrae (Figure 5.1). Once the point markers were drawn, the participant performed the second series of trunk flexion-extension cycles. Participants' trunk flexion-extension range of motion (ROM) was controlled by having them touch targets adjusted to shoulder and knee height without any constraints (Figure 5.1). One full trunk flexion-extension cycle was signaled by three metronome beats, which consisted of the following actions: with outstretched arms with one hand atop the other, participants touched the target placed at shoulder height (beat one), the participant flexed forward to touch the target 50 cm in front of their knees (beat two), and extended to return to the initial position touching the target at shoulder height (beat three) (Figure 5.1).

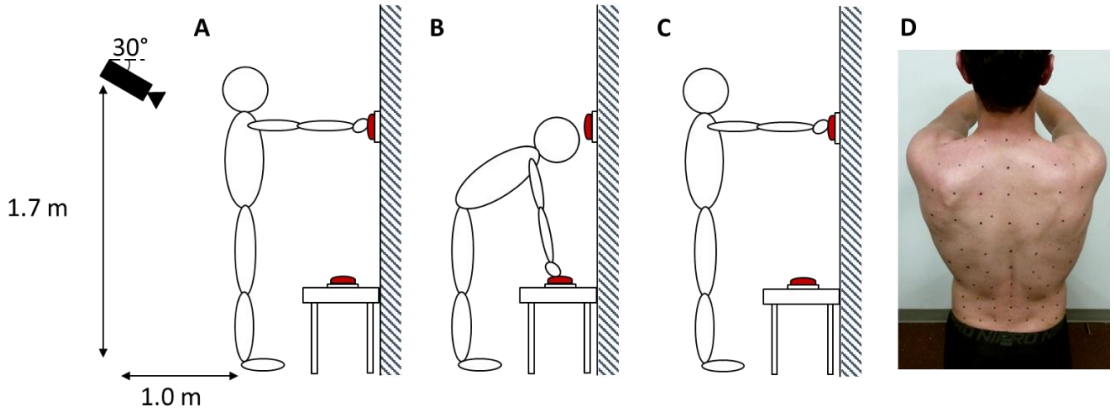

Figure 5.1 *Experimental setup, task protocol and participant preparation for the marked condition . (A) A single RGB-D camera was located 1 metre behind the participant, 1.7 metres high, and angled to 30 degrees from the horizontal. To start the trunk flexion-extension cycle, the participant stood upright with arms outstretched touching a target adjusted to shoulder height , (B) the participant fully flexed their trunk to touch a target adjusted to knee height, (C) the participant extended to a standing position and touched the target adjusted to shoulder height to finish the task cycle. (D) Starting at C7 and finishing at S1 a horizontal line of seven point markers were drawn on every second vertebrae with a black dry erase marker.*

5.3.2 Dataset

To ensure that the analyzed movements were continuous movements and more in synch with the metronome beats, only a subsample of five consistent (i.e. hitting targets synchronous with metronome, not moving too fast or too slow) continuous trunk flexion-extension cycles for each participant were included in the dataset.

The RGB-D camera's IR and Depth data were preprocessed to match the RGB image format and to enrich features. Raw IR images were contrast and brightness normalized across all images to better identify the drawn point markers and image features. Raw depth data were encoded as per (Eitel et al., 2015; Rahman et al., 2017): the "jet" colour map was used to convert the 13-bit (values: 0-8000) grey-scale pixels to 8-bit per colour channel (RGB) "Colourized" depth pixels (values: 0-255) and the apparent 3D "Surface Normal" was calculated by determining the difference between adjacent depth pixels and encoding "*xyz"* normal vectors as scaled RGB values, respectively.

To create the ground truth segmented images, colour images from the marked trunk flexion-extension cycles were manually labelled into four classes: spine, upper back, lower back, and background. All labelling was done using the video editing software Hitfilm Express (FXhome Limited, Norwich, NOR, England) and its Mocha Hitfilm visual effects software plug-in (Boris FX, Boston, MA, USA). More specifically, the Mocha plane tracking tool was used to define tracking planes on top of the markers that belong to the spine segmentation class; defined as the region between the 3rd and 5th markers across all vertebral marker groups from C_7 to S_1, as shown on Figure 5.2. Upper and lower back annotations were parsed for the full back on every frame using a lazy snapping algorithm, then the limits of the upper and lower back were defined as the regions between the C_7 and T_{12} marker groups for the upper back and between T_{12} and S_1 marker groups for the lower back. To register annotations on the RGB-D camera 's IR and depth data, C_7, T_{12} and S_1 marker groups were tracked on both colour and IR

images. Then, by using the tracked marker groups as control points, an affine geometric transformation was applied on colour labels to fit the IR and depth data inputs. Moreover, the RGB-D camera's IR and depth data channels were measured by the same sensor, having the same resolution and point of origin; therefore, IR and depth data were inherently registered with each other. Algorithms and functions used during the annotation phase (i.e., lazy snapping and affine geometric transformation) were provided by MATLAB (R2019a, The MathWorks Inc., Natick, MA, USA). Every pixel that did not fall into one of the three back classes was labelled "background". The final ground truth labelling scheme is illustrated in Figure 5.2. Figure 5.3 illustrates the workflow of the RGB-D camera's data prior to input into SpineNet.

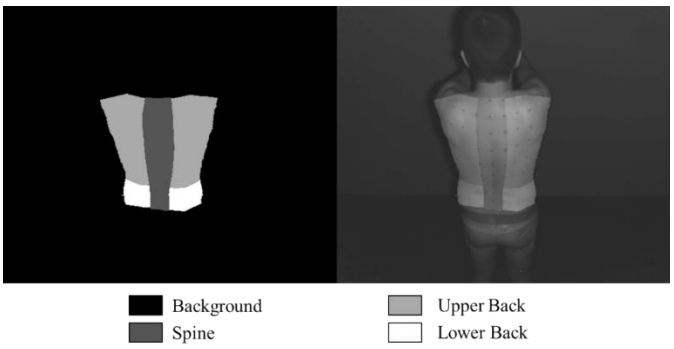

Figure 5.2 *Label Classes and IR Label Classes Overlay*

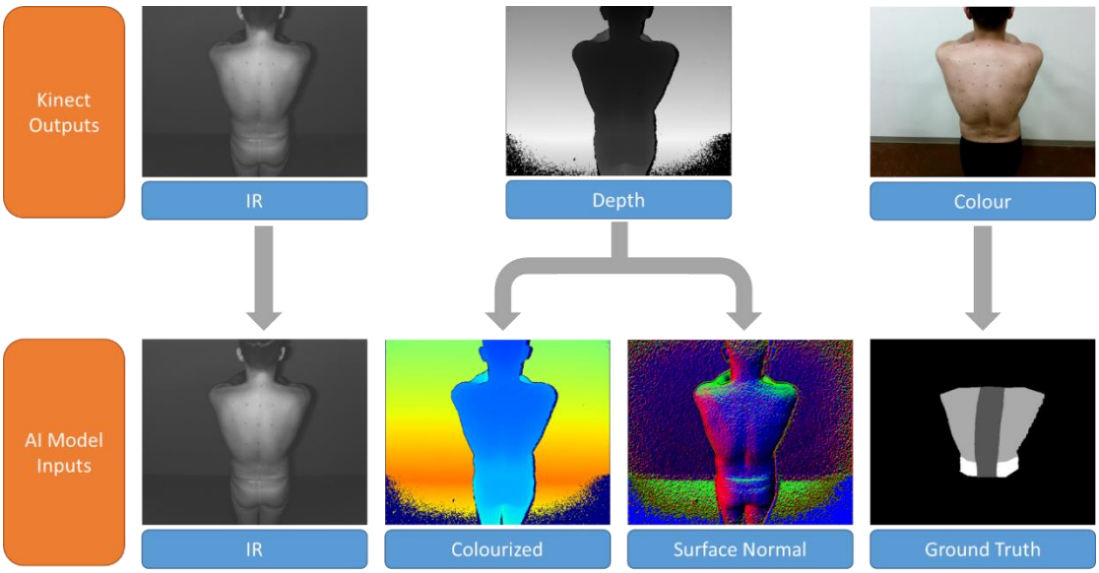

Figure 5.3 *RGB-D camera's data outputs and AI model inputs. An illustration of how each output from the RGB-D camera was used for the proposed AI model. IR output data were directly inputted into our AI model. Depth data were preprocessed to create a colourized and a surface normal input. Colour data output was used to create the ground truth.*

After preprocessing, data were randomly split participant-wise into three datasets: train dataset, test dataset, and a challenge dataset. The train and test datasets were composed of IR, colourized depth and surface normal depth annotated images of ten participants completing five cycles of the trunk flexion-extension task with point markers drawn on their backs for a total of 18000 annotated images with a resolution of 512 by 424 pixels. Eight participants were assigned to the training set and two participants were assigned to the test set, resulting in a train-test ratio of 80:20. The challenge dataset consisted of IR, colourized depth, surface normal depth, and unlabelled colour images from the unmarked trunk flexion-extension cycles of the remaining five participants totalling 9000 unannotated images with a resolution of 512 by 424 pixels. The test set was used to quantitatively evaluate SpineNet's image segmentation performance on marked people, while the challenge set was used to evaluate the generalizability of SpineNet on unmarked people, further details on utilization of each dataset for performance analysis are discussed on section 5.3.4. The organization of data into the test, train, and challenge set can be visualized in Figure 5.4.

5.3.3 SpineNet Architecture and Training

SpineNet is composed of four modules. In parallel, the first three modules pixel-wise segment the RGB-D camera's data streams into anatomical classes using 1) IR images, 2) pre-processed depth images encoded as the "jet" colour map and 3) pre-processed depth images encoded as 3D surface normal data, respectively. These anatomical segmentations are then fused using a final module, which combines the predictions from the first three modules to produce a consensus segmentation of the anatomical landmarks. An overview of the SpineNet architecture is illustrated in Figure 5.5.

Each module was built from U-Net 34. The U-Net 34 building block and all of its parameters including quantity, size, type of layers, nonlinearity, encoder-decoder design, and concatenation of feature maps were based on the U-Net architecture with 34 layers as proposed

by Ronneberger and colleagues (2015), which was found in the PyTorch (v1.2.0) and Fast.AI (v1.0.58) libraries (Howard et al., 2018; Paszke et al., 2019).

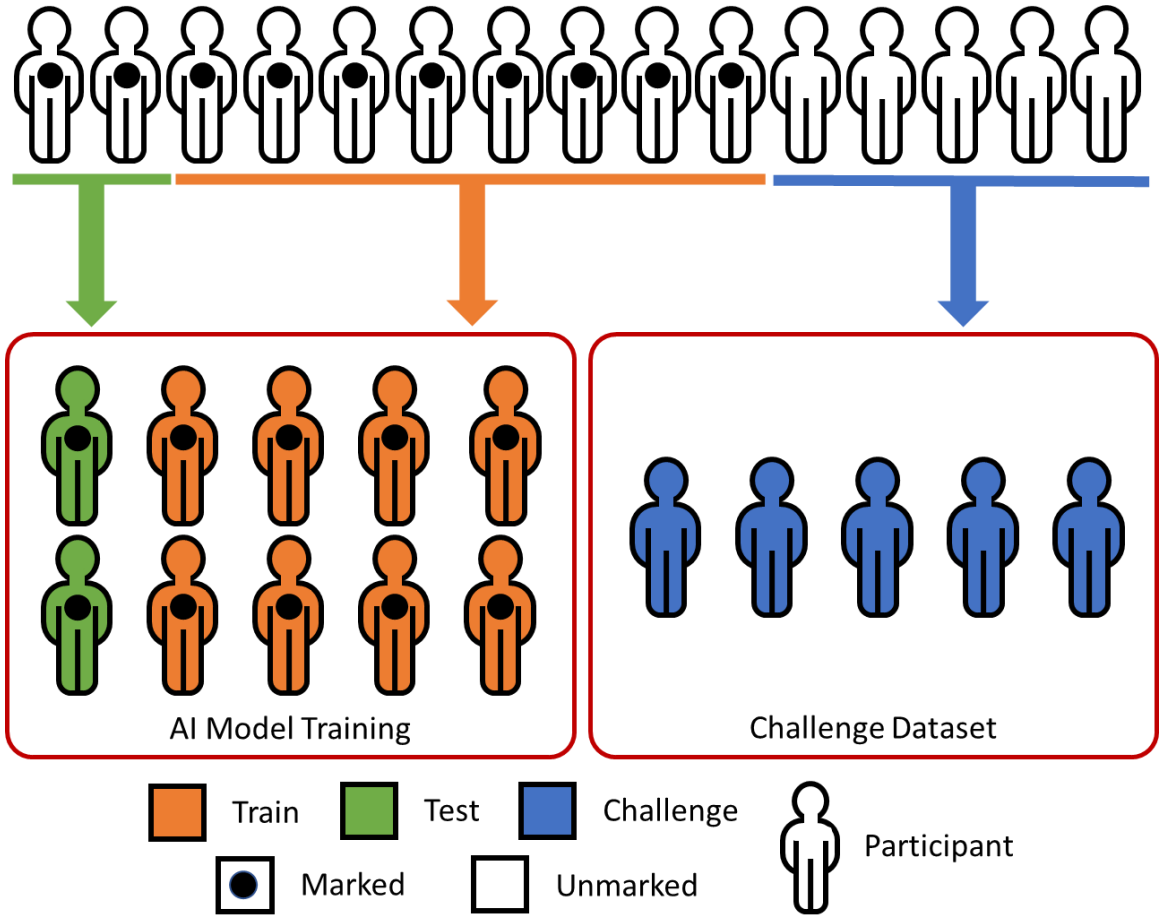

Figure 5.4 *Dataset split. An illustration of how participants were organized to define our train, test and challenge datasets. The train dataset was created with images of eight marked participants (**orange**), the test dataset was created with images of two marked participants (**green**) and the challenge dataset (**blue**) was created with images of five unmarked participants.*

Each of the three parallel input modules were trained separately using their respective data in their original dimensions. To increase dataset variability, training input data were augmented: each image taken as input to our AI model has its parameters randomized (i.e., contrast, brightness, warping, rotation, padding, and flipping). Transfer learning was used: starting weights and biases for the AI model were pre-trained on ImageNet, then fine tuned to our dataset. To avoid model divergence, the training session was paused every three epochs for training loss evaluation and optimal learning rate selection. The model loss was tested using a range of learning rates for a few iterations using a small sample of the training set, then each

iteration was plotted as means to choose the best learning rate (i.e., the one that most decreased the model loss). On each evaluation pause, if the model loss decreased when compared to its previously selected learning rate, then a new learning rate was selected, and training continued for three more epochs. This process was repeated until each input module of SpineNet converged. On average, each module was trained for 12 epochs with a learning rate of 10^{-5}.

The output of each of the three parallel input modules are pixel-wise class predictions. Each of the predictions were converted to grey-scale images and assigned to their respective RGB colour channel to form a new RGB input image for the final Fusion module. Training procedures for the Fusion module were identical to the three input modules, including participant-wise dataset selection for training, validation and testing sets.

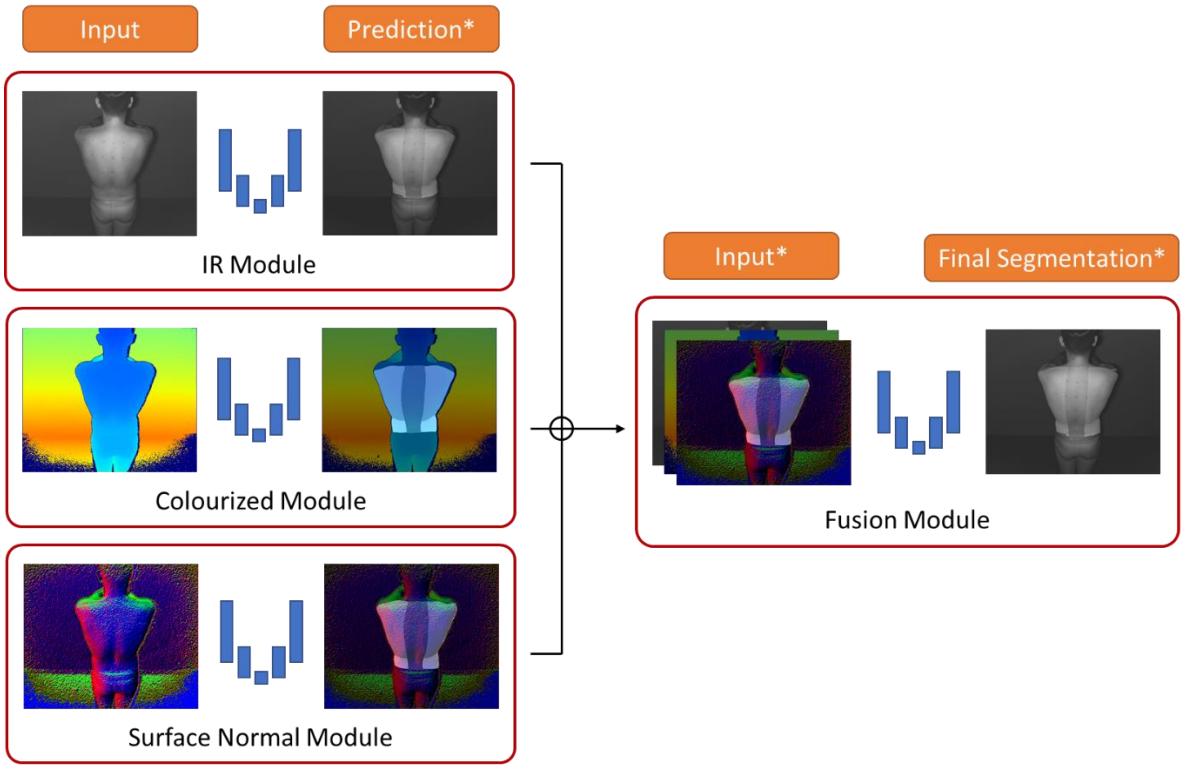

Figure 5.5 *AI Architecture Overview. Each RGB-D camera's data stream was used as input for each of the three individualized U-Net modules. Individual modules' anatomical segmentation predictions were then fused and used as input for the final U-Net module to generate a final segmentation prediction. (*) Prediction*, Input* and Final Segmentation* illustrations are shown as predictions overlaid over their respective data stream for better visualization.*

5.3.3.1 Kinematics from Image Segmentation

To calculate lumbar spine kinematics, the spine class was split into two masks: the upper and lower spine. To do this, a splitting line connecting the intersection of the upper back, lower back, and spine was drawn through the spine class. To ensure consistent data point selection, the upper and lower spine masks were refined, the vertical border sizes of mask borders were locked to a maximum distance, and resized over their respective bottom horizontal borders. The upper and lower spine masks were applied over the depth image, then a first-degree linear polynomial surface was fit onto each of the upper and lower spine segments. 3D global points *(x,y,z)* were defined as numerically equal to *(i,j,p)*, where *i* and *j* are the pixel position of the mask's corners and *p* is the point value that belongs to the first degree linear polynomial surface. 3D global coordinates of the extracted masks' corners were used to define the upper and lower spine's right-handed local coordinate systems (LCSs). Rotation matrices were defined for each LCS, then a relative rotation matrix was calculated, and Cardan angles were extracted using the "*xzy"* sequence (flexion-extension, lateral bending, axial twisting). Final LCS placement and step-by-step creation process of upper and lower spine masks are illustrated on Figures 5.6 and 5.7.

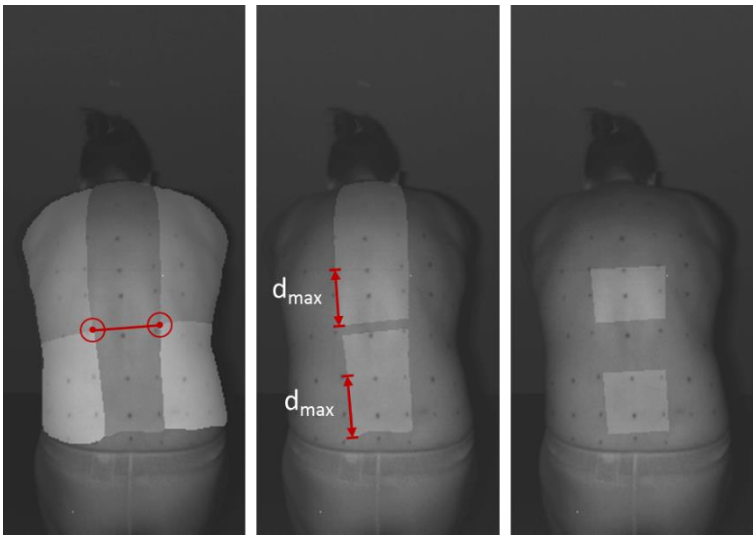

Figure 5.6 *Creation of upper and lower spine masks. From left to right: 1) Spine class predictions were split based on the position of the upper and lower back classes; 2) upper and lower spine masks were cropped based on the maximum distance of their vertical borders; 3) final upper and lower spine masks were obtained.*

Mean trajectories and angles for each participant were calculated by: 1) dividing the whole trial into individual trunk flexion-extension cycles, 2) normalizing cycles to 101 data points (i.e., 0-100% of the cycle), and 3) calculating the ensemble data from each cycle to obtain a mean trajectory and angle. Flexion-extension (FE), lateral bending (LB) and axial twisting (AT) ROM were calculated as defined in Chapter 4 equations 4.6 to 4.8.

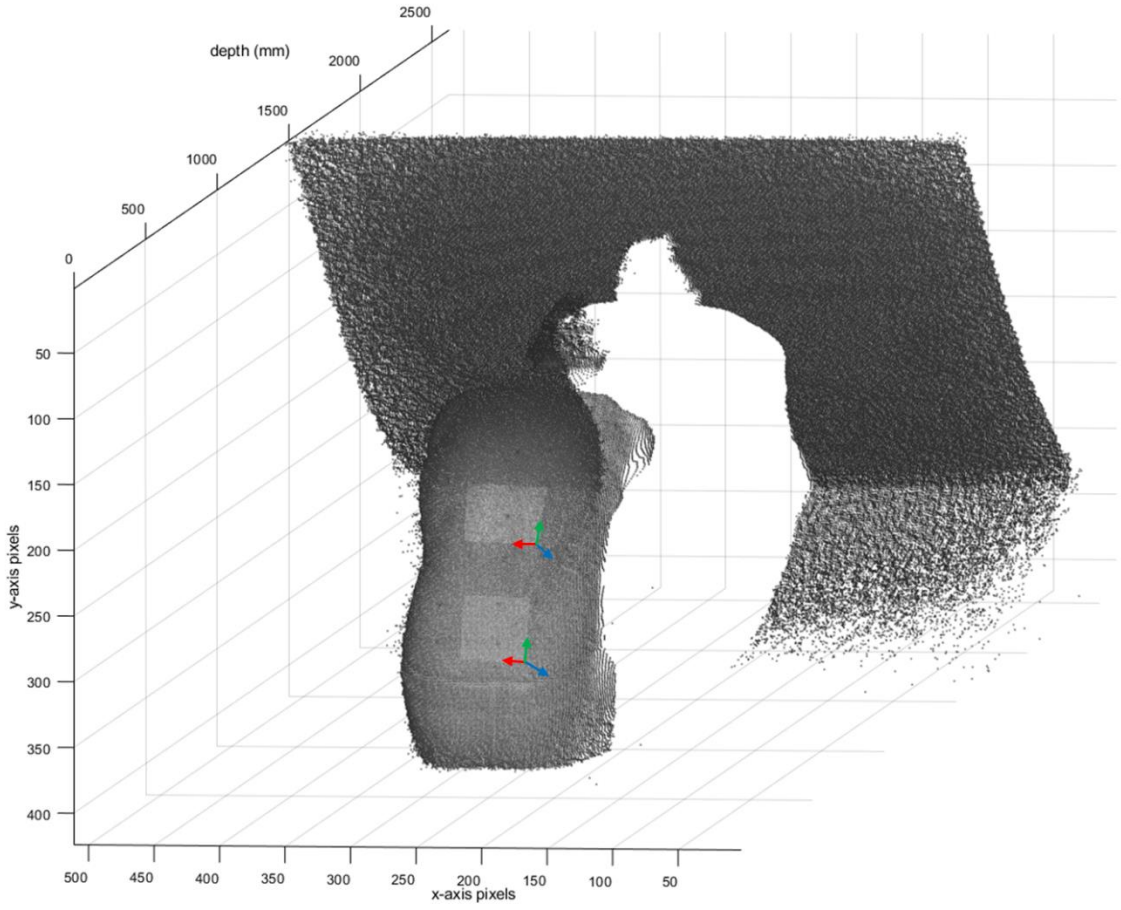

Figure 5.7 *RGB-D camera's 3D point cloud of depth data with IR overlaid illustrates the final LCS placement. Upper and lower spine masks were projected in 3D depth data (grey rectangles), then origin of right-handed 3D LCS were defined as the lowest right corner of upper spine and lower spine masks, represented as red (x), green (y) and blue (z) arrows. Figure axes x (pixels), y (pixels) and z (mm) show pixel location in 3D.*

5.3.4 Performance Analysis: Image Segmentation and Kinematics

SpineNet was evaluated on two performance criteria: 1) on image segmentation performance and 2) the quality of spine kinematics. For image segmentation, the test dataset's image segmentation was evaluated quantitatively using a common set of image segmentation metrics (section 5.3.4.1), and qualitatively by reviewing videos of the segmentation and scoring

them based on class borders and shapes (section 5.3.4.2). Extracted lumbar spine kinematic performance was evaluated for the test and challenge datasets quantitatively under two perspectives: 1) the accuracy of the lumbar spine kinematics extracted from predictions done across all data modules on marked participants compared against the lumbar spine kinematics extracted from their labels (i.e., test's dataset ground truth) and 2) general assessment of the ensemble average movement profiles of the lumbar spine kinematics extracted on predictions done across all modules on unmarked participants (section 5.3.4.3).

5.3.4.1 Quantitative Evaluation of Image Segmentation

SpineNet's semantic segmentation was quantitively evaluated using common metrics (Thoma, 2016; Garcia-Garcia et al., 2017): pixel accuracy *(PA)*, mean pixel accuracy *(mPA)*, mean Jaccard index *(mJ)*, and frequency weighted Jaccard index *(fwJ)*. These metrics are evaluated under three quality measures: true positives (TP), false positives (FP) and false negatives (FN), each one carrying the notation n_{ii} (TP), n_{ij} (FP) and n_{ji} (FN). Where n_{ij} is the number of pixels that belong to class *i* labelled as class *j* for *k* classes, and let $t_i = \Sigma_j n_{ij}$ be the total number of pixels of class i. Thus, we formally defined each metric as follows:

PA is a broad measure of how well the image was segmented. I.e., the ratio of all true positives (i.e., n_{ii}) over all pixels that belong to each class

$$PA = \frac{\Sigma_i^k n_{ii}}{\Sigma_i^k t_i} \tag{5.1}$$

mPA is similar to *PA*, but are averaged by the number of classes of a given image

$$mPA = \frac{1}{k} \Sigma_{i=1}^{k} \frac{n_{ii}}{t_i} \tag{5.2}$$

mJ, also known as "Intersection Over Union", calculates the ratio of pixels that belong to class *i* predicted as class *i*, over the number of all pixels classified as *i*, whether they were misclassified or not

$$mJ = \frac{1}{k} \Sigma_{i=1}^{k} \frac{n_{ii}}{\left(t_i - n_{ii} + \Sigma_{j=1}^{k} n_{ji}\right)} \tag{5.3}$$

fwJ weighs each pixel class by its frequency of appearance in the image

$$fwJ = \left(\Sigma_{i=1}^{k} t_i\right)^{-1} \Sigma_{i=1}^{k} t_i \frac{n_{ii}}{\left(t_i - n_{ii} + \Sigma_{j=1}^{k} n_{ji}\right)} \tag{5.4}$$

5.3.4.2 Qualitative Evaluation of Image Segmentation

Qualitative evaluation of image segmentation was performed on all segmented images across all modules using the video editing software Hitfilm Express (FXhome Limited, Norwich, NOR, England). Sequences of image predictions from each data type (i.e., IR, Colourized depth, Surface Normal depth, and Fusion) were overlaid on the IR input images and then transformed into videos for visual appraisal. Both challenge and test datasets were rated by one image analysis expert, and the objective observer criteria were to evaluate the boundaries and shape of each prediction class: borders should touch black point markers drawn on the participant's skin as shown in the Figure 5.8, and segmentation class morphology should be similar to labelled anatomical landmark structure. Borders were appraised on a continuum of four levels: excellent, good, moderate, poor. Where an excellent rating represents the borders as touching the class markers and ratings progressively transitioned to good, moderate and poor as the borders moved further away from the class markers. Segmentation class morphology was classified as adequate when it was similar to the ground truth label shape, and inadequate when it was not. Final image qualitative performance was achieved by combining border and

morphology qualifications; where initial border qualification was assessed and then if morphology was deemed inadequate, final image qualitative performance would fall in one rank. For example, if an image border was qualified as excellent but had an inadequate morphology, it would have received a final performance rank of good.

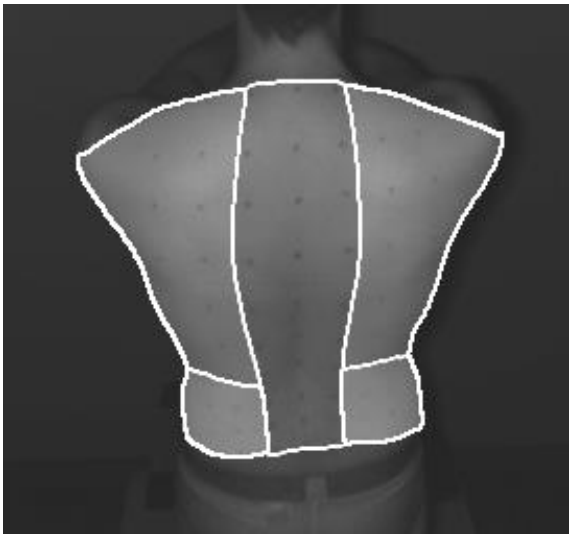

Figure 5.8 *Qualitative analysis objective criteria. The colourized module prediction is overlaid on IR images. Borders of each class prediction (highlighted in white) should touch black point markers drawn on the participant's skin. Morphology of segmentation classes are similar to anatomical landmarks labelled.*

5.3.4.3 Quantitative Evaluation of Spine Kinematics Extraction

Lumbar spine kinematics extracted from the segmented images of marked participants were quantitatively analysed by calculating root mean square error (*RMSE)* throughout the entire trial, and two way random intraclass coefficients *($ICC_{2,1}$)* were used to assess reliability between average ROM angles of the test dataset (marked participant's data) compared to their ground truth labelled counterparts. Average ensemble curves of lumbar spine kinematics from unmarked participants were assessed, their movement peaks, shapes, and profiles were visually compared for each data module against marked participants and other studies available in the literature. All statistical analyses were performed using Python statistical packages from Pingouin v0.3.7 (Vallat, 2018) and SciPy v1.4.1 (Virtanen et al., 2020).

5.4 Results

5.4.1 Image Segmentation

5.4.1.1 Quantitative Analysis

Since the background class consists of a greater number of pixels than the classes of the back (86% of the image vs. 14%), quantitative performance of all modules (IR, Colourized depth, Surface Normal depth, and Fusion) were analysed when considering all four classes (background included; BKG) and foreground only (the spine, upper back, and lower back classes; FG). Expectedly, *PA, mPA, mJ, and fwJ* performance metrics were all elevated when the background class was included. However, despite having a class imbalance, overall trends from both the BKG and FG perspectives of SpineNet indicated that the IR and Fusion modules slightly outperformed the Colourized depth and Surface Normal depth modules across all metrics.

For both the BKG and FG comparisons, the IR and Fusion modules performed better across all performance metrics compared to the Colourized depth and Surface Normal depth modules. However, all modules had good standard accuracy and similarity analysis, where their scores varied from 0 to 1, with 1 being the maximum and best score *($PA_{BKG} \geq 0.9822$; $PA_{FG} \geq 0.8840$; $mPA_{BKG} \geq 0.9135$; $mPA_{FG} \geq 0.8855$; $mJ_{BKG} \geq 0.8391$; $mJ_{FG} \geq 0.7884$; $fwJ_{BKG} \geq 0.9672$; $fwJ_{FG} \geq 0.8087$).* All results for each module for "background included" and "foreground only" analyses are presented in Tables 5.1 and 5.2, respectively.

Table 5.1 *Image segmentation metrics across all modules including background pixels.*

	PA	mPA	mJ	fwJ
IR	0.9885	0.9493	0.9108	0.9781
Colourized	0.9822	0.9135	0.8391	0.9672
Surface Normal	0.9828	0.9160	0.8504	0.9681
Fusion	0.9882	0.9468	0.9041	0.9775

Note Colourized and Surface Normal were derived from the depth data. IR = infrared, PA = pixel accuracy, mPA = mean pixel accuracy, mJ = mean Jaccard index, fwJ = frequency weighted Jaccard index.

Table 5.2 *Image segmentation metrics across all modules considering only foreground pixels.*

	PA	mPA	mJ	fwJ
IR	0.9382	0.9334	0.8837	0.8948
Colourized	0.8840	0.8855	0.7884	0.8087
Surface Normal	0.8900	0.8887	0.8034	0.8198
Fusion	0.9336	0.9299	0.8746	0.8885

Note Colourized and Surface Normal were derived from the depth data. IR = infrared, PA = pixel accuracy, mPA = mean pixel accuracy, mJ = mean Jaccard index, fwJ = frequency weighted Jaccard index.

5.4.1.2 Qualitative Analysis

On average, marked image segmentation had an excellent performance for the IR and Fusion modules: segmentation class borders touched most of drawn markers and overall morphology of classes was satisfactory. However, there were segmentation predictions throughout the trial where the IR and Fusion modules presented some errors, creating distortions on class borders as shown in Figure 5.9. For the Colourized depth and Surface Normal depth modules, performance was considered good on average; overall morphology of classes was satisfactory and segmentation class borders did not touch some of the drawn markers. Specifically, the sides of spine class and the bottom of lower back class did not touch the reference markers but they were close, thus, combined evaluation criteria indicated good average performance. Figure 5.10 displays an example of the average performance of all modules for segmenting the test dataset images. On the challenge set, the IR and Fusion modules had poor performance on average, while Colourized depth and Surface Normal depth modules show an overall satisfactory morphology of classes indicating a good average performance. Average performance of segmentation across all modules on the challenge dataset images are illustrated in Figure 5.11.

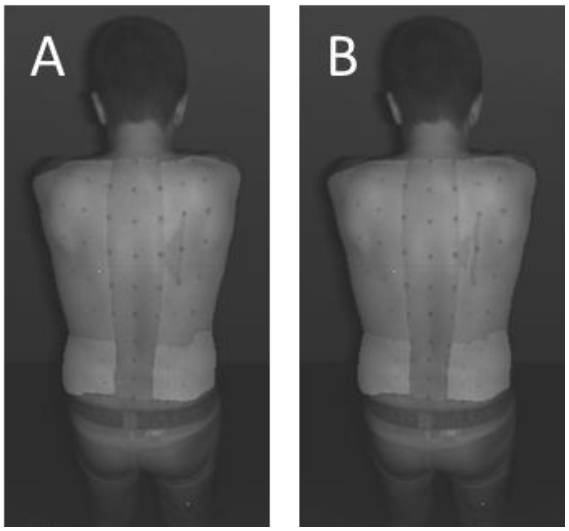

Figure 5.9 *Test dataset qualitative analysis failure case. An example of a frame where image segmentation failed and generated and artifact (or segmentation error) overlaid on an IR image. (A) IR module prediction and (B) Fusion module prediction. The artifact is located on the right side of spine segmentation class near the participant's scapula. Failure cases on the Fusion module predictions have smoother edges and a smaller error area than the IR module counterpart.*

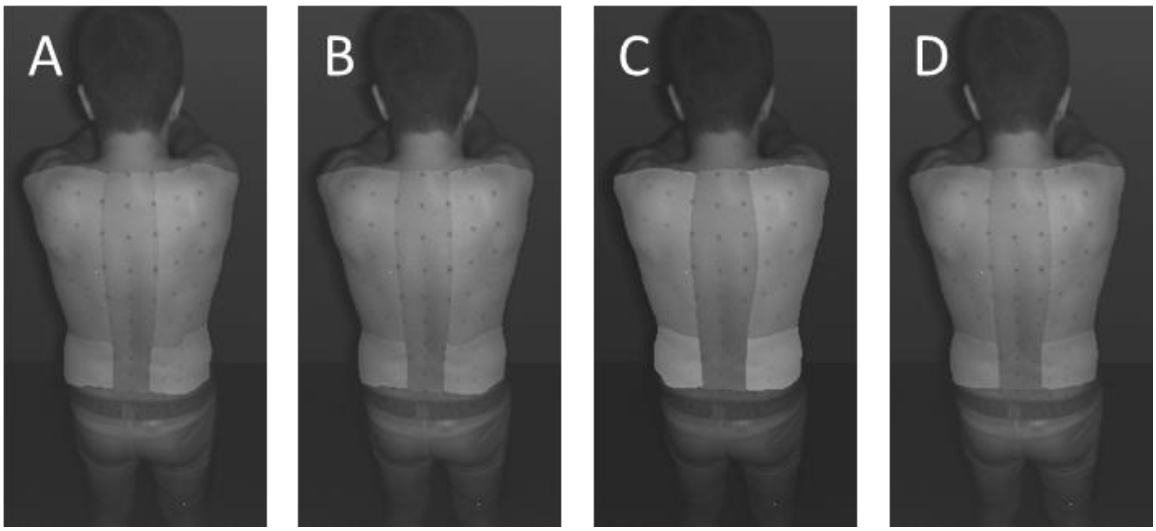

Figure 5.10 *Average test dataset qualitative analysis performance. The average performance of each module prediction overlaid on an IR image from the test dataset. (A) IR module, (B) Fusion module, (C) Colourized module and (D) Surface Normal module. The IR and Fusion modules' class prediction boundaries touch most of the drawn point markers and morphology is satisfactory, qualified as excellent performance, while Colourized depth and Surface Normal depth modules' class prediction boundaries are close to the drawn point markers and morphology is satisfactory, qualified as good performance.*

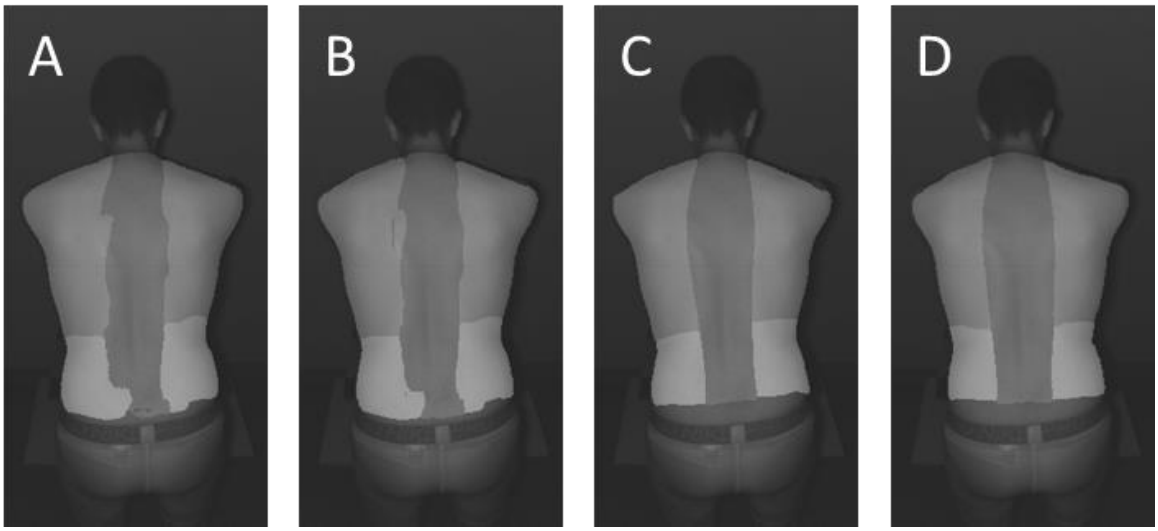

Figure 5.11 *Average challenge dataset qualitative analysis performance. The average performance of each module prediction overlaid on an IR image from the test dataset. (A) IR module, (B) Fusion module, (C) Colourized depth module and (D) Surface Normal depth module. The IR and Fusion modules' class prediction morphology is not satisfactory, qualified as poor performance, while the Colourized depth and Surface Normal depth modules' class predictions morphology is satisfactory, qualified as good performance. The Fusion module presented smoother edges than the IR module counterpart along the whole trial.*

5.4.2 Kinematic Analysis

Comparing the kinematics calculated from the test dataset (marked participants) compared to ground truth labels resulted in low *RMSE* values across all modules. *RMSE* values in the FE movement axes ranged from 1.28° to 2.48°, LB *RMSE* values ranged from 2.80° to 3.66° and AT *RMSE* values ranged from 1.12° to 2.47°. All *RMSE* values for each module and movement axis are presented in Table 5.3.

Table 5.3 *Error analysis (RMSE; SD) between ground truth labels and the test dataset for lumbar spine angles.*

	Flexion-Extension	**Lateral Bending**	**Axial Twisting**
IR	1.56 (±0.21)	3.08 (±1.14)	1.15 (±0.39)
Colourized	1.28 (±0.40)	2.80 (±0.04)	1.98 (±0.20)
Surface Normal	2.48 (±0.03)	3.66 (±0.56)	2.47 (±0.52)
Fusion	1.83 (±0.67)	3.15 (±0.31)	1.12 (±0.35)

IR = Infrared; RMSE = root mean square error; SD = standard deviation. Colourized and Surface normal data are derived from the depth data.

Calculated reliability from the cycle-to-cycle ROM angle measurements of the test dataset (marked participants) compared to the ground truth labels varied from poor to excellent depending on movement axis rather than the data module. Moderate to excellent $ICC_{2,1}$ in the

FE and AT axes was found across all modules *($ICC_{2,1}$ > 0.907; CI 95% [0.640, 0.990])*, while spine ROM in the LB axis had poor reliability when compared to LB ROM calculated using the ground truth image labels, resulting in negative (and unrealistic) $ICC_{2,1}$ values and wide confidence intervals *(-0.212 < $ICC_{2,1}$ <0.630; CI 95% [-6,990, 0.910])*. All $ICC_{2,1}$ values for each module and movement axis are presented in Table 5.4.

Table 5.4 *Reliability analysis ($ICC_{2,1}$; 95% CI lower-upper) between ground truth labels and predictions of test dataset lumbar spine.*

	Flexion-Extension	**Lateral Bending**	**Axial Twisting**
IR	0.965 (0.860-0.990)	0.150 (-3.060-0.800)	0.963 (0.850-0.990)
Colourized	0.995 (0.980-1.000)	0.354 (-2.130-0.850)	0.907 (0.640-0.980)
Surface Normal	0.952 (0.700-0.990)	0.630 (-0.600-0.910)	0.942 (0.760-0.990)
Fusion	0.928 (0.680-0.980)	-0.212 (-6.990-0.730)	0.957 (0.830-0.990)

IR = Infrared; $ICC_{2,1}$ = intraclass correlation coefficient; CI = confidence interval. Colourized and Surface normal data are derived from depth data.

Ensemble averages of the test dataset also varied based on the movement axis rather than the module. The magnitudes of the test dataset's kinematics in the FE axis were very similar across modules throughout the entire cycle, while the LB movement axis was underestimated between 30% and 70% of the cycle across all modules. For AT, a slight underestimation of angle magnitude was found for the colourized depth module between 20% and 80% of the cycle, while all other modules had an excellent match between prediction and ground truth labels. Ensemble averages calculated on the test dataset are organized by data module in Figures 5.12 to 5.15.

Despite the lack of a direct comparison, ensemble averages of the challenge dataset's lumbar spine kinematics in three dimensions exhibited a movement profile that is visually compatible to movements performed by participants under marked condition and to movements performed in other studies under similar task conditions (i.e., standing trunk flexion-extension without constrains on pelvic movement). Furthermore, standard deviations varied depending on the module; Colourized and Surface Normal modules have the lowest standard deviations, followed by Fusion and then IR module with the highest standard deviation across all axes.

Ensemble averages calculated presented similar profile across all modules, and they are organized by data module in Figures 5.16 to 5.19.

Overall, the marked condition achieved low levels of error and high indices of reliability between kinematic extraction methods (i.e., from predicted segmentation images and ground truth), while lumbar spine angles measured on participants from unmarked condition were visually compatible with trunk flexion-extension motion.

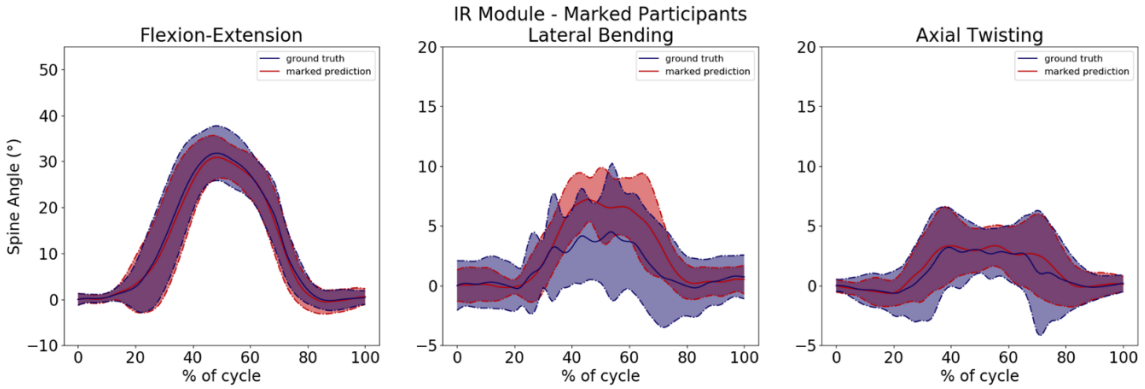

Figure 5.12 *IR module kinematic results – test dataset. Ground truth (blue) vs IR marked prediction (red) ensemble averages (solid) and standard deviations (dashed) of relative lumbar spine joint angles for flexion-extension, lateral bending and axial twisting movement axes.*

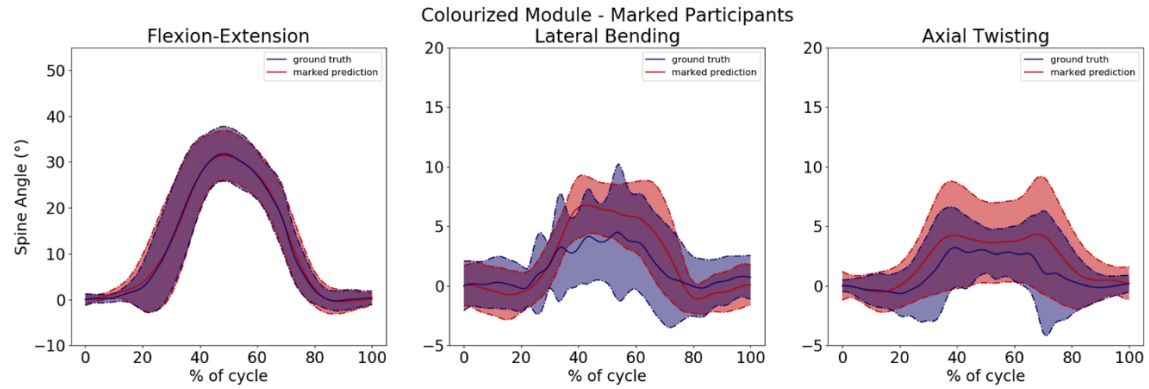

Figure 5.13 *Colourized depth module kinematic results – test dataset . Ground truth (blue) vs Colourized marked prediction (red) ensemble averages (solid) and standard deviations (dashed) of relative lumbar spine joint angles for flexion-extension, lateral bending and axial twisting movement axes.*

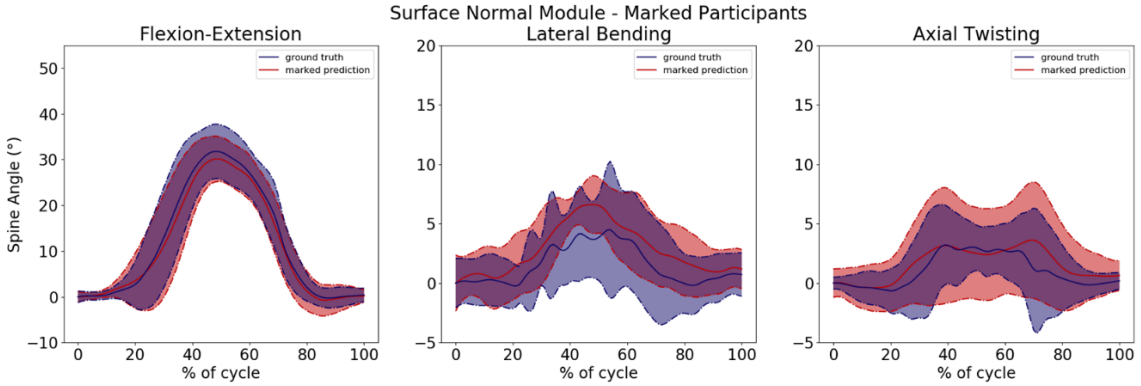

Figure 5.14 *Surface Normal depth module kinematic results – test dataset. Ground truth (blue) vs Surface Normal marked prediction (red) ensemble averages (solid) and standard deviations (dashed) of relative lumbar spine joint angles for flexion-extension, lateral bending and axial twisting movement axes.*

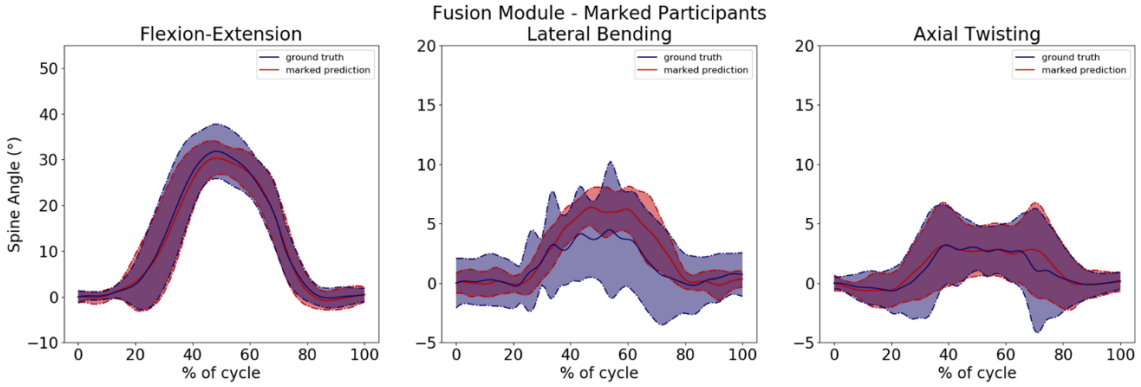

Figure 5.15 Fusion module kinematic results – test dataset . *Ground truth (blue) vs Fusion marked prediction (red) ensemble averages (solid) and standard deviations (dashed) of relative lumbar spine joint angle of flexion-extension, lateral bending and axial twisting axes movement axes.*

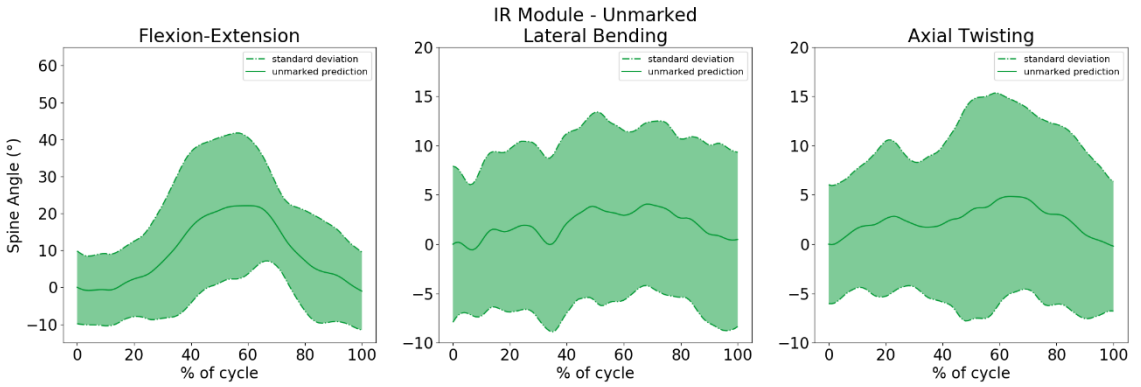

Figure 5.16 *IR module kinematic results – challenge dataset. IR unmarked prediction (green) ensemble averages (solid) and standard deviations (dashed) of relative lumbar spine joint angle of flexion-extension, lateral bending and axial twisting movement axes.*

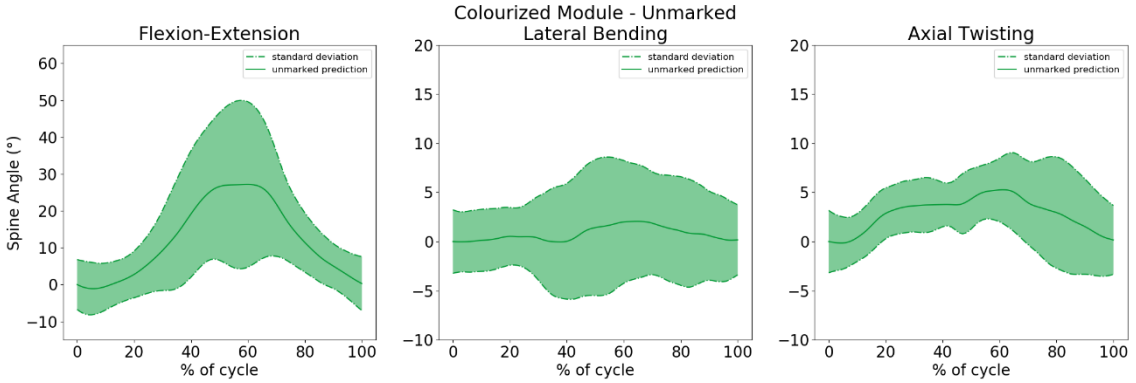

Figure 5.17 *Colourized depth module kinematic results – challenge dataset. Colourized unmarked prediction (green) ensemble averages (solid) and standard deviations (dashed) of relative lumbar spine joint angle of flexion-extension, lateral bending and axial twisting movement axes.*

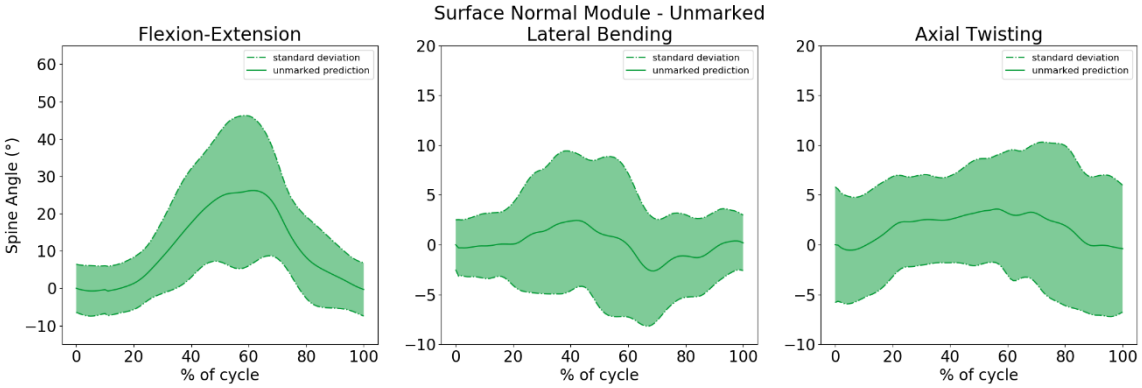

Figure 5.18 *Surface normal depth module kinematic results – challenge dataset. Surface Normal unmarked prediction (green) ensemble averages (solid) and standard deviations (dashed) of relative lumbar spine joint angle of flexion-extension, lateral bending and axial twisting movement axes.*

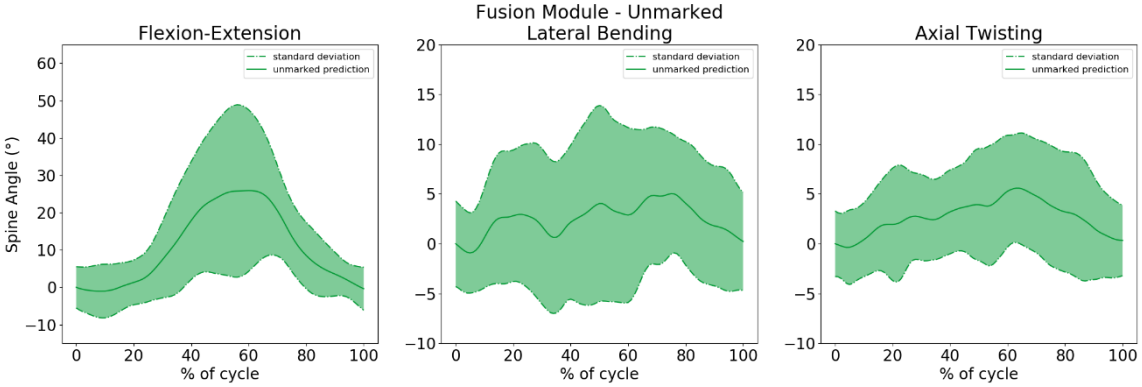

Figure 5.19 *Fusion module kinematic results – challenge dataset. Fusion unmarked prediction (green) ensemble averages (solid) and standard deviations (dashed) of relative lumbar spine joint angle of flexion-extension, lateral bending and axial twisting movement axes.*

5.5 Discussion

In the present study, we developed a deep learning model capable of segmenting the spine, upper back and lower back from images captured by a single RGB-D camera and used

these segmented outputs to extract lumbar spine joint angles for a repetitive trunk flexion-extension task. Below our results are discussed in two main subsections: 1) image segmentation analysis (i.e., quantitative and qualitative analysis) and 2) Kinematic extraction evaluation.

5.5.1 Image Segmentation

5.5.1.1 Quantitative Analysis

Analysing the collected images with the background class can be misleading, since the accuracy achieved for the spine, upper back and lower back classes are of much greater interest, and including the background class falsely boosts the apparent performance of the model. Therefore, only the performance on the foreground pixels will be discussed.

Considering only foreground pixels, the overall quantitative analysis of all dependent variables across all data channels for the test set present the same trend: the IR data module is the most accurate *(PA = 0.9382, mPA = 0.9334, mJ = 0.8837, fwJ = 0.8948)*, closely followed by the Fusion module *(PA = 0.9336, mPA = 0.9299, mJ = 0.8746, fwJ = 0.8885)* and a similar performance was achieved by the Colourized depth and Surface Normal depth modules, with all dependent variables greater than *0.7884 ($PA \geq 0.8840$, $mPA \geq 0.8855$, $mJ \geq 0.7884$, $fwJ \geq 0.8087$)*. This analysis suggests that Fusion is not better than the IR module for segmenting anatomical landmarks of the back. These results show that the IR module outperforms the other modules for image segmentation on the marked dataset. Also, the Fusion module achieves a high score but it is not superior than the IR module. Finally, Colourized depth and Surface Normal depth modules also achieve adequate scores, despite slightly inferior performance in comparison to IR and Fusion modules.

Using depth data encoding for improving AI performance was already tested by several studies (Eitel et al., 2015b; Gupta et al., 2014; Hazirbas et al., 2017; Rahman et al., 2017) and they have brought improvement for the state-of-the-art. For example, Rahman et al. AI model achieved an accuracy of 92.2 *(SD = 1.3)* for object classification using two encoded depth

parallel branches at the beginning of their model, and Hazirbas et al. achieved high similarity and accuracy *(PA = 76.27; mPA = 48.30; mJ = 37.29)* on semantic segmentation using slow fusion. On both cases, the applied techniques boosted baseline results (e.g. using not encoded depth data) to values comparable with state-of-the-art methods. Our results achieved higher scores than Rahman et al. and Hazirbas and colleagues, however, analysis conditions between AI models are not same; each network had its own purpose, also its training and testing set; Rahman et al. (2017)'s AI model was used to classify everyday objects and it was trained on the dataset SUN RGB-D, Hazirbas et al. (2017)'s AI model was used to pixel-wise segment indoor scenes and it was trained on the Washington RGB-D dataset, while SpineNet was used to parse anatomical landmarks and it was trained on a custom dataset. Therefore, despite the apparent better performance from SpineNet, in reality the aforementioned AI models are not directly comparable.

5.5.1.2 Qualitative Analysis

Qualitative analysis on the test dataset was performed to clarify if the Fusion module could successfully clean any segmentation errors from the initial input modules. Hazirbas et al. created an AI model (FuseNet) that fused RGB and depth data, producing accuracy and similarity results that are comparable with state-of-the-art semantic segmentation *($PA_{FUSENET}$ = 0.7627; $mPA_{FUSENET}$ = 0.4830; $mJ_{FUSENET}$ = 0.3729)* and an improvement in if compared with individual modules *(PA_{DEPTH} = 0.6906; mPA_{DEPTH} = 0.4280; mJ_{DEPTH} = 0.2849; PA_{RGB} = 0.7214; mPA_{RGB} = 0.4714; mJ_{RGB} = 0.3247)*, thus, it was expected that the Fusion module would have better quantitative results than any other module, but that was not the case: our fusion module had an excellent agreement and similarity, but it was still slightly inferior to IR module operation. Thus, further investigation on Fusion module revealed that, despite not increasing quantitative outcome variables, the Fusion module could successfully clean some segmentation errors from the initial input modules.

We observed artifacts (or errors) in both the IR and Fusion segmentation predictions, which would potentially interfere with the kinematic calculations. Errors found in the Fusion predictions, despite being in the same position as the IR predictions were slightly smaller and smoother, which suggests that the Fusion module does attenuate segmentation errors to some degree. Colourized depth and Surface Normal depth predictions, despite having slightly inferior quantitative performance than IR and Fusion, detected anatomical landmarks more consistently while producing no artifacts (segmentation errors) across all frames. Moreover, artifacts found in the IR and Fusion predictions did not appear in Colourized depth and Surface Normal depth's module predictions.

SpineNet's qualitative performance on the challenge dataset decreased. The IR predictions appear to have heavily relied on the features extracted from the markers, since its qualitative performance on unmarked data were lower than marked data. Colourized depth and Surface Normal depth predictions had the best performance for the unmarked condition: class segments presented an excellent morphology. Since the Fusion predictions combine all features from the input modules, it had a slight improvement in morphology (i.e., smoother edges and boundaries) compared to the IR module but was not superior to either depth module.

In summary, the IR and Fusion modules are better than the Colourized depth and Surface Normal depth modules on marked data, but the opposite occurs on unmarked data, showing that SpineNet's IR and Fusion modules rely on the markers to make good predictions. In contrast, the Colourized depth and Surface Normal depth modules had good performance on marked data (although slightly inferior to the IR and Fusion modules) but an excellent performance on unmarked data, showing that Colourized depth and Surface Normal depth modules can segment RGB-D camera images independently from the use of markers and, therefore, can better generalize their predictions to unmarked data.

5.5.2 Kinematic Evaluation

Kinematics were extracted from the test dataset across all data modules and evaluated against the ground truth test dataset. When analysing the test dataset, average total lumbar spine ROM angles achieved excellent levels of $ICC_{2,1}$ indices in comparison to the ground truth labels in the FE and AT movement axes, while extracted ROM angles in the LB movement axis was considered unreliable across all modules. The absence of a trend toward any specific module suggests that there are no differences on the predicted segmentations done by the modules that would cause an adverse impact to the extracted kinematics using the proposed methodology. Furthermore, the low reliability levels of ROM measurements obtained in the LB movement axis are directly linked to the proposed extraction methodology since this method creates LCSs based on the morphology of the segmented classes. Therefore, movements that occur in the frontal plane (i.e., same as the image space plane) are more affected by morphing segmented classes. It is possible that further processing could eliminate errors in the LB movement axis by improving the segmentation data to help eliminate inconsistent class morphology, thus improving the accuracy of the kinematic extraction model, since it relies on the bottom corners to define the LCS.

When analysing the generalizability of SpineNet's ability to measure lumbar spine kinematics we found that mean ensemble averages of the challenge dataset (unmarked) are compatible with standing trunk flexion-extension tasks, exhibiting a movement profile that is similar to the task conditions; trunk flexion peaks align between studies, although, magnitudes were lower on FE movement axis magnitude in comparison with previous studies (Laird et al., 2019; McGill et al., 1999; Ng, et al., 2001). These studies reported lumbar spine overall ROM between 70º and 50º on FE movement axis, while our current study reported angles between 20º and 30º. However, the aforementioned studies performed slightly different movement tasks, as participants completed full trunk flexions (i.e. no restriction on movement

ROM for FE axis), while our study limited participant's ROM including targets on shoulder and knee height. Thus, lower overall lumbar spine a ROM values were expected to be found. For LB and AT movement axes, amplitude matched previous studies (Laird et al., 2019; McGill et al., 1999; Ng, et al., 2001), but movement peak positions and profiles were not compatible with the normal behaviour for this average ensemble curves. This is most likely to occur because of inconsistencies on our model LCS positioning. While the aforementioned studies define their LCS over L_5, our unmarked predictions model attempts to do the same, however, due to image segmentation errors, lower spine LCS may change its position and may not be consistently located over the same level as the other system for being able to compare. More promising results were found when comparing lumbar spine kinematics extracted from unmarked participants against extractions done on marked participants; lumbar spine kinematic movement profiles, peaks, shapes and magnitudes of the ensemble curve match very well on FE and AT movement axes, while LB average ensemble curve exhibit divergencies with the observed criteria (i.e., movement profile, peaks, shapes and magnitudes). In this analysis, the poor performance found on LB movement axis can also be explained by inconsistencies on our model LCS positioning.

Despite not being able to generate remarkably strong findings, since this work does not directly validate unmarked ROM measurements, our results indicate that SpineNet trained on marked participants and our kinematic extraction method can measure general movement trends of lumbar spine kinematics on unmarked participants during a trunk flexion-extension task using images from a single RGB-D camera. Furthermore, we have illustrated that it is possible to extract kinematic data given a segmented point cloud. Our kinematic extraction model was simple, and further development of the model may lead to improved results.

5.5.3 Limitations

While results found in this study are promising, our findings must be taken with caution considering that this work is a proof of concept and has limitations in its development. Despite the total number of images in the study being high (approximately 27000 images), the subject variability was very low as the whole study was done on 15 male participants from university population. This might limit the generalization power of SpineNet to other populations. Also, qualitative analysis was done by only by one image expert analyst that pertained to the research group, which might generate bias on the ratings of this analysis.

5.6 Conclusion

In this work a proof of concept novel framework to measure lumbar spine kinematics using alternative devices is presented. The SpineNet image segmentation framework successfully parsed anatomical landmarks of the human back from RGB-D camera images of people with and without drawn point markers while performing a repetitive trunk flexion-extension task. The IR and Fusion modules had better performance on marked datasets, while the Colorized depth and Surface Normal depth modules performed better on unmarked datasets. Lumbar spine kinematics extracted from the RGB-D camera images of marked participants were adequate for FE and AT movement axes when compared to the ground truth labels; however, the kinematic extraction method produced unreliable data in the LB movement axis, although, movement amplitude is low *(≈ 5°)*, making signal to noise ratio very high on this movement axis. In addition, all data modules had similar reliability, error, and correlation scores for kinematic calculations; therefore, there was no preferred image segmentation method. General assessment of the ensemble averages of lumbar spine kinematics extracted from images of unmarked participants exhibited a movement profile compatible with results from previous research on standing trunk flexion-extension tasks. Thus, overall, segmentation results obtained from all classification modules gave acceptable predictions of the anatomical

landmarks of the back in a standardized setting. Despite these promising results, kinematics calculated from the segmentations were unreliable for LB movement axis, thus, and thus further refinement of the kinematic extraction method is required.

5.7 Future Directions

Future studies should validate kinematic results from participants in an unmarked condition, and should also improve kinematic extraction from the predicted segmentations by investigating the addition of preprocessing steps such as morphological filters to reduce segmentation artifacts or creating a kinematic extraction method that does not rely on segmented classes morphology. Reliability, agreement, consistency, and validity of the kinematic measurements, including comparisons between individual and combined channels and other kinematic analyses common to spine research should also be investigated in the future. Future work with SpineNet should also increase the participant pool by collecting both sexes, and people of varying ages, heights, and weights. Treating the acquired images as a time series by implementing other models such as Long-Short Term Memory and Recurrent Neural Networks are also methodologies that could prove useful to improve the SpineNet's performance. Also, to address potential bias on the qualitative analysis, at least a couple of external image expert analysists should be brought onboard the project to qualitatively rate image segmentations.

CHAPTER 6 GENERAL DISCUSSION

This thesis describes a proof of principle adaptation framework to use an inexpensive and portable tool capable of quantifying lumbar spine kinematics during a repetitive trunk flexion-extension task by leveraging the use of an RGB-D camera's depth and infrared (IR) sensors. This work was divided into two studies: *Concurrent validity of a custom computer vision algorithm for measuring lumbar spine motion from RGB-D depth data* where depth data from a single RGB-D camera was validated against an optoelectronic reference system using reflective IR marker clusters (Chapter 4); and *Development and testing of a custom markerless deep learning algorithm for spine segmentation and motion assessment using RGB-D images,* where a deep learning method for image segmentation was developed to detect the spine, upper and lower back segments, which were then used to calculate lumbar spine kinematics during a repetitive trunk flexion-extension task. (Chapter 5).

Study 1 was designed to validate the RGB-D camera's depth data against an optoelectronic motion capture system to ensure that the outputs of the RGB-D camera's depth sensors were appropriate for capturing and calculating lumbar spine kinematics of participants performing a trunk flexion-extension task. To perform this validation, reflective IR markers were placed on participants' backs over T_{10} to T_{12} and over the sacrum. It was found that the RGB-D camera's depth data had an adequate performance in comparison to the optoelectronic motion capture system. Results showed a low error rate over the whole trial for all movement axes *($RMSE \leq 2.05°$)*, and a good level of agreement between the systems was achieved for measuring relative spine ROM *($ICC_{2,1} \geq 0.849$)*; however, Bland Altman plots revealed a bias on the RGB-D camera's measures: the device underestimated angles on the FE axis *($\approx 1.9°$)* and overestimates angles in the LB *($\approx 0.6°$)* and AT axes *($\approx 0.2°$)*. Despite the promising results yielded on the first study, the results in LB and AT must be taken with caution since the movement amplitude in these axes was very small. Thus, study 1 shows that the RGB-D

camera's depth data is valid in comparison to the optoelectronic reference system for measuring spine kinematics during a trunk flexion-extension task using IR markers as trackers, achieving the clinical benchmark for accuracy of human movement tracking. However, appropriate data point selection on the RGB-D camera's depth data is essential for achieving high accuracy levels when measuring kinematic variables, as in study one by tracking the IR reflective markers correctly positioned over anatomical landmarks of interest.

In study 2, we used the validated RGB-D camera's depth data, and its IR data to train an AI model to detect and segment anatomical landmarks of the back, and then used those segmented images to extract and calculate lumbar spine kinematics. The AI model was developed using the U-Net 34 architecture (Ronneberger et al.,2015) as a building block on a bigger architecture, where the three input modules (each one being composed by one U-Net 34) used IR, Colourized depth, and Surface Normal depth data from the RGB-D camera as input, and a fourth Fusion module (also a U-Net 34 block) took predictions from the previous three modules as input to create a final consensus image segmentation. When evaluating the image segmentation from each module, it was found that the IR and Fusion modules achieved better performance on people with markers drawn on their backs than without markers *(mean pixel accuracy (mPA) ≥ 0.9299; mean Jaccard index (mJ) ≥ 0.8746)*; however, the qualitative evaluation of patients without markers revealed that the morphology of the segmentation classes was not adequate, showing distortions in all classes as shown in Chapter 5, Figure 5.11. In contrast, the Colourized depth and Surface Normal depth modules had a good segmentation performance both quantitatively and qualitatively, obtaining high accuracy and similarity indices on patients with markers *(mPA ≥ 0.8855; mJ ≥ 0.7884)* and satisfactory results in the qualitative analysis (Figure 5.11), showing more robustness in the predictions in comparison to the IR and Fusion modules with and without markers.

Kinematic analysis of the AI model on participants under the marked condition showed no significant difference between modules' performance within each movement axis, for example, the FE axis agreement on marked participants ranged between *0.928* and *0.995*, where the Fusion module obtained the lowest result and Colourized depth module obtained the highest, and, therefore, all modules performed quite similarly. Furthermore, the kinematics extracted from the predictions in comparison with the ground truth during the marked condition obtained poor and unrealistic agreement index (i.e., negative mean values) on the LB axis *($-0.212 \leq ICC_{2,1\ LB} \leq 0.630$)*, while agreement on FE and AT axes was excellent *($ICC_{2,1\ FE,\ AT} \geq 0.907$)*. For lumbar spine kinematic analysis of unmarked participants, mean ensemble curves revealed that the method could detect the general trunk flexion-extension movement peaks and movement profiles across all axes independently of the image segmentation module used (IR, Colourized, Surface Normal and Fusion) in spite of the error in magnitudes throughout this axis. Although, LB and AT axes ensemble curves had the correct magnitude, movement profiles and standard deviations do not match current literature (Laird et al., 2019; McGill et al., 1999; Ng, et al., 2001), this is mostly likely to errors in image segmentation that affect LCS position and consequentially kinematic extraction. Standard deviations of the ensemble curves across LB and AT axes were low on Colourized and Surface Normal modules, followed by Fusion and then IR with the highest standard deviations.

Depth data encoding and data fusion was already tested by several studies (Eitel et al., 2015b; Gupta et al., 2014; Hazirbas et al., 2017; Rahman et al., 2017) showing results comparable with state-of-art on their respective AI models. In our study, the use of the Fusion model did not improve our model performance, although, encoding depth data as colourized and surface normal modules was sufficient to achieve a high standard on image segmentation and kinematics extraction. Even though our study metrics are the same as the reference studies (Eitel et al., 2015b; Gupta et al., 2014; Hazirbas et al., 2017;

Rahman et al., 2017), given the differences in methodology (i.e., use of pretrained modules; dataset chosen for testing) absolute quantities are not directly comparable.

Overall, the RGB-D camera's raw depth data achieved adequate results for extracting lumbar spine kinematics against an optoelectronic reference system. The proposed AI image segmentation model showed adequate accuracy and similarity for detecting and segmenting the anatomical landmarks of the back; better results were achieved by the IR and Fusion modules for participants wearing markers, while the Colourized depth and Surface Normal depth modules performed better on participants who were not marked. The extraction of kinematic data was considered adequate under the marked condition in the FE and AT movement axes but not in the LB movement axis, and finally, kinematic extraction under the unmarked condition the model could detect the general movement profile of the performed movements.

Despite the promising results, this work has some limitations. First, the sample size was small and the images that compose our dataset were taken from a university student population, not assuring AI model generalization on all populations. Thus, the sample size was not large enough to address the whole spectrum of human body shapes, genders and ethnic variability. Second, due to lack of a robust visual tracking feature, manually labelling the unmarked condition was considered infeasible. Consequently, the image segmentation quantitative analysis and kinematic analysis of agreement and error on unmarked participants was impractical. Thus, future research projects will continue to develop and optimize image segmentation and kinematic extraction methods to accurately measure and validate markerless measurement of lumbar spine kinematics using an RGB-D camera. And third, qualitative analysis was done by only one image analysis expert in our research group, which might have had a bias on the analysis ratings. Thus, future studies should recruit several independent image analysis experts to rate the segmented images.

CHAPTER 7 GENERAL CONCLUSION

Throughout this work, a framework was developed that uses an inexpensive and portable tool that can be used for measuring lumbar spine kinematics in variety of settings such as research centres, physiotherapy clinics, and patients' homes (i.e. telemedicine), and potentially allowing faster and more assertive assessments. In the first study, the RGB-D camera's raw depth data was validated against an optoelectronic motion capture reference system. In the second study, a method to extract lumbar spine kinematics from the RGB-D camera's depth and IR data using a deep learning model was developed.

In study one, the RGB-D camera's depth data was considered valid when compared to an optoelectronic motion capture system for tracking and calculating lumbar spine kinematics during a repetitive trunk flexion-extension task while participants wore IR reflective markers. The kinematic results achieved excellent agreement in all axes and error indices within clinical benchmark for measuring human motion in clinics (i.e., error index inferior to 2°). However, this method is limited by the use of IR reflective markers, where a markerless system would be more desirable.

In study two, depth and IR data were collected from a single RGB-D camera while participants performed a repetitive trunk flexion-extension movement task under two conditions: with and without drawn point markers on the participant's back. An AI model (SpineNet) was developed that uses three parallel modules (i.e. IR, colourized depth, and surface normal depth data) as inputs and outputted segmented images classifying the participant's spine, upper back, and lower back. A fourth module fused these segment predictions to produce a consensus segmentation. From these segmentations, FE, LB, and AT joint angles of the lumbar spine were calculated. Segmentation predictions made by the IR and Fusion modules had excellent performance for participants wearing markers and moderate performance for unmarked participants, while Colourized depth and Surface Normal depth

modules had a constant good performance independent from participant's condition. Kinematic results were considered excellent in the FE and AT axes in the marked condition; however, the LB axis results were considered poor. The poor performance of the kinematic extraction of the LB axis occurred due to method sensitivity to morphological alterations on image segmentation that would mostly affect LB movement axis. SpineNet was also able to calculate kinematics on unmarked participants that resemble movement patterns stereotypical of the trunk flexion-extension task performed.

Future studies should validate the kinematic extraction against a gold standard optoelectronic systems and improve the kinematic extraction model's robustness, making it less sensitive to morphology of class segmentation and potentially increasing the model accuracy. Furthermore, future studies should make improvements in the current AI model by increasing participant variability by adding a larger number of participants of both genders, ages, and body sizes. Also, image segmentation quality should be appraised by multiple external image analysis experts (i.e. outer from the research group). Another important future direction is adding a wider variety of movements to the research protocol. And lastly, clinical validity should be investigated by adding a couple of elements: 1) one software application that assembles all the technologies described in this research project, delivering all of its advantages to the hands of clinicians and 2) the participation of low back pain patients in the study, to confirm the benefits provided by the proposed system.

CHAPTER 8 REFERENCES

Alvarez, A. (2017). Validation of Microsoft Kinect for Use in Detecting Balance Impairment in ACL Repaired Patients. *Open Access Theses*. http://scholarlyrepository.miami.edu/oa_theses/650

Andersson, G. B. J. (1999). Epidemiological features of chronic low-back pain. *The Lancet*, *354*(9178), 581–585. https://doi.org/http://dx.doi.org/10.1016/S0140-6736(99)01312-4

Ashouri, S., Abedi, M., Abdollahi, M., Dehghan Manshadi, F., Parnianpour, M., & Khalaf, K. (2017). A novel approach to spinal 3-D kinematic assessment using inertial sensors: Towards effective quantitative evaluation of low back pain in clinical settings. *Computers in Biology and Medicine*, *89*(August), 144–149. https://doi.org/10.1016/j.compbiomed.2017.08.002

Asif, U., Bennamoun, M., & Sohel, F. (2015). Efficient RGB-D object categorization using cascaded ensembles of randomized decision trees. *Proceedings - IEEE International Conference on Robotics and Automation*, *2015-June*(June), 1295–1302. https://doi.org/10.1109/ICRA.2015.7139358

Auvinet, E., Multon, F., Manning, V., Meunier, J., & Cobb, J. P. (2017). Validity and sensitivity of the longitudinal asymmetry index to detect gait asymmetry using Microsoft Kinect data. *Gait and Posture*, *51*, 162–168. https://doi.org/10.1016/j.gaitpost.2016.08.022

Bauer, C. M., Rast, F. M., Ernst, M. J., Kool, J., Oetiker, S., Rissanen, S. M., Suni, J. H., & Kankaanpää, M. (2015). Concurrent validity and reliability of a novel wireless inertial measurement system to assess trunk movement. *Journal of Electromyography and Kinesiology*, *25*(5), 782–790. https://doi.org/10.1016/j.jelekin.2015.06.001

Beange, K. H. E., Chan, A. D. C., Beaudette, S. M., & Graham, R. B. (2019). Concurrent validity of a wearable IMU for objective assessments of functional movement quality

and control of the lumbar spine. *Journal of Biomechanics*, *97*, 109356. https://doi.org/10.1016/j.jbiomech.2019.109356

Benson, L. C., Clermont, C. A., Bošnjak, E., & Ferber, R. (2018). The use of wearable devices for walking and running gait analysis outside of the lab: A systematic review. *Gait and Posture*, *63*(March), 124–138. https://doi.org/10.1016/j.gaitpost.2018.04.047

Biely, S. A., Silfies, S. P., Smith, S. S., & Hicks, G. E. (2014a). Clinical observation of standing trunk movements: What do the aberrant movement patterns tell us? *Journal of Orthopaedic and Sports Physical Therapy*, *44*(4), 262–272. https://doi.org/10.2519/jospt.2014.4988

Biely, S. A., Silfies, S. P., Smith, S. S., & Hicks, G. E. (2014b). *Clinical Observation of Standing Trunk Movements: What do the Aberrant Movement Patterns Tell Us? 44*(4), 262–272. https://doi.org/10.2519/jospt.2014.4988

Bone and Joint Canada. (2017). *Low Back Pain*.

Bonnechère, B., Jansen, B., & Van Sint Jan, S. (2016). Cost-effective (gaming) motion and balance devices for functional assessment: Need or hype? *Journal of Biomechanics*, *49*(13), 2561–2565. https://doi.org/10.1016/j.jbiomech.2016.07.011

Carlsson, H., & Rasmussen-Barr, E. (2013). Clinical screening tests for assessing movement control in non-specific low-back pain. A systematic review of intra- and inter-observer reliability studies. *Manual Therapy*, *18*(2), 103–110. https://doi.org/10.1016/j.math.2012.08.004

Castro, A. P. G., Pacheco, J. D., Lourenço, C., Queirós, S., Moreira, A. H. J., Rodrigues, N. F., & Vilaça, J. L. (2017). Evaluation of spinal posture using Microsoft Kinect™: A preliminary case-study with 98 volunteers. *Porto Biomedical Journal*, *2*(1), 18–22. https://doi.org/10.1016/j.pbj.2016.11.004

Chakraborty, S., Nandy, A., Yamaguchi, T., Bonnet, V., & Venture, G. (2020). Accuracy of

image data stream of a markerless motion capture system in determining the local dynamic stability and joint kinematics of human gait. *Journal of Biomechanics*, *104*, 109718. https://doi.org/10.1016/j.jbiomech.2020.109718

Cippitelli, E., Gasparrini, S., Spinsante, S., & Gambi, E. (2015). Kinect as a tool for gait analysis: Validation of a real-time joint extraction algorithm working in side view. *Sensors (Switzerland)*, *15*(1), 1417–1434. https://doi.org/10.3390/s150101417

Clark, R. A., Bower, K. J., Mentiplay, B. F., Paterson, K., & Pua, Y. H. (2013). Concurrent validity of the Microsoft Kinect for assessment of spatiotemporal gait variables. *Journal of Biomechanics*, *46*(15), 2722–2725. https://doi.org/10.1016/j.jbiomech.2013.08.011

Clark, R. A., Mentiplay, B. F., Hough, E., & Pua, Y. H. (2019). Three-dimensional cameras and skeleton pose tracking for physical function assessment: A review of uses, validity, current developments and Kinect alternatives. *Gait and Posture*, *68*, 193–200. https://doi.org/10.1016/j.gaitpost.2018.11.029

Clark, R. A., Pua, Y. H., Bryant, A. L., & Hunt, M. A. (2013). Validity of the Microsoft Kinect for providing lateral trunk lean feedback during gait retraining. *Gait and Posture*, *38*(4), 1064–1066. https://doi.org/10.1016/j.gaitpost.2013.03.029

Clark, R. A., Pua, Y. H., Fortin, K., Ritchie, C., Webster, K. E., Denehy, L., & Bryant, A. L. (2012). Validity of the Microsoft Kinect for assessment of postural control. *Gait and Posture*, *36*(3), 372–377. https://doi.org/10.1016/j.gaitpost.2012.03.033

Clark, R. A., Pua, Y. H., Oliveira, C. C., Bower, K. J., Thilarajah, S., McGaw, R., Hasanki, K., & Mentiplay, B. F. (2015). Reliability and concurrent validity of the Microsoft Xbox One Kinect for assessment of standing balance and postural control. *Gait and Posture*, *42*(2), 210–213. https://doi.org/10.1016/j.gaitpost.2015.03.005

Croft, P. R., Macfarlane, G. J., Papageorgiou, A. C., Thomas, E., & Silman, A. J. (1998). General practice a prospective study. *British Medical Journal*, *316*(January 2005),

1356–1359. https://doi.org/10.1136/bmj.316.7141.1356

Cuesta-Vargas, A. I., Galán-Mercant, A., & Williams, J. M. (2010). The use of inertial sensors system for human motion analysis. *Physical Therapy Reviews*, *15*(6), 462–473. https://doi.org/10.1179/1743288X11Y.0000000006

Delitto, a, Erhard, R. E., & Bowling, R. W. (1995). A treatment-based classification approach to low back syndrome: identifying and staging patients for conservative treatment. *Physical Therapy*, *75*(6), 470–485; discussion 485-489. https://doi.org/10.1197/j.jht.2007.12.001

Denteneer, L., Stassijns, G., De Hertogh, W., Truijen, S., & Van Daele, U. (2017). Inter- and Intrarater Reliability of Clinical Tests Associated With Functional Lumbar Segmental Instability and Motor Control Impairment in Patients With Low Back Pain: A Systematic Review. *Archives of Physical Medicine and Rehabilitation*, *98*(1), 151-164.e6. https://doi.org/10.1016/j.apmr.2016.07.020

Dillingham, T. R. (1995). Evaluation and management of low back pain: an overview. *Spine (Phila-Hanley and Belfus)*, *9*, 559–596.

Dolatabadi, E., Taati, B., & Mihailidis, A. (2016). Concurrent validity of the Microsoft Kinect for Windows v2 for measuring spatiotemporal gait parameters. *Medical Engineering and Physics*, *38*(9), 952–958. https://doi.org/10.1016/j.medengphy.2016.06.015

Dugan, S. A., & Bhat, K. P. (2005). Biomechanics and analysis of running gait. *Physical Medicine and Rehabilitation Clinics of North America*, *16*(3), 603–621. https://doi.org/10.1016/j.pmr.2005.02.007

Eitel, A., Springenberg, J. T., Spinello, L., Riedmiller, M., & Burgard, W. (2015a). Multimodal deep learning for robust RGB-D object recognition. *IEEE International Conference on Intelligent Robots and Systems*, *2015-Decem*(11), 681–687.

https://doi.org/10.1109/IROS.2015.7353446

Eitel, A., Springenberg, J. T., Spinello, L., Riedmiller, M., & Burgard, W. (2015b). Multimodal deep learning for robust RGB-D object recognition. *2015 IEEE/RSJ International Conference on Intelligent Robots and Systems (IROS), 2015-Decem*, 681–687. https://doi.org/10.1109/IROS.2015.7353446

Eltoukhy, M. A., Kuenze, C., Oh, J., & Signorile, J. F. (2018). Validation of Static and Dynamic Balance Assessment Using Microsoft Kinect for Young and Elderly Populations. *IEEE Journal of Biomedical and Health Informatics*, *22*(1), 147–153. https://doi.org/10.1109/JBHI.2017.2686330

Eltoukhy, M., Oh, J., Kuenze, C., & Signorile, J. (2017). Improved kinect-based spatiotemporal and kinematic treadmill gait assessment. *Gait and Posture*, *51*, 77–83. https://doi.org/10.1016/j.gaitpost.2016.10.001

Fritz, J. M., Cleland, J. A., & Childs, J. D. (2007). Subgrouping patients with low back pain: evolution of a classification approach to physical therapy. *The Journal of Orthopaedic and Sports Physical Therapy*, *37*(6), 290–302. https://doi.org/10.2519/jospt.2007.2498

Galna, B., Barry, G., Jackson, D., Mhiripiri, D., Olivier, P., & Rochester, L. (2014). Accuracy of the Microsoft Kinect sensor for measuring movement in people with Parkinson's disease. *Gait and Posture*, *39*(4), 1062–1068. https://doi.org/10.1016/j.gaitpost.2014.01.008

Garcia-Garcia, A., Orts-Escolano, S., Oprea, S., Villena-Martinez, V., & Garcia-Rodriguez, J. (2017). *A Review on Deep Learning Techniques Applied to Semantic Segmentation*. 1–23. https://doi.org/10.1007/978-1-4471-4640-7

Geerse, D. J., Coolen, B. H., & Roerdink, M. (2015). Kinematic Validation of a Multi-Kinect v2 Instrumented 10-Meter Walkway for Quantitative Gait Assessments. *PLOS ONE*, *10*(10), e0139913. https://doi.org/10.1371/journal.pone.0139913

Graham, R. B., Oikawa, L. Y., & Ross, G. B. (2014). Comparing the local dynamic stability of trunk movements between varsity athletes with and without non-specific low back pain. *Journal of Biomechanics*, *47*(6), 1459–1464. https://doi.org/10.1016/j.jbiomech.2014.01.033

Granata, K. P., & England, S. A. (2006). Stability of dynamic trunk movement. *Spine*, *31*(10), E271--E276. https://doi.org/10.1097/01.brs.0000216445.28943.d1

Gupta, S., Girshick, R., Arbeláez, P., & Malik, J. (2014). Learning rich features from RGB-D images for object detection and segmentation. *Lecture Notes in Computer Science (Including Subseries Lecture Notes in Artificial Intelligence and Lecture Notes in Bioinformatics)*, *8695 LNCS*(PART 7), 345–360. https://doi.org/10.1007/978-3-319-10584-0_23

Hannink, E., Shannon, T., Barker, K. L., & Dawes, H. (2020). The reliability and reproducibility of sagittal spinal curvature measurement using the Microsoft Kinect V2. *Journal of Back and Musculoskeletal Rehabilitation*, *33*(2), 295–301. https://doi.org/10.3233/BMR-191554

Hazirbas, C., Ma, L., Domokos, C., & Cremers, D. (2017). FuseNet: Incorporating depth into semantic segmentation via fusion-based CNN architecture. *Lecture Notes in Computer Science (Including Subseries Lecture Notes in Artificial Intelligence and Lecture Notes in Bioinformatics)*, *10111 LNCS*. https://doi.org/10.1007/978-3-319-54181-5_14

Hemming, R., Sheeran, L., van Deursen, R., & Sparkes, V. (2018). Non-specific chronic low back pain: differences in spinal kinematics in subgroups during functional tasks. *European Spine Journal*, *27*(1), 163–170. https://doi.org/10.1007/s00586-017-5217-1

Hicks, G. E., Fritz, J. M., Delitto, A., & Mishock, J. (2003). Interrater Reliability of Clinical Examination Measures for Identification of Lumbar Segmental Instability. *Archives of Physical Medicine and Rehabilitation*, *84*(12), 1858–1864.

https://doi.org/10.1016/S0003-9993(03)00365-4

Hotrabhavananda, B., Mishra, A. K., Skubic, M., Hotrabhavananda, N., & Abbott, C. (2016). Evaluation of the microsoft kinect skeletal versus depth data analysis for timed-up and go and figure of 8 walk tests. *Proceedings of the Annual International Conference of the IEEE Engineering in Medicine and Biology Society, EMBS*, *2016-Octob*, 2274–2277. https://doi.org/10.1109/EMBC.2016.7591183

Howard, J. and others. (2018). *fastai*. GitHub. https://github.com/fastai/fastai

Jaspers, E., Desloovere, K., Bruyninckx, H., Klingels, K., Molenaers, G., Aertbeliën, E., Van Gestel, L., & Feys, H. (2011). Three-dimensional upper limb movement characteristics in children with hemiplegic cerebral palsy and typically developing children. *Research in Developmental Disabilities*, *32*(6), 2283–2294. https://doi.org/10.1016/j.ridd.2011.07.038

Kjaer, P., Kongsted, A., Ris, I., Abbott, A., Rasmussen, C. D. N., Roos, E. M., Skou, S. T., Andersen, T. E., & Hartvigsen, J. (2018). GLA:D ® Back group-based patient education integrated with exercises to support self-management of back pain - Development, theories and scientific evidence - Development, t. *BMC Musculoskeletal Disorders*, *19*(1), 1–21. https://doi.org/10.1186/s12891-018-2334-x

Lai, K., Bo, L., Ren, X., & Fox, D. (2011). A large-scale hierarchical multi-view RGB-D object dataset. *Proceedings - IEEE International Conference on Robotics and Automation*, 1817–1824. https://doi.org/10.1109/ICRA.2011.5980382

Laird, R. A., Keating, J. L., Ussing, K., Li, P., & Kent, P. (2019). Does movement matter in people with back pain? Investigating “atypical” lumbo-pelvic kinematics in people with and without back pain using wireless movement sensors. *BMC Musculoskeletal Disorders*, *20*(1), 1–15. https://doi.org/10.1186/s12891-018-2387-x

Lebel, K., Boissy, P., Hamel, M., & Duval, C. (2013). Inertial measures of motion for clinical

biomechanics: Comparative assessment of accuracy under controlled conditions - Effect of velocity. *PLoS ONE*, *8*(11). https://doi.org/10.1371/journal.pone.0079945

Lebel, K., Boissy, P., Hamel, M., & Duval, C. (2015). Inertial measures of motion for clinical biomechanics: Comparative assessment of accuracy under controlled conditions - Changes in accuracy over time. *PLoS ONE*, *10*(3), 1–12. https://doi.org/10.1371/journal.pone.0118361

Macpherson, T. W., Taylor, J., McBain, T., Weston, M., & Spears, I. R. (2016). Real-time measurement of pelvis and trunk kinematics during treadmill locomotion using a low-cost depth-sensing camera: A concurrent validity study. *Journal of Biomechanics*, *49*(3), 474–478. https://doi.org/10.1016/j.jbiomech.2015.12.008

Mavor, M. P., & Graham, R. B. (2015). Exploring the relationship between local and global dynamic trunk stabilities during repetitive lifting tasks. *Journal of Biomechanics*, *48*(14), 3955–3960. https://doi.org/10.1016/j.jbiomech.2015.09.026

Mazzone, B., Wood, R., & Gombatto, S. (2016). Spine Kinematics During Prone Extension in People With and Without Low Back Pain and Among Classification-Specific Low Back Pain Subgroups. *The Journal of Orthopaedic and Sports Physical Therapy*, *1*(7), 1–33. https://doi.org/10.2519/jospt.2016.6159

McGill, S. M., Yingling, V. R., & Peach, J. P. (1999). Three-dimensional kinematics and trunk muscle myoelectric activity in the elderly spine - A database compared to young people. *Clinical Biomechanics*, *14*(6), 389–395. https://doi.org/10.1016/S0268-0033(98)00111-9

McGinley, J. L., Baker, R., Wolfe, R., & Morris, M. E. (2009). The reliability of three-dimensional kinematic gait measurements: A systematic review. *Gait and Posture*, *29*(3), 360–369. https://doi.org/10.1016/j.gaitpost.2008.09.003

Mentiplay, B. F., Clark, R. A., Mullins, A., Bryant, A. L., Bartold, S., & Paterson, K.

(2013a). Reliability and validity of the Microsoft Kinect for evaluating static foot posture. *Journal of Foot and Ankle Research*, *6*(1), 14. https://doi.org/10.1186/1757-1146-6-14

Mentiplay, B. F., Clark, R. A., Mullins, A., Bryant, A. L., Bartold, S., & Paterson, K. (2013b). Reliability and validity of the Microsoft Kinect for evaluating static foot posture. *Journal of Foot and Ankle Research*, *6*(1), 1–10. https://doi.org/10.1186/1757-1146-6-14

Mentiplay, B. F., Perraton, L. G., Bower, K. J., Pua, Y. H., McGaw, R., Heywood, S., & Clark, R. A. (2015). Gait assessment using the Microsoft Xbox One Kinect: Concurrent validity and inter-day reliability of spatiotemporal and kinematic variables. *Journal of Biomechanics*, *48*(10), 2166–2170. https://doi.org/10.1016/j.jbiomech.2015.05.021

Microsoft. (2020). *JointType Enumeration*.

Mokhtarinia, H. R., Sanjari, M. A., Chehrehrazi, M., Kahrizi, S., & Parnianpour, M. (2016). Trunk coordination in healthy and chronic nonspecific low back pain subjects during repetitive flexion-extension tasks: Effects of movement asymmetry, velocity and load. *Human Movement Science*, *45*, 182–192. https://doi.org/10.1016/j.humov.2015.11.007

Moreno, F. Á., Merchán-Baeza, J. A., González-Sánchez, M., González-Jiménez, J., & Cuesta-Vargas, A. I. (2017). Experimental validation of depth cameras for the parameterization of functional balance of patients in clinical tests. *Sensors (Switzerland)*, *17*(2). https://doi.org/10.3390/s17020424

Müller, B., Ilg, W., Giese, M. A., & Ludolph, N. (2017). Validation of enhanced kinect sensor based motion capturing for gait assessment. *PLOS ONE*, *12*(4), e0175813. https://doi.org/10.1371/journal.pone.0175813

Ng, J. K. F., Kippers, V., Richardson, C. A., & Parnianpour, M. (2001). Range of motion and lordosis of the lumbar spine: Reliability of measurement and normative values. *Spine*,

26(1), 53–60. https://doi.org/10.1097/00007632-200101010-00011

O'Sullivan, P. (2005). Diagnosis and classification of chronic low back pain disorders: Maladaptive movement and motor control impairments as underlying mechanism. *Manual Therapy*, *10*(4), 242–255. https://doi.org/10.1016/j.math.2005.07.001

Ono, T., & Takahashi, M. (2019). Walking Measurement System Including Turning Motion Assessment Using Depth Sensors. *2019 12th Asian Control Conference, ASCC 2019*, 861–866.

Otte, K., Kayser, B., Mansow-Model, S., Verrel, J., Paul, F., Brandt, A. U., & Schmitz-Hübsch, T. (2016). Accuracy and reliability of the kinect version 2 for clinical measurement of motor function. *PLoS ONE*, *11*(11), 1–17. https://doi.org/10.1371/journal.pone.0166532

Papi, E., Bull, A. M. J., & McGregor, A. H. (2018). Is there evidence to use kinematic/kinetic measures clinically in low back pain patients? A systematic review. *Clinical Biomechanics*, *55*(April), 53–64. https://doi.org/10.1016/j.clinbiomech.2018.04.006

Papi, E., Murtagh, G. M., & McGregor, A. H. (2016). Wearable technologies in osteoarthritis: A qualitative study of clinicians' preferences. *BMJ Open*, *6*(1), 1–7. https://doi.org/10.1136/bmjopen-2015-009544

Paszke, A., Gross, S., Massa, F., Lerer, A., Bradbury, J., Chanan, G., Killeen, T., Lin, Z., Gimelshein, N., Antiga, L., Desmaison, A., Köpf, A., Yang, E., DeVito, Z., Raison, M., Tejani, A., Chilamkurthy, S., Steiner, B., Fang, L., … Chintala, S. (2019). *PyTorch: An Imperative Style, High-Performance Deep Learning Library*. *NeurIPS*. http://arxiv.org/abs/1912.01703

Paterson, K. L., Clark, R. A., Mullins, A., Bryant, A. L., & Mentiplay, B. F. (2015). Predicting dynamic foot function from static foot posture: Comparison between visual assessment, motion analysis, and a commercially available depth camera. *Journal of*

Orthopaedic and Sports Physical Therapy, *45*(10), 789–798. https://doi.org/10.2519/jospt.2015.5616

Plantard, P., Shum, H. P. H., Le Pierres, A. S., & Multon, F. (2017). Validation of an ergonomic assessment method using Kinect data in real workplace conditions. *Applied Ergonomics*, *65*, 562–569. https://doi.org/10.1016/j.apergo.2016.10.015

Quek, J., Brauer, S. G., Treleaven, J., & Clark, R. A. (2017). The concurrent validity and intrarater reliability of the Microsoft Kinect to measure thoracic kyphosis. *International Journal of Rehabilitation Research*, *40*(3), 279–284. https://doi.org/10.1097/MRR.0000000000000237

Rabin, A., Shashua, A., Pizem, K., & Dar, G. (2013). The interrater reliability of physical examination tests that may predict the outcome or suggest the need for lumbar stabilization exercises. *Journal of Orthopaedic and Sports Physical Therapy*, *43*(2), 83–90. https://doi.org/10.2519/jospt.2013.4310

Rahman, M. M., Tan, Y., Xue, J., & Lu, K. (2017). RGB-D Object Recognition with Multimodal Deep Convolutional Neural Networks. *IEEE International Conference on Multimedia and Expo (ICME)*, *July*, 991–996.

Ricci, L., Taffoni, F., & Formica, D. (2016). On the orientation error of IMU: Investigating static and dynamic accuracy targeting human motion. *PLoS ONE*, *11*(9). https://doi.org/10.1371/journal.pone.0161940

Roland, M., & Van Tulder, M. (1998). Should radiologists change the way they report plain radiography of the spine? *Lancet*, *352*(9123), 229–230. https://doi.org/10.1016/S0140-6736(97)11499-4

Ronneberger, O., Fischer, P., & Brox, T. (2015). U-net: Convolutional networks for biomedical image segmentation. *Lecture Notes in Computer Science (Including Subseries Lecture Notes in Artificial Intelligence and Lecture Notes in Bioinformatics)*,

9351, 234–241. https://doi.org/10.1007/978-3-319-24574-4_28

Rosenberg, M., Thornton, A. L., Lay, B. S., Ward, B., Nathan, D., Hunt, D., & Braham, R. (2016). Development of a kinect software tool to classify movements during active video gaming. *PLoS ONE*, *11*(7), 1–14. https://doi.org/10.1371/journal.pone.0159356

Ross, G. B., Mavor, M., Brown, S. H. M., & Graham, R. B. (2015). The Effects of Experimentally Induced Low Back Pain on Spine Rotational Stiffness and Local Dynamic Stability. *Annals of Biomedical Engineering*, *43*(9), 2120–2130. https://doi.org/10.1007/s10439-015-1268-9

Saleh, M., & Murdoch, G. (1985). In defence of gait analysis. Observation and measurement in gait assessment. *Journal of Bone and Joint Surgery - Series B*, *67*(2), 237–241. https://doi.org/10.1302/0301-620x.67b2.3980533

Samir, M., Golkar, E., & Rahni, A. A. A. (2016). Comparison between the Kinect™ V1 and Kinect™ V2 for respiratory motion tracking. *IEEE 2015 International Conference on Signal and Image Processing Applications, ICSIPA 2015 - Proceedings*, 150–155. https://doi.org/10.1109/ICSIPA.2015.7412180

Sánchez-Zuriaga, D., López-Pascual, J., Garrido-Jaén, D., De Moya, M. F. P., & Prat-Pastor, J. (2011). Reliability and validity of a new objective tool for low back pain functional assessment. *Spine*, *36*(16), 1279–1288. https://doi.org/10.1097/BRS.0b013e3181f471d8

Sarbolandi, H., Lefloch, D., & Kolb, A. (2015). Kinect range sensing: Structured-light versus Time-of-Flight Kinect. *Computer Vision and Image Understanding*, *139*, 1–20. https://doi.org/10.1016/j.cviu.2015.05.006

Schneider, E., Copsey, S., & Irastorza, X. (2010). *OSH [Occupational Safety and Health] in figures: Work-related musculoskeletal disorders in the EU-Facts and Figures*. https://doi.org/10.2802/10952

Schwarz, L. A., Mkhitaryan, A., Mateus, D., & Navab, N. (2012). Human skeleton tracking

from depth data using geodesic distances and optical flow. *Image and Vision Computing*, *30*(3), 217–226. https://doi.org/10.1016/j.imavis.2011.12.001

Shum, G. L. K., Crosbie, J., & Lee, R. Y. W. (2005). Effect of low back pain on the kinematics and joint coordination of the lumbar spine and hip during sit-to-stand and stand-to-sit. *Spine*, *30*(17), 1998–2004. https://doi.org/10.1097/01.brs.0000176195.16128.27

Silfies, S. P., Bhattacharya, A., Biely, S., Smith, S. S., & Giszter, S. (2009). Trunk control during standing reach: A dynamical system analysis of movement strategies in patients with mechanical low back pain. *Gait and Posture*, *29*(3), 370–376. https://doi.org/10.1016/j.gaitpost.2008.10.053

Simon, S. R. (2004). Quantification of human motion: Gait analysis - Benefits and limitations to its application to clinical problems. *Journal of Biomechanics*, *37*(12), 1869–1880. https://doi.org/10.1016/j.jbiomech.2004.02.047

Smeets, R., Köke, A., Lin, C. W., Ferreira, M., & Demoulin, C. (2011). Measures of function in low back pain/disorders: Low Back Pain Rating Scale (LBPRS), Oswestry Disability Index (ODI), Progressive Isoinertial Lifting Evaluation (PILE), Quebec Back Pain Disability Scale (QBPDS), and Roland-Morris Disability Questionnaire . *Arthritis Care and Research*, *63*(SUPPL. 11), 158–173. https://doi.org/10.1002/acr.20542

Socher, R., Huval, B., Bhat, B., Manning, C. D., & Ng, A. Y. (2012). Convolutional-recursive deep learning for 3D object classification. *Advances in Neural Information Processing Systems*, *1*(i), 656–664.

Spinelli, B. A., Wattananon, P., Silfies, S., Talaty, M., & Ebaugh, D. (2015). Using kinematics and a dynamical systems approach to enhance understanding of clinically observed aberrant movement patterns. *Manual Therapy*, *20*(1), 221–226. https://doi.org/10.1016/j.math.2014.07.012

Springer, S., & Seligmann, G. Y. (2016). Validity of the kinect for gait assessment: A focused review. *Sensors (Switzerland)*, *16*(2), 194. https://doi.org/10.3390/s16020194

Stanton, T. R., Fritz, J. M., Hancock, M. J., Latimer, J., Maher, C. G., Wand, B. M., & Parent, E. C. (2011a). Evaluation of a Treatment-Based Classification Algorithm for Low Back Pain: A Cross-Sectional Study. *Physical Therapy*, *91*(4), 496–509.

Stanton, T. R., Fritz, J. M., Hancock, M. J., Latimer, J., Maher, C. G., Wand, B. M., & Parent, E. C. (2011b). Pain : A Cross-Sectional Study. *Physical Therapy*, *91*(4), 496–509.

Stone, E. E., & Skubic, M. (2011). Passive in-home measurement of stride-to-stride gait variability comparing vision and Kinect sensing. *Conference Proceedings : ... Annual International Conference of the IEEE Engineering in Medicine and Biology Society. IEEE Engineering in Medicine and Biology Society. Conference*, *2011*, 6491–6494.

Thoma, M. (2016). *A Survey of Semantic Segmentation*. 1–16. http://arxiv.org/abs/1602.06541

Vallat, R. (2018). Pingouin: statistics in Python. *Journal of Open Source Software*, *3*(31), 1026. https://doi.org/10.21105/joss.01026

van Tulder, M. W., Assendelft, W. J. J., Koes, B. W., & Bouter, L. M. (1997). Spinal Radiographic Findings and Nonspecific Low Back Pain. *Spine*, *22*(4), 427–434. https://doi.org/10.1097/00007632-199702150-00015

Vernon, S., Paterson, K., Bower, K., McGinley, J., Miller, K., Pua, Y. H., & Clark, R. A. (2015). Quantifying individual components of the timed up and go using the kinect in people living with stroke. *Neurorehabilitation and Neural Repair*, *29*(1), 48–53. https://doi.org/10.1177/1545968314529475

Virtanen, P., Gommers, R., Oliphant, T. E., Haberland, M., Reddy, T., Cournapeau, D., Burovski, E., Peterson, P., Weckesser, W., Bright, J., van der Walt, S. J., Brett, M.,

Wilson, J., Millman, K. J., Mayorov, N., Nelson, A. R. J., Jones, E., Kern, R., Larson, E., … van Mulbregt, P. (2020). SciPy 1.0: fundamental algorithms for scientific computing in Python. *Nature Methods*, *17*(3), 261–272. https://doi.org/10.1038/s41592-019-0686-2

Visser, J. E., Carpenter, M. G., van der Kooij, H., & Bloem, B. R. (2008). The clinical utility of posturography. *Clinical Neurophysiology*, *119*(11), 2424–2436. https://doi.org/10.1016/j.clinph.2008.07.220

Wasenmüller, O. (2016). *Comparison of Kinect v1 and v2 Depth Images in Terms of Accuracy and Precision*. *October*.

Wattananon, P., Ebaugh, D., Biely, S. A., Smith, S. S., Hicks, G. E., & Silfies, S. P. (2017). Kinematic characterization of clinically observed aberrant movement patterns in patients with non-specific low back pain: A cross-sectional study. *BMC Musculoskeletal Disorders*, *18*(1), 1–12. https://doi.org/10.1186/s12891-017-1820-x

Whittle, M. W. (1996). Clinical gait analysis: A review. *Human Movement Science*, *15*(3), 369–387. https://doi.org/10.1016/0167-9457(96)00006-1

Workplace Safety and Insurance Board of Ontario. (2016). *WSIB by the Numbers 2016*.

Xiao, Z., Mengyin, F., Yi, Y., & Lv, N. (2012). 3D human postures recognition using kinect. *Proceedings of the 2012 4th International Conference on Intelligent Human-Machine Systems and Cybernetics, IHMSC 2012*, *1*, 344–347. https://doi.org/10.1109/IHMSC.2012.92

Xu, X., McGorry, R. W., Chou, L. S., Lin, J. hua, & Chang, C. chi. (2015). Accuracy of the Microsoft Kinect™ for measuring gait parameters during treadmill walking. *Gait and Posture*, *42*(2), 145–151. https://doi.org/10.1016/j.gaitpost.2015.05.002

Yang, L., Zhang, L., Dong, H., Alelaiwi, A., & Saddik, A. El. (2015). Evaluating and improving the depth accuracy of Kinect for Windows v2. *IEEE Sensors Journal*, *15*(8),

4275–4285. https://doi.org/10.1109/JSEN.2015.2416651

Yang, Y., Pu, F., Li, Y., Li, S., Fan, Y., & Li, D. (2014). Reliability and validity of kinect RGB-D sensor for assessing standing balance. *IEEE Sensors Journal*, *14*(5), 1633–1638. https://doi.org/10.1109/JSEN.2013.2296509

Zhou, H., & Hu, H. (2008). Human motion tracking for rehabilitation-A survey. *Biomedical Signal Processing and Control*, *3*(1), 1–18. https://doi.org/10.1016/j.bspc.2007.09.001

Zimmermann, T., Taetz, B., & Bleser, G. (2018). IMU-to-segment assignment and orientation alignment for the lower body using deep learning. *Sensors (Switzerland)*, *18*(1), E302. https://doi.org/10.3390/s18010302

APPENDIX A

Concurrent validity of a custom computer vision algorithm for measuring lumbar spine motion from RGB-D depth data – Consent Form and Ethics Certificate

Research Consent Form

Research Project Title: The effect of focus of attention on local dynamic stability during repetitive spine flexion

Principal Investigators:

613-562-5800 X 1025; ryan.graham@uottawa.ca
University of Ottawa
Faculty of Health Sciences
Department of Human Kinetics
200 Lees Ave (E020)
Ottawa, ON K1N6N5

Université d'Ottawa
Faculté des sciences de la santé

École des sciences de l'activité physique

University of Ottawa
Faculty of Health Sciences

School of Human Kinetics

+1 613 562 5800 ext. 1025
Ryan.Graham@uottawa.ca

200 Lees Ave. (E020)
Ottawa ON K1N 6N5 Canada

www.uOttawa.ca

Background and Purpose of the Study:
Spine stability during dynamic movements is achieved through complex interactions between multiple systems of the body. It is important to understand how different factors affect stability so that conditions can be optimized to improve stability. Focus of attention has previously been found to affect performance of movement tasks from sport to postural balance. The goal of this study is to assess how an individual's focus of attention can affect stability of the spine during a dynamic flexion task. Stability will be evaluated using a local dynamic stability analysis.

Description of Study Procedures:
You are invited to participate in a one-day motion analysis procedure for approximately 1 hour at the University of Ottawa Human Movement Biomechanics Laboratory (200 Lees Avenue, E020). The study protocol consists of completion of a repetitive spine flexion task three times under different conditions. The task includes 35 cycles of moving from an upright standing position, into forward spine flexion and back to standing. More specifically, you will be asked to touch a target placed at shoulder height, then move into spine flexion to touch a target placed 50cm anterior to your knee. You will be asked to touch the targets at a frequency of 0.5 Hz, resulting in each cycle lasting 4 seconds. The three conditions will involve changing the focus of attention during the protocol. Further instructions will be given prior to completion of the trial. These conditions will be completed in a randomized order, and a minimum three minute break will be provided between conditions. More time will be provided if it is required to ensure no signs of fatigue are present.

Before the procedure, you will be asked to change into form fitting spandex clothing for the remainder of the data collection. Reflective markers will be placed on anatomical landmarks with double sided tape. Marker clusters will be attached to the lower back and pelvis with tape around your trunk and waist. For the flexion task, your waist will be secured to a brace with a strap on the line of your anterior superior iliac spines in order to limit lower limb movement and isolate the trunk.

Following the flexion protocol, you will be asked to fill out a follow-up questionnaire regarding any pain or fatigue experienced during the protocol.

Possible Risks and Discomforts:
There are no significant risks associated with participating in this study. You may experience pain and fatigue due to the nature of the flexion task. However, sufficient rest will be given to reduce these effects. Should you experience any major discomfort, please tell us immediately and seek primary care from a medical professional on campus (100 Marie Curie, Ottawa, Tel.: 613-564-3950) or a medical professional of your choosing.

Possible Benefits:
You will not directly benefit from participating in this study. However, the results of this study will greatly add to our knowledge of how focus of attention affects local dynamic stability during spine flexion tasks.

Voluntary Participation:
You are not obliged to participate in this study; participation in this study is voluntary. You may also withdraw from the study at any time with no penalty or coercion.

Confidentiality:
All personal information is kept confidential unless release is required by law. Information gained from this study will be stored electronically and will need a password to access. Paper study records are stored in a locked cabinet and will be destroyed after 5 years; electronic records will be deleted and paper records will be shredded. You will not be identified by name in any reports of the completed study. Your anonymity will be strictly maintained – you will not be identified by your name, but will be determined by an independent study number.

Compensation:
No monetary compensation will be provided for participation in this study. However the data will provide significant contributions to understanding how focus of attention can affect dynamic movements.

Exclusion Criteria
You will be excluded from participation in this study if you have a history of low back pain. Also if you have previously experienced any: cardiovascular conditions, neurologic disorders (neuropathy, neurodegenerative conditions), low back pain (discogenic, mechanical, myofascial), ankle injury (sprained, fractured) use of medication (anti-inflammatories, analgesics, anticonvulsants, antidepressants), history of low back injury (discogenic mechanical) use of anticoagulent therapy, stroke or TIA, spine trauma, motor vehicle accident, lumbar spine surgery,

hypertension, CTD and focal neurological symptoms (sensory/motor) you will be excluded from participation.

Questions about the Study:
You are free to ask questions at any time; you can contact the principal investigators by email: Wantuir Junior , Eric Bourdon and/or Dr. Ryan Graham (ryan.graham@uottawa.ca). This project is funded by the Natural Sciences and Engineering Research Council of Canada. This protocol has been approved by the University of Ottawa research ethics board. If you have any questions regarding the ethical conduct of this study, you may contact the Protocol Officer for Ethics in Research, University of Ottawa, Tabaret Hall, 550 Cumberland Street, Room 154, Ottawa ON, K1N 6N5. Tel.: (613) 562-5387 Email: ethics@uottawa.ca

Research Project Title: **The effect of focus of attention on local dynamic stability during repetitive spine flexion**

Consent:
I have read this consent form, and I agree to participate in the procedures of this study.

_____
Printed Name of Participant

_____ _____
Signature of Participant Date

Investigator Statement (or Person Explaining the Consent):
I have carefully explained to the research participant the nature of the above research study. To the best of my knowledge, the research participant signing this consent form understands the nature, demands, risks and benefits involved in participating in this study. I acknowledge my responsibility for the care and well-being of the above research participant, to respect the rights and wishes of the research participant, and to conduct the study according to applicable Good Clinical Practice guidelines and regulations.

_____
Name of Investigator/Delegate (printed)

_____ _____
Signature of Investigator/Delegate Date

Informed Consent to have Pictures Taken:
I consent to have side view pictures taken of myself completing the experiment, and understand that no pictures will be taken at any point without me knowing. I also understand that if any of these pictures are used in a subsequent presentation or publication, that my face and any other identifiers will be blurred. You can still participate in the research study without consenting to have pictures taken.

_____ _____
Name Date

_____
Signature

_____ _____
Witness Name Witness Signature

Future Participation:

- ☐ I am interested in being contacted to participate in future research performed by this laboratory (your email information will be saved in a password protected file).

Université d'Ottawa
Faculté des sciences de la santé

École des sciences de l'activité physique

University of Ottawa
Faculty of Health Sciences

School of Human Kinetics

☎ +1 613 562 5800 ext. 1025
Ryan.Graham@uottawa.ca

200 Lees Ave. (E020)
Ottawa ON K1N 6N5 Canada

www.uOttawa.ca

Formulaire de consentement à la recherche

Titre du projet de recherche: L'effet de l'attention sur la stabilité dynamique locale pendant la flexion répétitive de la colonne vertébrale

Chercheurs principaux:

Wantuir Carlos Ramos Junior

Eric Bourdon

Dr. Ryan Graham
613-562-5800 X 1025; ryan.graham@uottawa.ca
University of Ottawa
Faculty of Health Sciences
Department of Human Kinetics
200 Lees Ave (E020)
Ottawa, ON K1N6N5

Contexte et objectif de l'étude:

La stabilité de la colonne vertébrale pendant les mouvements dynamiques est obtenue par des interactions complexes avec divers systèmes du corps. Il est important de comprendre comment différents facteurs affectent la stabilité dans le but que les conditions peuvent être optimisées et ainsi, améliorer la stabilité. On a constaté auparavant que l'attention avait eu une influence sur la performance des tâches de mouvement du sport ainsi que l'équilibre postural. L'objectif de cette étude est d'évaluer comment l'attention d'un individu peut affecter la stabilité de la colonne vertébrale pendant l'exécution d'une tâche de flexion dynamique. La stabilité sera évaluée à l'aide d'une analyse de stabilité dynamique locale.

Description des procédures de l'étude:

Vous êtes invités à participer à une procédure d'analyse pendant environ 1 heure 20 minutes au Laboratoire de biomécanique des mouvements humains de l'Université d'Ottawa (200, avenue Lees, E020). Le protocole d'étude est d'accomplir une tâche répétitive de flexion de la colonne vertébrale trois fois dans des conditions différentes. La tâche comprend 35 cycles de déplacement d'une position debout, en flexion de la colonne vertébrale et de retour à la position debout. Plus précisément, on vous demandera de toucher une cible placée à la hauteur de l'épaule, puis ensuite de vous déplacer pour toucher une cible placée à 50 cm antérieurs de votre genou. On vous demandera de toucher les cibles à une fréquence de 0,5 Hz, ce qui est un cycle de 4 secondes. Les trois conditions impliquent de varier votre foyer d'attention pendant l'expérience. D'autres instructions seront données avant les essais. Ces conditions seront complétées de façon aléatoire, et une pause de trois minutes

(minimum) sera enforcée entre les conditions. Du temps supplémentaire sera accordé s'il est nécessaire de s'assurer qu'aucun signe de fatigue n'est présent.

Avant la procédure, on vous demandera de vous changer en tenue style spandex pour de la collecte de données. Les marqueurs réfléchissants seront placés sur des repères anatomiques avec du ruban adhésif double face. Des grappes de marqueur seront attachées au bas du dos et au bassin avec du ruban adhésif autour de votre tronc et de votre taille. Pour la tâche de flexion, votre taille sera fixée à une attelle avec une sangle sur la ligne de vos épines iliaque antérieure supérieure afin de limiter le mouvement des membres inférieurs et d'isoler le tronc. Après le protocole de flexion, on vous demandera de remplir un questionnaire concernant toute douleur ou fatigue vécu au cours du protocole. Following the flexion protocol, you will be asked to fill out a follow-up questionnaire regarding any pain or fatigue experienced during the protocol.

Risques et inconforts possibles:
Il n'y a aucun risque significatif associé avec la participation à cette étude. Il est possible de ressentir de la douleur et de la fatigue en raison de nature de la tâche de flexion. Cependant, un repos suffisant sera fourni pour réduire ces effets. Si vous ressentez un inconfort majeur, veuillez nous le signaler immédiatement et demander les soins primaires d'un professionnel de la santé sur le campus (100 Marie Curie, Ottawa, Tél.: 613-564-3950) ou un professionnel médical de votre choix.

Avantages possibles:
Vous ne bénéficierez pas directement de la participation à cette étude. Cependant, les résultats contribueront grandement à notre connaissance de la façon dont la focalisation de l'attention affecte la stabilité dynamique locale pendant les tâches de flexion de la colonne vertébrale.

Participation volontaire:
Vous n'êtes pas obligé de participer à cette étude. La participation à cette étude est volontaire. Vous pouvez également vous retirer de l'étude à tout moment sans pénalité.

Confidentialité:
Tous les renseignements personnels sont gardés confidentiels à moins que la libération ne soit requise par la loi. Les renseignements tirés de cette étude seront enregistre électroniquement et auront besoin d'un mot de passe pour y accéder. Les dossiers d'études sur papier sont entreposés dans un cabinet verrouillé et seront détruits après 5 ans. Aussi, les dossiers électroniques seront supprimés et les documents papier seront détruits. Vous ne serez pas identifié par nom dans les rapports finaux de l'étude. Votre anonymat sera strictement maintenu - vous ne serez pas identifié par votre nom, mais sera déterminé par un numéro d'étude.

Compensation:
Aucune compensation monétaire ne sera accordée pour participer à cette étude. Cependant, les données fourniront d'importantes contributions à la compréhension.

Critère d'exclusion:
Vous serez exclu de la participation à cette étude si vous avez des antécédents de lombalgie. En outre, si vous avez déjà vécu: des troubles cardiovasculaires, des troubles neurologiques

(neuropathie, maladies neurodégénératives), des douleurs lombaires (discogène, mécanique, myofasciale), une blessure à la cheville (sprainée, fracturée) l'utilisation de médicaments (anti-inflammatoires, antidépresseurs), antécédents de lésions lombaires (mécanique discogène) utilisation d'une thérapie anticoagulante, AVC ou AIT, traumatisme de la colonne vertébrale, accident de véhicule, chirurgie de la colonne lombaire, hypertension, CTD et symptômes neurologiques focaux (sensoriels / moteurs) .

Questions sur l'étude:
Vous êtes bienvenue de poser des questions à tout moment; Vous pouvez communiquer avec les chercheurs principaux par courriel: Wantuir Junior Eric Bourdon et / ou le Dr Ryan Graham (ryan.graham@uottawa.ca). Ce projet est financé par le Conseil de recherches en sciences naturelles et en génie du Canada.
Ce protocole a été approuvé par le Conseil d'éthique de la recherche de l'Université d'Ottawa. Si vous avez des questions sur la conduite éthique de cette étude, vous pouvez communiquer avec l'agent de protocole pour l'éthique en recherche, Université d'Ottawa, Hall Tabaret, 550, rue Cumberland, pièce 154, Ottawa ON, K1N 6N5. Tél.: (613) 562-5387 Courriel: ethics@uottawa.ca

Titre du projet de recherche: **L'effet de l'attention sur la stabilité dynamique locale pendant la flexion répétitive de la colonne vertébrale**

Consentement:
J'ai lu ce formulaire de consentement et j'accepte de participer aux procédures de cette étude.

_____
Nom imprimé du participant

_____ _____
Signature du participant Date

Déclaration de l'enquêteur:
J'ai soigneusement expliqué au participant de la recherche la nature de l'étude de recherche ci-dessus. À ma connaissance, le participant à la recherche signant ce formulaire comprend la nature, les exigences, les risques et les avantages associés à la participation à cette étude. Je reconnais ma responsabilité pour la sécurité et le bien-être du participant à la recherche susmentionné, de respecter les droits et les besoins du participant à la recherche et de mener l'étude conformément aux lignes directrices et aux règlements applicables en matière de bonnes pratiques cliniques.

_____
Nom de l'enquêteur / délégué

_____ _____
Signature de l'enqueteur/Delegue Date

Consentement à prendre des photos:
Je consens à avoir des photos de vue latérale de moi-même complétant l'expérience, et comprends que les photos ne seront prises à aucun moment sans me savoir. Je comprends également que si l'une de ces images est utilisée dans une présentation ou une publication ultérieure, mon visage et tout autre identifiant seront flous. Vous pouvez toujours participer à l'étude sans consentir à prendre des photos.

_____ _____
Nom Date

_____
Signature

Nom du témoin Signature du témoin

Participation future:

- ☐ Je suis intéressé à être contacté pour participer à de f recherches futures effectuées par ce laboratoire (vos informations de courriel seront enregistrées dans un fichier protégé par mot de passe).

File Number: H02-17-11 **Date (mm/dd/yyyy):** 03/17/2017

Université d'Ottawa University of Ottawa
Bureau d'éthique et d'intégrité de la recherche Office of Research Ethics and Integrity

Ethics Approval Notice

Health Sciences and Science REB

Principal Investigator / Supervisor / Co-investigator(s) / Student(s)

First Name	Last Name	Affiliation	Role
Ryan	Graham	Health Sciences / Others	Supervisor
Eric	Bourdon	Health Sciences / Human Kinetics	Student Researcher
Wantuir Carlos	Ramos Junior	Health Sciences / Human Kinetics	Student Researcher

File Number: H02-17-11

Type of Project: Independent Student Project

Title: The effect of focus of attention on local dynamic stability during repetitive spine flexion

Approval Date (mm/dd/yyyy)	Expiry Date (mm/dd/yyyy)	Approval Type
03/17/2017	03/16/2018	Approval

Special Conditions / Comments:
N/A

File Number: H02-17-11 **Date (mm/dd/yyyy):** 03/17/2017

Université d'Ottawa University of Ottawa
Bureau d'éthique et d'intégrité de la recherche Office of Research Ethics and Integrity

This is to confirm that the University of Ottawa Research Ethics Board identified above, which operates in accordance with the Tri-Council Policy Statement (2010) and other applicable laws and regulations in Ontario, has examined and approved the ethics application for the above named research project. Ethics approval is valid for the period indicated above and subject to the conditions listed in the section entitled "Special Conditions / Comments".

During the course of the project, the protocol may not be modified without prior written approval from the REB except when necessary to remove participants from immediate endangerment or when the modification(s) pertain to only administrative or logistical components of the project (e.g., change of telephone number). Investigators must also promptly alert the REB of any changes which increase the risk to participant(s), any changes which considerably affect the conduct of the project, all unanticipated and harmful events that occur, and new information that may negatively affect the conduct of the project and safety of the participant(s). Modifications to the project, including consent and recruitment documentation, should be submitted to the Ethics Office for approval using the "Modification to research project" form available at: https://research.uottawa.ca/ethics/forms.

Please submit an annual report to the Ethics Office four weeks before the above-referenced expiry date to request a renewal of this ethics approval. To close the file, a final report must be submitted. These documents can be found at: https://research.uottawa.ca/ethics/forms.

If you have any questions, please do not hesitate to contact the Ethics Office at extension 5387 or by e-mail at: ethics@uOttawa.ca.

Gabriel Petitti
Protocol Officer for Ethics in Research
For Daniel Lagarec, Chair of the Health Sciences and Sciences REB

APPENDIX B

Development and testing of a custom markerless deep learning algorithm for spine segmentation and motion assessment using RGB-D images – Consent Form and Ethics Certificate

uOttawa

Research Consent Form

Research Project Title:

Validation of wearable sensor and video-based depth sensor for the evaluation of spine movement quality

Principal Investigator and Co-Investigators:

Dr. Ryan Graham
613-562-5800 X 1025; ryan.graham@uottawa.ca

Wantuir Junior
613-562-5800 X 1739;

University of Ottawa
Faculty of Health Sciences
Department of Human Kinetics
200 Lees Avenue (E020)
Ottawa, ON K1N6N5

Université d'Ottawa
Faculté des sciences de la santé

École des sciences de l'activité physique

University of Ottawa
Faculty of Health Sciences

School of Human Kinetics

☎ +1 613 562 5800 ext. 1025
Ryan.Graham@uottawa.ca
☎ +1 613 562 5800 ext. 1739

200 Lees Ave. (E020)
Ottawa ON K1N 6N5 Canada

www.uOttawa.ca

Background and Purpose of the Study:
Despite the vast population of low back pain sufferers, accurate diagnosis and treatment of the disorder is insufficient. There is currently a lack of understanding regarding the various mechanisms that drive the disorder, resulting in inappropriate treatment. It is documented that people with low back pain move differently based on the dominant factor driving the disorder. The ability for health care providers to objectively measure spinal movement quality in clinics will greatly improve diagnostic procedures and spine care. Our lab has developed and is refining a framework for performing video-based spine movement quality analyses in clinical settings. In this specific study, we are improving a video-based depth sensor method to classify anatomical landmarks by remodeling its artificial intelligence. Therefore, the goal of this study is to create a deep learning algorithm capable of accurately classifying anatomical landmarks of the back through a video-based depth sensor input (i.e. colour infrared, and depth images).

Description of Study Procedures:
You are invited to participate in a one day motion analysis procedure at the University of Ottawa Human Movement Biomechanics Laboratory (200 Lees Avenue, E020). The study visit will last approximately 1 hour. For the study visit, prior the data collection, you will be asked to change into appropriate outfit for being able to collect images of their backs. Male participants will be asked to wear spandex pants only, and female participants will be asked to wear spandex pants and a hospital gown during the task protocol.

During the study, you will complete 2 trials of 10 rate-controlled cycles of repetitive trunk flexion-extension tasks. In the first trial, the trunk flexion-extension task will be completed without the use of any markers. Prior the start of the second trial, 70 tracking dots will be drawn on your back using dry-erase black marker. During both repetitive trunk movement tasks, you will be asked to touch two targets with your hands that represent end range of motion in each direction. You will be given a 5-minute rest between tasks to prevent fatigue, and will be allowed to practice the tasks to ensure you are comfortable and understand the instructions. More time will be provided if it is required to ensure no signs of fatigue are present. You will not be constrained in any way during the duration of the movement protocol.

Possible Risks and Discomforts:
There are no significant risks associated with participating in this study. You may experience pain and fatigue due to the nature of the movement protocol. However, sufficient rest will be given, where possible, to reduce these effects. Should you experience any major discomfort, please tell us immediately and seek primary care from a medical professional on campus (100 Marie Curie, Ottawa, Tel.: 613-564-3950) or a medical professional of your choosing.

Possible Benefits:
You will not directly benefit from participating in this study. However, the results of this study will help advance the evaluation of spine movement quality in clinical settings.

Voluntary Participation:
You are not obliged to participate in this study; participation in this study is voluntary. You may also withdraw from the study at any time with no penalty or coercion.

Confidentiality:
All personal information is kept confidential unless release is required by law. Information gained from this study will be stored electronically and will need a password to access. Paper study records are stored in a locked cabinet and will be destroyed after 5 years; electronic records will be deleted and paper records will be shredded. You will not be identified by name in any reports of the completed study. Your anonymity will be strictly maintained – you will not be identified by your name, but will be determined by an independent study number.

Compensation:
No monetary compensation will be provided for participation in this study. However the data will provide significant contributions to validating the Microsoft Kinect for evaluation of spine movement quality.

Exclusion Criteria:
You will be excluded from the study if you have any history of the following: allergy to contact with marker ink (contact dermatitis), cardiovascular conditions, neurologic disorders (neuropathy, neurodegenerative conditions), specific LBP (discogenic, mechanical, myofascial), use of medication (anti-inflammatories, analgesics, anticonvulsants, antidepressants), history of low back injury (discogenic mechanical) use of anticoagulent therapy, stroke or TIA, spine trauma, motor vehicle accident, lumbar spine surgery, hypertension, CTD and focal neurological symptoms (sensory/motor).

Questions about the Study:
You are free to ask questions at any time; you can contact the principal investigators by email: Wantuir Junior and/or Dr. Ryan Graham (ryan.graham@uottawa.ca). This project is funded by the Natural Sciences and Engineering Research Council of Canada. The University of Ottawa research ethics board has approved all ethical aspects of this research project. If you have any questions regarding the ethical conduct of this study, you may contact the Protocol Officer for Ethics in Research, University of Ottawa, Tabaret Hall, 550 Cumberland Street, Room 154, Ottawa ON, K1N 6N5. Tel.: (613) 562-5387 Email: ethics@uottawa.ca

Research Project Title: **Validation of wearable sensor and video-based depth sensor for the evaluation of spine movement quality**

Consent:
I have read this consent form, and I agree to participate in the procedures of this study.

_____
Printed Name of Participant

_____ _____
Signature of Participant Date

Investigator Statement (or Person Explaining the Consent):
I have carefully explained to the research participant the nature of the above research study. To the best of my knowledge, the research participant signing this consent form understands the nature, demands, risks and benefits involved in participating in this study. I acknowledge my responsibility for the care and well-being of the above research participant, to respect the rights and wishes of the research participant, and to conduct the study according to applicable Good Clinical Practice guidelines and regulations.

_____
Name of Investigator/Delegate (printed)

_____ _____
Signature of Investigator/Delegate Date

Informed Consent to have Pictures Taken:
I consent to have side view pictures taken of myself completing the experiment, and understand that no pictures will be taken at any point without me knowing. I also understand that if any of these pictures are used in a subsequent presentation or publication, that my face and any other identifiers will be blurred. You can still participate in the research study without consenting to have pictures taken.

_____ _____
Name Date

_____
Signature

_____ _____
Witness Name Witness Signature

Future Participation:

- ☐ I am interested in being contacted to participate in future research performed by this laboratory (your email information will be saved in a password protected file).

uOttawa

Formulaire de consentement à la recherche

Titre du projet de recherche:

Validation de la performance de capteur portable et le capteur de profondeur basé sur la vidéo pour l'évaluation de la qualité du mouvement de la colonne vertébrale

Chercheurs Principaux et Co-chercheurs:

Dr. Ryan Graham
613-562-5800 X 1025; ryan.graham@uottawa.ca

Wantuir Junior
613-562-5800 X 1739;

Université d'Ottawa
Faculté des sciences de la santé
École des sciences de l'activité physique
200, Avenue Lees (E020)
Ottawa, ON K1N6N5

Contexte et objectif de l'étude:
Malgré la vaste population de personnes souffrant de douleurs lombaires, la précision du diagnostic et du traitement de la maladie est insuffisante. Il existe un manque de compréhension concernant les différents mécanismes qui entraînent le désordre, ce qui entraîne un traitement inapproprié. Il est documenté que les personnes souffrant de lombalgie se déplacent différemment en fonction du facteur dominant responsable du désordre. La capacité des fournisseurs de soins de santé à mesurer objectivement la qualité du mouvement de la colonne vertébrale dans les cliniques améliorera grandement les procédures de diagnostic et les soins de la colonne vertébrale. Notre laboratoire a mis au point et perfectionne un système permettant d'effectuer les analyses des vidéos pour voir la qualité des mouvements de la colonne vertébrale en milieu clinique. Dans cette étude spécifique, nous améliorons une méthode de capteur de profondeur basée sur la vidéo pour classer les repères anatomiques en remodelant son intelligence artificielle. Par conséquent, l'objectif de cette étude est de créer un algorithme d'apprentissage en profondeur capable de classer avec précision les repères anatomiques du dos au moyen d'une entrée de capteur de profondeur vidéo (images couleur, infrarouge et de profondeur).

Description des procédures d'étude:
Vous êtes invités à participer à une procédure d'analyse de mouvement d'une journée au Laboratoire de biomécanique du mouvement humain de l'Université d'Ottawa (200, avenue Lees, E020). La visite d'étude durera environ une heure. Pour la visite d'étude, avant qu'on collecte des données, on vous sera demandé

Université d'Ottawa
Faculté des sciences de la santé

École des sciences de l'activité physique

University of Ottawa
Faculty of Health Sciences

School of Human Kinetics

+1 613 562 5800 ext. 1025
ryan.graham@uottawa.ca

200, Avenue Lees (E020)
Ottawa, ON K1N 6N5 Canada

www.uOttawa.ca

de changer de tenue pour pouvoir collecter des images de votre dos. Les participants masculins ne devront porter que des pantalons en spandex, et les participantes seront tenues de porter des pantalons en spandex et une blouse d'hôpital lors du protocole de la tâche.

Au cours de l'étude, vous effectuerez deux essais de 10 cycles de tâches répétitives de flexion-extension du tronc qui sont contrôlé par une métronome. Lors du premier essai, la tâche d'extension de la flexion du tronc sera complétée sans utilisation de marqueur. Avant le début du deuxième essai, 70 points seront dessinés sur votre dos à l'aide d'un marqueur noir effaçable à sec. Au cours des deux tâches de mouvement du tronc répétitives, il vous sera demandé de toucher deux cibles avec vos mains qui représentent l'amplitude de fin de mouvement dans chaque direction. Vous aurez cinq minutes de repos entre les tâches pour éviter la fatigue et vous pouvez exercer à exécuter les tâches pour vous assurer que vous êtes à l'aise et que vous comprenez bien les instructions. Plus de temps sera alloué s'il est nécessaire de s'assurer qu'aucun signe de fatigue est présent. Vous ne serez en aucune manière contraint pendant la durée du protocole de mouvement.

Risques et inconforts possibles:
Il n'y a aucun risque significatif associé avec la participation à cette étude. Il est possible de ressentir de la douleur et de la fatigue en raison de nature de la tâche de flexion. Cependant, un repos suffisant sera fourni pour réduire ces effets. Si vous ressentez un inconfort majeur, veuillez nous le signaler immédiatement et demander les soins primaires d'un professionnel de la santé sur le campus (100 Marie Curie, Ottawa, Tél.:(613-564-3950) ou un professionnel médical de votre choix.

Avantages possibles:
Vous ne bénéficierez pas directement de la participation à cette étude. Cependant, les résultats de cette étude aideront à progresser l'évaluation de la qualité du mouvement de la colonne vertébrale dans les milieux cliniques.

Participation volontaire :
Vous n'êtes pas obligé de participer à cette étude. La participation à cette étude est volontaire. Vous pouvez également vous retirer de l'étude à tout moment sans pénalité.

Confidentialité:
Tous les renseignements personnels sont gardés confidentiels à moins que la libération ne soit requise par la loi. Les renseignements tirés de cette étude seront enregistrés électroniquement et auront besoin d'un mot de passe pour y accéder. Les dossiers d'études sur papier sont entreposés dans un cabinet verrouillé et seront détruits après 5 ans. Aussi, les dossiers électroniques seront supprimés et les documents papier seront détruits. Vous ne serez pas identifié par nom dans les rapports finaux de l'étude. Votre anonymat sera strictement maintenu - vous ne serez pas identifié par votre nom, mais sera déterminé par un numéro d'étude.

Compensation:
Aucune compensation monétaire ne sera accordée pour participer à cette étude. Cependant, les données fourniront d'importantes contributions pour valider les capteurs portables de centrale

inertielle et Microsoft Kinect pour l'évaluation de la qualité du mouvement de la colonne vertébrale.

Critère d'exclusion:
Tous les participants: Vous serez exclu de la participation à cette étude si vous avez déjà vécu: allergie au contact avec l'encre de marqueur (dermatite de contact), des difficultés cardio-vasculaires, des difficultés neurologiques (neuropathie, maladies neurodégénératives), des douleurs lombaires (discogène, mécanique, myofasciale), une blessure à la cheville (foulée, fracturée) l'utilisation de médicaments (anti-inflammatoires, antidépresseurs), antécédents de lésions lombaires (mécanique discogène) utilisation d'une thérapie anticoagulante, AVC ou AIT, traumatisme de la colonne vertébrale, accident de véhicule, chirurgie de la colonne lombaire, hypertension, CTD et symptômes neurologiques focaux (sensoriels / moteurs).

Questions sur l'étude:
Vous êtes bienvenue de poser des questions à tout moment; Vous pouvez communiquer avec les chercheurs principaux par courriel: Wantuir Junior et/ou Dr. Ryan Graham (ryan.graham@uottawa.ca). Ce projet est financé par le Conseil de recherches en sciences naturelles et en génie du Canada. Le Conseil d'éthique de la recherche de l'Université d'Ottawa a approuvé tous les aspects éthiques de ce projet de recherche. Si vous avez des questions sur la conduite éthique de cette étude, vous pouvez communiquer avec l'agent de protocole pour l'éthique en recherche, Université d'Ottawa, Hall Tabaret, 550, rue Cumberland, pièce 154, Ottawa ON, K1N 6N5. Tél.: (613) 562-5387 Courriel: ethics@uottawa.ca

Titre du projet de recherche: **Validation de la performance de capteur portable et le capteur de profondeur basé sur la vidéo pour l'évaluation de la qualité du mouvement de la colonne vertébrale**

Consentement:
J'ai lu ce formulaire de consentement et j'accepte de participer aux procédures de cette étude.

_____
Nom imprimé du participant

_____ _____
Signature du participant Date

Déclaration de l'enquêteur:
J'ai soigneusement expliqué au participant de la recherche la nature de l'étude de recherche ci-dessus. À ma connaissance, le participant à la recherche signant ce formulaire comprend la nature, les exigences, les risques et les avantages associés à la participation à cette étude. Je reconnais ma responsabilité pour la sécurité et le bien-être du participant à la recherche susmentionné, de respecter les droits et les besoins du participant à la recherche et de mener l'étude conformément aux lignes directrices et aux règlements applicables en matière de bonnes pratiques cliniques.

_____
Nom de l'enquêteur / délégué

_____ _____
Signature de l'enqueteur/Delegue Date

Consentement à prendre des photos:
Je consens à avoir des photos de vue latérale de moi-même complétant l'expérience, et comprends que les photos ne seront prises à aucun moment sans me savoir. Je comprends également que si l'une de ces images est utilisée dans une présentation ou une publication ultérieure, mon visage et tout autre identifiant seront flous. Vous pouvez toujours participer à l'étude sans consentir à prendre des photos.

_____ _____
Nom Date

_____
Signature

Nom du témoin Signature du témoin

Participation future:

- ☐ Je suis intéressé à être contacté pour participer à de f recherches futures effectuées par ce laboratoire (vos informations de courriel seront enregistrées dans un fichier protégé par mot de passe).

File Number: H08-17-26 **Date (mm/dd/yyyy):** 11/12/2019

Université d'Ottawa University of Ottawa
Bureau d'éthique et d'intégrité de la recherche Office of Research Ethics and Integrity

Ethics Approval Notice

Health Sciences and Science REB

Principal Investigator / Supervisor / Co-investigator(s) / Student(s)

First Name	Last Name	Affiliation	Role
Ryan	Graham	Health Sciences / Human Kinetics	Principal Investigator
Sean	Beaudette	Others / Others	Co-investigator
Kristen	Beange	Health Sciences / Human Kinetics	Research Assistant
Wantuir Carlos	Ramos Junior	Health Sciences / Human Kinetics	Research Assistant

File Number: H08-17-26

Type of Project: Professor

Title: Validation of a wearable sensor mobile application for the investigation of spine movement quality

Renewal Date (mm/dd/yyyy)	Expiry Date (mm/dd/yyyy)	Approval Type
11/08/2019	11/07/2020	Renewal

Special Conditions / Comments:
N/A

1 550, rue Cumberland, pièce 154
550 Cumberland Street, room 154 Ottawa (Ontario) K1N 6N5 Canada
Ottawa, Ontario K1N 6N5 Canada
(613) 562-5387 • Téléc./Fax (613) 562-5338
www recherche.uottawa.ca/deontologie/ www research.uottawa.ca/ethics/

Number: H08-17-26 **Date (mm/dd/yyyy):** 11/12/2019

Université d'Ottawa University of Ottawa

Bureau d'éthique et d'intégrité de la recherche Office of Research Ethics and Integrity

This is to confirm that the University of Ottawa Research Ethics Board identified above, which operates in accordance with the Tri-Council Policy Statement (2010) and other applicable laws and regulations in Ontario, has examined and approved the ethics application for the above named research project. Ethics approval is valid for the period indicated above and subject to the conditions listed in the section entitled "Special Conditions / Comments".

During the course of the project, the protocol may not be modified without prior written approval from the REB except when necessary to remove participants from immediate endangerment or when the modification(s) pertain to only administrative or logistical components of the project (e.g., change of telephone number). Investigators must also promptly alert the REB of any changes which increase the risk to participant(s), any changes which considerably affect the conduct of the project, all unanticipated and harmful events that occur, and new information that may negatively affect the conduct of the project and safety of the participant(s). Modifications to the project, including consent and recruitment documentation, should be submitted to the

Ethics Office for approval using the "Modification to research project" form available at: https://research.uottawa.ca/ethics/forms.

Please submit an annual report to the Ethics Office four weeks before the above-referenced expiry date to request a renewal of this ethics approval. To close the file, a final report must be submitted. These documents can be found at: https://research.uottawa.ca/ethics/forms.

If you have any questions, please do not hesitate to contact the Ethics Office at extension 5387 or by e-mail at: ethics@uOttawa.ca.

Marc Alain Bonenfant
Research Ethics Coordinator
For Catherine Paquet, Director of the Office of Research Ethics and Integrity

File Number: H08-17-26 **Date (mm/dd/yyyy):** 10/18/2018

Université d'Ottawa University of Ottawa
Bureau d'éthique et d'intégrité de la recherche Office of Research Ethics and Integrity

Ethics Approval Notice

Health Sciences and Science REB

Principal Investigator / Supervisor / Co-investigator(s) / Student(s)

First Name	Last Name	Affiliation	Role
Ryan	Graham	Health Sciences / Human Kinetics	Principal Investigator
Sean	Beaudette	Others / Others	Co-investigator
Kristen	Beange	Health Sciences / Human Kinetics	Research Assistant
Wantuir Carlos	Ramos Junior	Health Sciences / Human Kinetics	Research Assistant

File Number: H08-17-26

Type of Project: Professor

Title: Validation of a wearable sensor mobile application for the investigation of spine movement quality

Renewal Date (mm/dd/yyyy)	Expiry Date (mm/dd/yyyy)	Approval Type
11/08/2018	11/07/2019	Renewal

Special Conditions / Comments:
N/A

File Number: H08-17-26 **Date (mm/dd/yyyy):** 10/18/2018

Université d'Ottawa University of Ottawa
Bureau d'éthique et d'intégrité de la recherche Office of Research Ethics and Integrity

This is to confirm that the University of Ottawa Research Ethics Board identified above, which operates in accordance with the Tri-Council Policy Statement (2010) and other applicable laws and regulations in Ontario, has examined and approved the ethics application for the above named research project. Ethics approval is valid for the period indicated above and subject to the conditions listed in the section entitled "Special Conditions / Comments".

During the course of the project, the protocol may not be modified without prior written approval from the REB except when necessary to remove participants from immediate endangerment or when the modification(s) pertain to only administrative or logistical components of the project (e.g., change of telephone number). Investigators must also promptly alert the REB of any changes which increase the risk to participant(s), any changes which considerably affect the conduct of the project, all unanticipated and harmful events that occur, and new information that may negatively affect the conduct of the project and safety of the participant(s). Modifications to the project, including consent and recruitment documentation, should be submitted to the Ethics Office for approval using the "Modification to research project" form available at: https://research.uottawa.ca/ethics/forms.

Please submit an annual report to the Ethics Office four weeks before the above-referenced expiry date to request a renewal of this ethics approval. To close the file, a final report must be submitted. These documents can be found at: https://research.uottawa.ca/ethics/forms.

If you have any questions, please do not hesitate to contact the Ethics Office at extension 5387 or by e-mail at: ethics@uOttawa.ca.

Marc Alain Bonenfant
Research Ethics Coordinator
For Catherine Paquet, Director of the Office of Research Ethics and Integrity